2015-03-30

Immunoassays of Potential Cancer Biomarkers in Microfluidic Devices

Jayson Virola Pagaduan
Brigham Young University - Provo

Immunoassays of Potential Cancer Biomarkers in Microfluidic Devices

Jayson Virola Pagaduan

A dissertation submitted to the faculty of
Brigham Young University
in partial fulfillment of the requirements for the degree of

Doctor of Philosophy

Adam T. Woolley, Chair
Steven W. Graves
Richard K. Watt
Steven R. Goates
Kim O'Neill

Department of Chemistry and Biochemistry

Brigham Young University

April 2015

ABSTRACT

Immunoassays of Potential Cancer Biomarkers in Microfluidic Devices

Jayson Virola Pagaduan
Department of Chemistry and Biochemistry, BYU
Doctor of Philosophy

Laboratory test results are important in making decisions regarding a patient's diagnosis and response to treatment. These tests often measure the biomarkers found in biological fluids such blood, urine, and saliva. Immunoassay is one type of laboratory test used to measure the level of biomarkers using specific antibodies. Microfluidics offer several advantages such as speed, small sample volume requirement, portability, integration, and automation. These advantages are motivating to develop microfluidic platforms of conventional laboratory tests. I have fabricated polymer microfluidic devices and developed immunoassays on-chip for potential cancer markers.

Silicon template devices were fabricated using standard photolithographic techniques. The template design was transferred to a poly(methyl methacrylate) (PMMA) piece by hot embossing and subsequently bonded to another PMMA piece with holes for reservoirs. I used these devices to perform microchip immunoaffinity electrophoresis to detect purified recombinant thymidine kinase 1 (TK1). Buffer with 1% methylcellulose acted as a dynamic coating that minimized nonspecific adsorption of protein and as sieving matrix that enabled separation of free antibody from antibody-TK1 complexes. Using this technique, I was able to detect TK1 concentration >80 nM and obtained separation results within 1 minute using a 5 mm effective separation length.

Detection of endogenous TK1 in serum is difficult because TK1 is present at the pM range. I compared three different depletion methods to eliminate high abundance immunoglobulin and human serum albumin. Cibacron blue columns depleted abundant protein but also nonspecifically bound TK1. I found that ammonium sulfate precipitation and IgG/albumin immunoaffinity columns effectively depleted high abundance proteins. TK1 was salted out of the serum with saturated ammonium sulfate and still maintained activity.

To integrate affinity columns in microfluidic devices, I have developed a fast and easy strategy for initial optimization of monolith affinity columns using bulk polymerization of multiple monolith solutions. The morphology, surface area, and porosity, were qualitatively assessed using scanning electron microscopy. This method decreased the time, effort, and resources compared to in situ optimization of monoliths in microfluidic devices. This strategy could be used when designing novel formulations of monolith columns.

I have also integrated poly(ethylene glycol dimethacrylate-glycidyl methacrylate) monolith affinity columns in polymer microfluidic devices to demonstrate the feasibility of extracting human interleukin 8 (IL8), a cancer biomarker, from saliva. Initial results have shown that the affinity column (~3 mm) was successfully integrated into the devices without prior surface modification. Furthermore, anti-IL8 was immobilized on the surface of the monolith. Electrochromatograms showed that 1 ng/mL of IL8 can be detected when in buffer while 10 ng/mL was detected when IL8 was spiked in saliva.

Overall, these findings can be used to further develop immunoassays in microfluidic platforms, especially for analyzing biological fluids.

Keywords: microchip electrophoresis, microfluidics, electrochromatography, monolith, immunoaffinity

ACKNOWLEDGEMENTS

I would like to thank my Heavenly Father for helping me go through this endeavor of graduate education. All the knowledge I have gained in this journey has helped me better understand the greatness of His power and His marvelous creations.

I will forever be grateful for my advisor, Dr. Adam T. Woolley. His passion for science is contagious. His comments and suggestions have guided me to be a better researcher and helped me complete this dissertation. I thank my committee, Dr. O'Neill, Dr. Goates, Dr. Graves and Dr. Watt for their recommendations and insightful questions so I could improve my work.

I thank my ATW lab mates especially Dr. Ming Yu, Dr. Pamgela Nge, Dr. Debolina Chatterjee, Dr. Chad Rogers and Dr. Vishal Sahore for your help and friendliness inside and outside the laboratory. I am also thankful for the O'Neill lab members especially Rachel Brog for sacrificing many Saturdays for the sake of research.

I thank the Department of Chemistry and Biochemistry at Brigham Young University for providing an excellent environment for learning both academically and spiritually.

I am very thankful for my family. My parents, Arsenio A. Pagaduan and Aida V. Pagaduan, have always been supportive with my decisions and who are always there to motivate me to do my best. My siblings, Kuya Ryan and Ate Cristy, my nieces Keziah and Hannah, Ate Jenny and Kuya Adrian, Ate Lilian and Kuya Jayson, my nephews J.E., ArJo, my niece Jalian, Kuya Ephraim, my nephew E.J, my niece Jasmine, Ate Joy, my niece Brianna, and Ate Amabel, thank you for your encouragements and Skype conversations.

I thank my friends especially Sambhav Kumbhani and Vikas Asthana.

Finally, I am thankful for my fiancé, Liz, for your encouragements, understanding, and listening ears. I love you very much.

TABLE OF CONTENTS

LIST OF FIGURES

LIST OF TABLES

CHAPTER 1: INTRODUCTION*

1.1 ADVANTAGES OF MICROCHIP ELECTROPHORESIS FOR CLINICAL MARKER ANALYSIS

The push for improved health care is increasing the need to develop diagnostic tools that are cost-effective, reliable, and fast. Lack of resources and expertise in many developing countries limits their ability to perform straightforward clinical diagnostic tests. On the other hand, developed countries often have a backlog of tests that results in longer waiting times for results to be dispensed to the physicians and ultimately to the patients. A causative factor in these problems with clinical diagnostics is that they are done using conventional benchtop analysis platforms that are effective yet slow, lab-bound, labor intensive, and consume large volumes of reagents and expensive samples. Because of some of the disadvantages of conventional methods, researchers adapted photolithography and chemical etching techniques from the microelectronics industry to make microfluidic analysis systems starting in the early 1990s.[1] The goal of this chapter is to describe advances in microchip electrophoresis over the last 5 years in the analysis of clinically relevant biomarkers, including lipids, carbohydrates, nucleic acids, and proteins. I further highlight the advantages over conventional benchtop techniques offered by microchip electrophoresis in the analyses of clinical samples.

Commonly used disease diagnostic tools process complex bodily fluids.[2,3] Microchip electrophoresis offers advantages for clinical analysis like speed, small sample volumes, low power, and integration of multiple sample manipulation processes into a compact format.[4] The

* Sections 1.1 and 1.4 adapted with permission from Pagaduan, J.; Sahore, V.; Woolley, A.T. *Anal. Bioanal. Chem.* 2015, accepted for publication.

manufacturing procedure for these devices is compatible with well-established semiconductor processing techniques. Moreover, microchip electrophoresis systems are compatible with point-of-care analysis that can be performed by semi-skilled workers in resource-limited locations.[5, 6]

1.2 MICROFLUIDIC DEVICE FABRICATION

The techniques used to fabricate the microfluidic devices were adapted from the methods previously developed in the microelectronics industry.[7] A schematic of the procedure for template and device fabrication is illustrated in Figure 1.1. Briefly, a <100> silicon wafer was thermally oxidized before spin coating with positive photoresist. The coated silicon wafer was exposed to UV light through a photomask containing the channel design. The wafer was developed to remove the exposed photoresist and then etched in 10% buffered HF solution to remove the oxide layer. Further etching with 40% aqueous KOH was done to obtain ~20-μm height features. The fluidic design was hot embossed onto 1.5 mm thick poly(methyl methacrylate) (PMMA) sheets by sandwiching the template and PMMA between glass and copper plates held by C-clamps. The assembly was held in a convection oven for 20 minutes at 110 °C. Then a 3.0 mm thick PMMA piece with precut holes for reservoirs was used as a cover plate. The two pieces were thermally bonded in an assembly in a convection oven at 138 °C for 27 minutes.

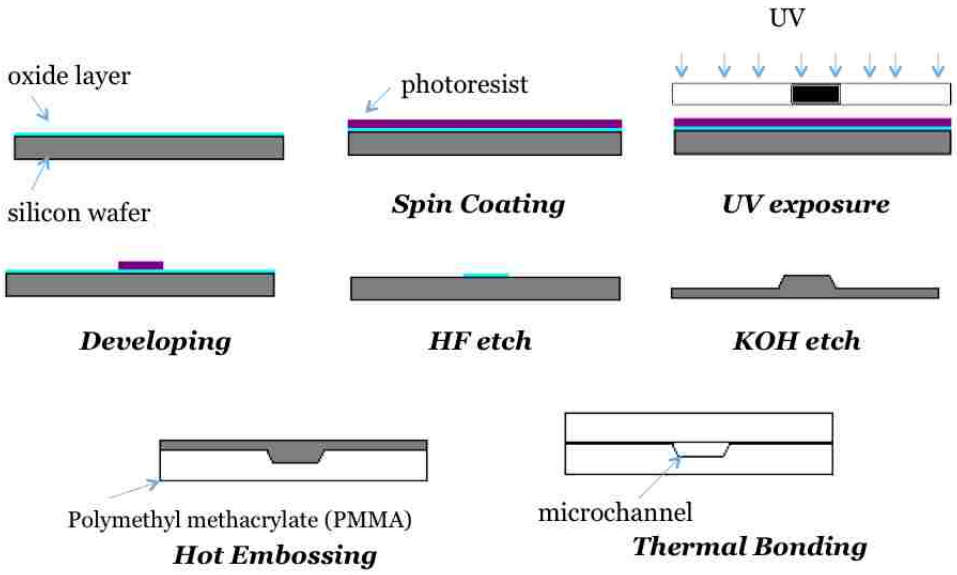

Figure 1.1 Fabrication of PMMA microfluidic devices.

1.3 MICROCHIP ELECTROPHORESIS

1.3.1 Introduction

Microchip electrophoresis (ME) is the miniaturization of capillary electrophoresis that was introduced in the early 1990's.[1] As described in section 1.2, ME devices are made using microfabrication techniques used by the electronics industry. The high surface area to volume ratio effectively dissipates Joule heating making it possible to use higher voltages in ME.[8] The simplicity of ME plus its further advantages that include fast analysis, multiplex separation, low sample volume, low cost, and portability resulted in increased interest in applying this technology for point-of-care analysis.[9]

1.3.2 Theory of Electrophoresis

Electrophoresis is the movement of charged analytes due to the influence of an applied potential difference. Electrophoretic flow and electroosmotic flow (EOF) are the two phenomena

observed in typical capillary electrophoresis that affect the migration velocity, v, of an analyte. The resulting migration phenomenon can be mathematically represented in equation 1.1,[10]

$$v = (\mu_e + \mu_{eof})E \qquad (1.1)$$

where μ_e is the electrophoretic mobility of the analyte, μ_{eof} is the EOF, and E is the electric field. The electrophoretic mobility is governed by the charge to mass ratio of the analyte expressed in equation 1.2,[10]

$$\mu_e = qE/6\pi\eta r \qquad (1.2)$$

where q is the charge of the analyte, E is the field strength (V/cm), η is the viscosity of the fluid and r is the radius, which is related to the mass of the analyte. The mass of an analyte is constant so manipulation of its charge by the buffer pH is the easiest way to change the separation of analytes with the same mass.

Surface channels with a net charge attract free ions of the opposite charge to create a thin Debye layer of mobile charges next to the charged surface and the potential difference in this double layer is called the zeta potential.[11] When an external field is applied, the fluid in this charged Debye layer is moved resulting in bulk fluid flow. This uniform velocity is described in the Helmholtz-Smoluchowski formula:[12]

$$\mu_{eo} = \varepsilon E\zeta/4\pi\eta \qquad (1.3)$$

Here, ε is the dielectric constant of the fluid, E is the applied electric field, and ζ is the zeta-potential at the liquid solid interface. Figure 1.2 illustrates the formation of the double layer near a negatively-charged channel wall.

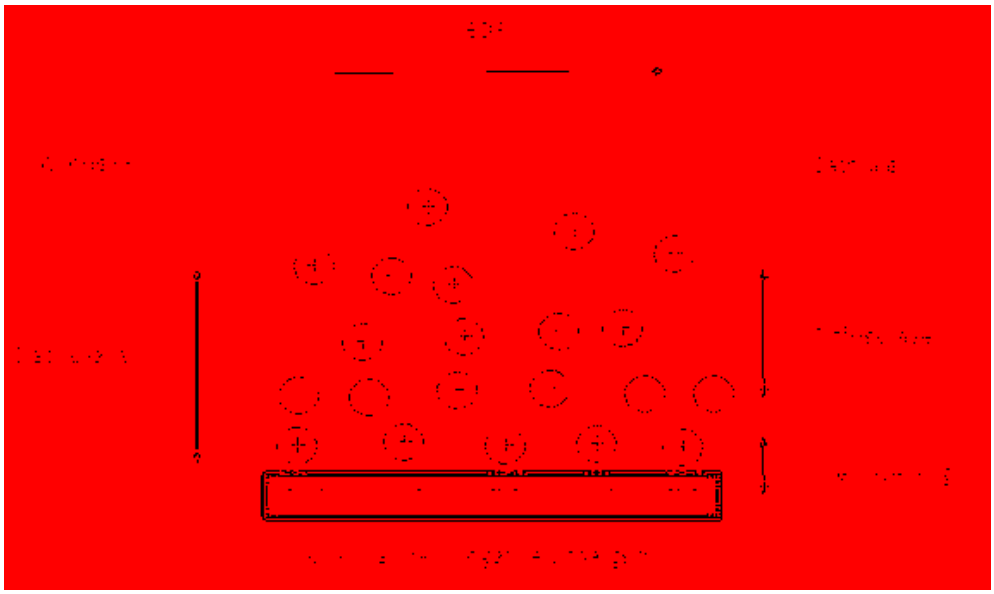

Figure 1.2 Direction of EOF with a negatively charged channel wall.

EOF is also affected by the pH, composition and concentration of background electrolyte; therefore, it is susceptible to changes that can alter the EOF during an experiment. However, when EOF is stabilized, it can reduce electrokinetic sample injection bias and make it possible to analyze cations, anions and neutral molecules simultaneously. The uniform plug flow profile produced by EOF that results in reduced sample dispersion is an important contrast to pressure driven flow.

1.3.3 Device Operation and Detection

Several injection methods are utilized in ME. Electrokinetic injection is commonly used because of its simplicity and no need for moving parts. This method uses an electric field to manipulate the direction of sample flow.[13] The two most common modes of electrokinetic injections are pinched and gated.[14] Pinched injection (see figure 1.3) provides an accurate, well-defined volume of sample plug and provides high separation efficiency. However, this technique limits the sample volume by the dimension of the intersection, which can be detrimental for

analysis of very dilute samples.[15] In gated injection, sample volume can be increased by changing the injection time while sample volume does not change with time in pinched injection.[16] Gated injection, like pinched injection, also produces injection bias due to the differences in the electrophoretic mobilities of analytes.[17]

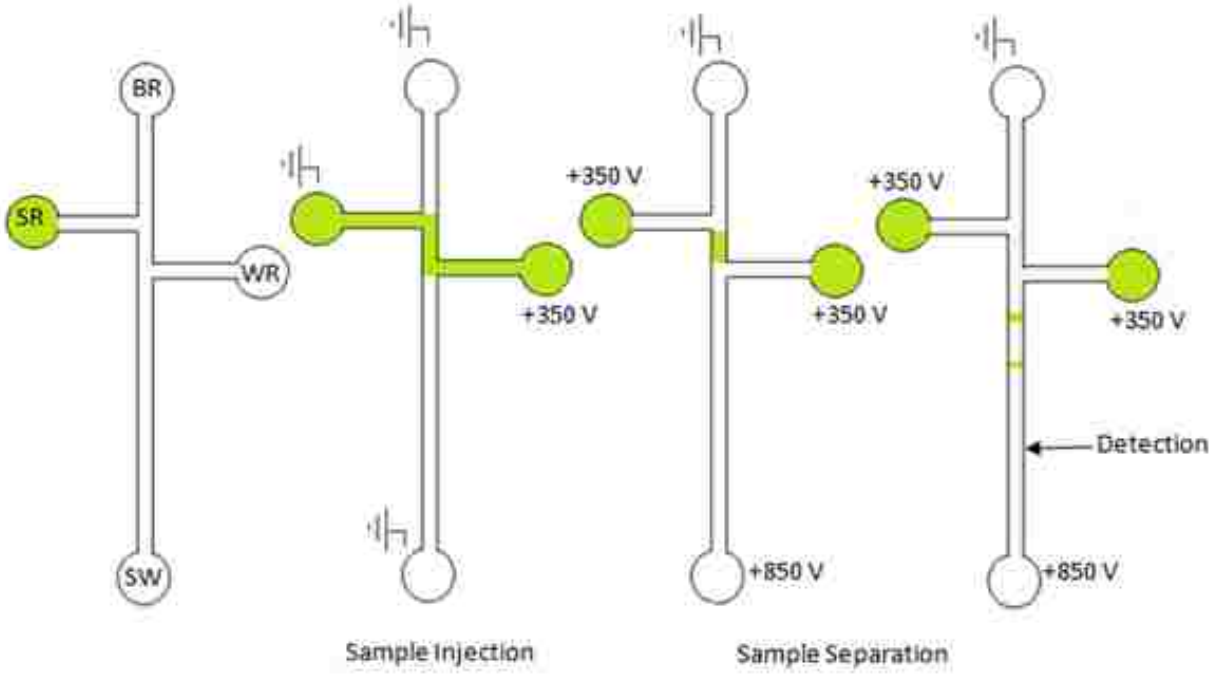

Figure 1.3 Schematic of voltage configuration for pinched injection. SR sample reservoir, BR buffer reservoir, WR waste reservoir, SW separation waste.

Laser induced fluorescence (LIF) detection was used in the experiments described in the succeeding chapters. Figure 1.4 illustrates a simplified schematic of the detection system. The diode laser excites the fluorescent molecules as they pass through the detection point. The emitted light passes through the dichroic mirror and is detected by the photomultiplier tube. The

quantity of photons that reach the detector is converted to an electrical signal that is then processed by LabView software on a computer.

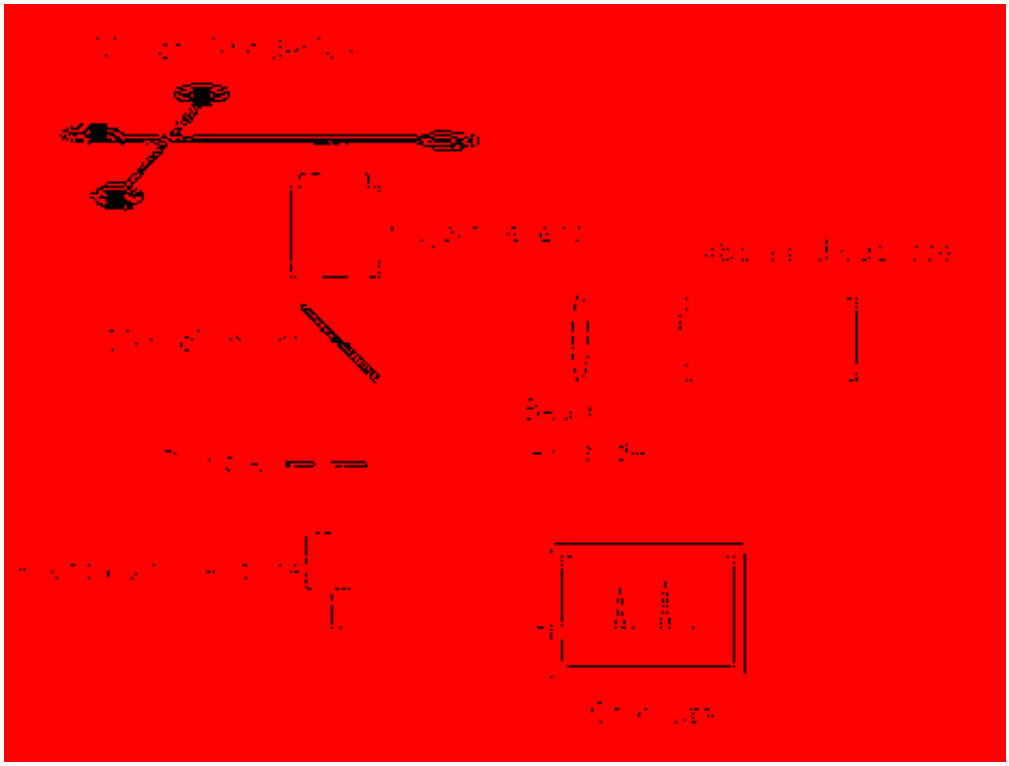

Figure 1.4 Schematic of laser induced fluorescence detection system.

1.4 RECENT ADVANCES IN MICROCHIP ELECTROPHORESIS OF BIOMARKERS

1.4.1 Introduction

Clinical diagnostics need to detect biological molecules that are disease indicators (biomarkers) in complex bodily fluidic samples. Thousands of biomarkers have been reported in literature, and nearly 100 of these are used in regular clinical practice.[18] ME is a promising technology that is being developed and tested for biomarker detection in clinical samples such as urine, serum, cerebrospinal fluid, and saliva. Application of different separation principles, such as isotachophoresis, capillary zone electrophoresis and micellar electrokinetic chromatography in

ME has been explored, resulting in improved separations. Use of different detection methods such as UV absorption, fluorescence, chemiluminescence, and electrochemistry allows analyses of different biomarkers. The following sections discuss various clinical biomarkers tested using ME including lipids, carbohydrates, nucleic acids, and proteins.

1.4.2 Lipids

In this section I discuss ME methods for assaying different classes of lipids including lipoproteins, cholesterol and phospholipid biomarkers. Lipoproteins are macromolecular complexes of lipids and globular proteins held together by hydrophobic and electrostatic interactions. Lipoproteins are involved in transport of lipids; and atherosclerosis, coronary heart disease, liver dysfunction and cancer are all associated with lipoproteins.[19-22] These complexes can be classified as high density lipoprotein (HDL), low density lipoprotein (LDL) or very low density lipoprotein (VLDL). Common methods of lipoprotein analysis are ultracentrifugation, enzymatic assays, nuclear magnetic resonance, and size exclusion chromatography.[23-25]

Cholesterol is an important marker for assessing risk for cardiovascular conditions such as atherosclerosis and hypertension. Total cholesterol detection using ME in poly(dimethylsiloxane) (PDMS) devices was reported by Ruecha et al.[26] Amperometric detection was used to quantify the total cholesterol by monitoring the reaction of cholesterol with cholesterol oxidase enzyme. Separation and detection of cholesterol and an interfering species (ascorbic acid) using ME resulted in reliable quantitation. The detection limit for cholesterol in serum without sample preparation was 1 nM, well below clinical levels, and the limit of quantitation was 1 μM. Sample stacking was achieved by diluting serum in water instead of separation buffer, and analysis took less than 100 seconds.

Fractionation into subclasses of lipoproteins can give a better understanding of the physiological condition of a patient. Wang et al.[27] described ME separation of two protein subclasses (large buoyant LDL and small, dense LDL) using a PDMS/glass microfluidic device. Modifying the channel surface with β-D-maltoside and adding hydroxypropyl cellulose in the running buffer achieved optimum separation. This combination of surface modification and sieving matrix enabled separation of fluorescently labeled HDL and the two LDL subclasses within 3 minutes. The optimized separation conditions were tested for the analysis of serum of patient before and after treatment with atorvastatin. The results showed a significant decrease in the quantity of short, dense LDL after treatment, indicating a possible prognostic application of ME.

Phospholipids are susceptible to reactive oxygen species (ROS); indeed, peroxidation of phospholipid arachidonyl residues by ROS generates prostaglandins, a complex group of biomarkers found in various biofluids.[28] Isoprostanes, a subset of prostaglandins, are a ROS indicator in cardiovascular disease.[29] Because lipids tend to aggregate in aqueous solutions typically used for electrophoretic separations, Gibson and Bohn[30] described a method for characterization of lipids using non-aqueous ME that could be applied to lipid biomarker detection. With their buffer system composed of a tetraalkylammonium salt in N-methylformamide, they observed that the separation of 3 model lipids depended on the voltage and timing of the injection pulse, the background electrolyte concentration, and the electric field strength. As expected, the number of theoretical plates increased with electric field and decreased with background electrolyte concentration. Separation of lipid mixtures was achieved with high resolution (>5) and theoretical plate counts in excess of 7.7×10^6 plates/m.

These recent results show that ME is an attractive alternative to traditional methods such as ultracentrifugation for lipid determination. Such microchip methods offer fast analysis, low sample consumption, and sufficient sensitivity for clinical application.

1.4.3 Carbohydrates

Glycosylation, the addition of a carbohydrate moiety, is a post-translational modification that affects the function of proteins; for example, carbohydrates expressed on the surface of cells vary in structural complexity. Understanding the significance and the function of these modifications requires robust methods for their characterization and quantitation. The most common method of analysis of glycoproteins is by mass spectrometry. Glycoproteins are often treated enzymatically to release the polysaccharides, which can be further cleaved into monosaccharides.[31, 32] Mass spectrometry is a powerful tool for carbohydrate analysis but is less well suited for point-of-care diagnostics. ME is an alternative to mass spectrometry that is a much better fit with point-of-care assays.

Mitra et al.[33] described electrophoretic analysis of N-glycans from RNase B and glycoproteins in the blood sera of an ovarian cancer patient and a disease-free individual using glass microchips with asymmetrically tapered turns that reduced dispersion. The plate count was 940,000 for a 36-cm channel and 600,000 for a 22-cm channel. The microchip devices were used to analyze both native and desialylated N-glycans. Isomer separation of mannose 7 and mannose 8 was observed in the longer (36 cm) but not in the shorter (22 cm) channels. The asymmetrically tapered turn geometry improved over the spiral geommetry reported earlier by Zhuang et al.[34] for separation of N-glycans that resulted in 400,000 to 655,000 plates. In both

designs, increasing the electric field from 75 V/cm to 1250 V/cm resulted in an increase in resolution, as well as a reduction of the analysis time.

Monosaccharides with similar structure, molecular weight and electric charge are difficult to separate. Nagata et al.[35] demonstrated the use of a discontinuous pH buffer system for the separation of neutral and amino monosaccharides. Stacking was achieved by using pH 6.0 borate solution for the sample buffer and pH 9.3 Tris-borate for the separation buffer. The sensitivity was improved by a factor of 65 compared to results in a continuous buffer system.

ME offers a simple and potentially less costly alternative to mass spectrometric analysis of carbohydrates, which could increase understanding of glycosylation that is implicated to different diseases. Importantly, ME allows the complexity of carbohydrate structure to be effectively resolved by manipulating the buffer conditions and geometry of the microfluidic devices.

1.4.4 Nucleic Acids

DNA and RNA analyses are important in disease diagnosis, forensics, and drug screening. Traditionally, fragments of nucleic acids are amplified through PCR and then analyzed. Reagents used in these processes can be expensive; therefore miniaturization of nucleic acid analysis is beneficial for clinical diagnostics. Sample preparation, PCR and electrophoresis can also be integrated using microfluidics resulting in a real lab on a chip.

Clinical genotyping is becoming important especially with the paradigm shift toward personalized medicine.[36] For example, warfarin is a common oral anticoagulant medication that is one of the top 20 most commonly prescribed medications in the US; however, the dosage of this drug to obtain a therapeutic effect varies among individuals.[37] Proper dosage is vital because

an incorrect dosage can have adverse effects and in extreme cases be fatal. Genotyping for warfarin dosage using a single PCR reaction and subsequent ME was reported by Poe et al.[38] By using microchip PCR, the amplification time was reduced to 30 minutes from 45 minutes with benchtop PCR, and the complete assay, combining PCR with ME, took only 60 minutes. The assay determined the patient's genotype using a tetraprimer amplification refractory mutation system in a single reaction. This reduction in reagent and sample consumption using microfluidics could enable low-cost genotyping for warfarin and other genotype-sensitive medications.

Multiplex PCR is commonly used to quickly detect aberrations in DNA sequences of large genes, such as short tandem repeat DNA sequences that have a repetitive unit of 1-6 base pairs and can be used to study polymorphisms or mutation rates important for forensic analysis and identification of genetic diseases.[39] Conventionally, PCR products from multiplex PCR are probed using a Southern blot that can take several hours to yield results. Also, in some cases quantitative analysis of the PCR products is necessary for a diagnosis, which is difficult to achieve via Southern blotting. Le Roux et al.[40] developed a prototype of an integrated microchip for multiplex PCR amplification and electrophoresis. They showed baseline separation of a 10 allele ladder with comparable separation results to a conventional benchtop PCR system. The valve less plastic microchip devices they used had an effective separation length of 7 cm. Under optimized separation conditions they were able to discriminate short tandem repeats having two-base or single-base differences. They also showed consistency of results over time and even when devices were transferred from one laboratory to another. These results suggest the possibility of using portable integrated PCR-ME devices without the need to calibrate before use.

These integrated microchips for multiplex PCR could be used in clinical analysis or personalized medicine.

1.4.5 Proteins

Enzyme linked immunosorbent assay and western blot analysis are commonly used methods as serological tests for different diseases such as HIV and hepatitis B. However, these methods take hours and require multiple processing steps. Furthermore, traditional on-plate assay or membrane analysis requires reagents that increase the cost. In western blot analysis, membrane processing is a slow step that may take at least one hour. An integrated ME system with western blotting developed by Jin et al.[41] reduced the time to 22-32 min for a complete immunoassay. They tested this system on a number of proteins, including actin, carbonic anhydrase and lysozyme. Proteins were detected at concentrations as low as 10 nM. Furthermore, with an increase to 9 samples in one membrane, the analysis time decreased to 6 min/sample. Integrating multiple channels in the microfluidic devices could result in still higher throughput analyses.

Single-cell protein analysis is an important step to elucidate cell signaling and determine cell heterogeneity, for example in drug discovery and cancer studies.[42] Hughes et al.[43] demonstrated single-cell western blotting in microfluidic devices made from a microscope slide coated with a thin, photoactive polyacrylamide gel. Cell lysis and western blotting were performed in situ. Proteins released from lysed neural stem cells were electrophoresed and immobilized on the polyacrylamide gel before probing with fluorescent antibodies for multiple differentiation markers. Kang et al.[44] further tested the application of these devices to study the heterogeneity of cells within a tumor and assess the response of tumor cells to a chemotherapeutic drug. The whole system consisted of single cell imaging, cell lysis, polyacrylamide gel electrophoresis, UV

crosslinking of proteins onto the gel and target probing with fluorescent antibodies. This system allowed correlation of cell phenotype to proteomic profile. They tested this set-up to study drug resistance of a glioblastoma cell line and were able to analyze up to 30 cells/min. This approach may become a valuable tool to identify small populations of drug resistant cells within a tumor that are currently difficult to identify using conventional methods.

One of the agreed upon hallmarks of etiology of Alzhiemer's disease is the accumulation of β-amyloid peptides in amyloid plaques found in cerebrospinal fluid (CSF), blood and urine.[45] However, detection of these peptides in blood and urine is more difficult because their concentrations are 10-100 times smaller than in CSF (1 to 10 ng/mL). Mohamadi et al.[46] described a two-step microchip analysis of five different β-amyloid peptides from CSF in PDMS devices. To enrich the target analytes, they performed immunocapture in a microchip and labeled the eluted analytes with fluorescent dye. They found that β-amyloid 42 could be detected by ME, but baseline separation of the five β-amyloids was not successfully achieved in purified samples or CSF samples. However, analysis of markers in CSF was obtained within 150 seconds. They also found that preconcentration of CSF was a necessary step to be able to detect the amyloid peptides. This detection method shows a promising application of ME in detecting Alzheimer's disease.

Haptoglobin (Hp) binds to hemoglobin released by dead red blood cells, and this complex is then transported to the liver for recycling. Thus, Hp testing is often done to determine how fast red blood cells are destroyed. Common methods for detecting haptoglobin phenotypes are based on electrophoretic separation using a polyacrylamide gel, but this method requires both separation and staining for detection.[47] Different Hp phenotypes have recently been shown to

have association with diseases: the Hp 2-2 phenotype is correlated with higher risk of developing refractory hypertension and schizophrenia;[48, 49] in contrast, Hp 2-2 appears to have protective benefit while Hp 1-1 increases the risk for cervical cancer. Huang et al.[50] tested ME for Hp phenotyping and showed that fluorescently labeled Hp from a liver cancer patient's serum had lower Hp 2-2 levels compared to normal serum. Hp was only clearly detected in serum upon depletion of the abundant human serum albumin and immunoglobulins. The analysis of processed serum took only 150 s by ME, while 400 s were needed for conventional capillary electrophoresis. Low cost, short separation time and sufficient sensitivity are the advantages of ME for the detection of diseases associated with haptoglobin.

In clinical diagnostics, selective detection of target biomarkers in complex biological samples is necessary for an accurate diagnosis. Often, immunoaffinity columns are utilized to purify and concentrate biomarkers, especially for low abundance ones.[51] Biological samples such as CSF and tissue biopsies are typically obtained only in limited amounts and also require sample preparation before analysis. Thus, developing microfluidic analysis of quantity-limited samples would be advantageous.

As one example, dermatological diseases like atopic dermatitis may require lesion biopsy and immunochemical analysis to determine if the lesion is caused by infiltrating neutrophils leading to clinical inflammation or by infiltrating T-cells suggesting prolonged associated inflammation. Kalish et al.[52] analyzed 6 μm diameter frozen biopsy sections from atopic dermatitis lesions for the presence of 5 chemokines by using an integrated microchip immunoaffinity capillary electrophoresis system. Only 200 nL of tissue homogenate with a total protein concentration of 1 μg/mL was used for analysis. The immunoaffinity disks allowed specific extraction of

biomarkers and the succeeding ME separation enabled quantification and confirmation of specificity. Quantifying the chemokines from the biopsy allowed the two types of clinically relevant allergic skin lesions to be distinguished. This method is advantageous over traditional immunoassays, because it uses a small sample volume so it is well suited for detection of disease biomarkers from skin biopsies. The integrated device demonstrates the promise of analyzing complex tissue homogenates.

ME has been combined with several common biochemical analysis methods such as western blot and immunoaffinity. Biomarkers from varied, complex specimens can be analyzed using ME, providing lower sample and reagent consumption as attractive advantages for clinical analysis of limited samples.

1.4.6 Conclusions about applications of microchip electrophoresis to biomarkers

ME has been demonstrated to be applicable for analysis of different biomarkers including lipids, carbohydrates, nucleic acids and proteins. The various materials available for fabricating microfluidic devices make it possible to use aqueous or non-aqueous buffers suitable for analysis of different biomarkers. Interfacing with different detection systems also expands the versatility and sensitivity of ME for various biomarkers. Finally, the relatively simple fabrication of these devices makes it easy to design layouts that can be adapted to various analyses.

Integration of multiple processes in a single microfluidic device offers totally automated sample analysis that may be applicable for clinical laboratories and point-of-care diagnostics. Recognition of the benefits offered by this technology no doubt played a key role in the development of commercial ME platforms offered by companies such as Agilent, BioRad and Bio-Techne. However, these commercial systems are still expensive and benchtop, rather than

point of care. Furthermore, validation of assays for clinically relevant biomarkers is needed for this technology to be widely used in clinical laboratories or point-of-care diagnostics.

The study and modification of the surface chemistry of materials used for microfluidic devices should improve control of the physical phenomena that affect electrophoresis and lead to more reproducible and predictable results. Further characterization of the effects of device layouts and engineering designs should shed additional light on the effects of channel dimensions and geometry on fluid dynamics and assays. Advances in fabrication methods can further decrease the channel dimensions and ease the integration of processes and electronics needed for automated analysis. Miniaturization and improved packaging of detection systems such as optical and electrochemical ones would move a step closer to complete lab-on-a-chip systems. Such advances should lead to low-cost, portable, sensitive and fast tools for analyzing clinical biomarkers from biological fluids or biopsies.

1.5 SURFACE MODIFICATION

1.5.1 Introduction

Surface modification is one of the factors manipulated for target analyte extraction or improved separation by suppressing non-specific adsorption and modulation of EOF. One of the challenges in analysis of complex biological samples such as blood is the non-specific adsorption of proteins on the channel wall. The focus of this section is to briefly discuss stable and dynamic coatings for surface modifications that demonstrate ability to inhibit nonspecific adsorption and provide uniform EOF for ME. Doherty et al.[53] gave an excellent detailed review on microchannel wall coatings.

1.5.2 Methods of surface modification

1.5.2.1 Stable Modification

Stable surface modification with biocompatible layers such as poly(ethylene glycol) (PEG) reduces nonspecific adsorption of biomolecules. There are four common strategies used in stable surface modification. Layer-by layer film deposition involves sequential deposition of polyelectrolyte to modify the surface charge that reduce nonspecific adsorption and resulted in EOF independent of pH.[54] Click chemistry is a covalent modification that results in robust and selective chemical reactions using azides that has been applied in glass microfluidic devices.[55] Atom transfer radical polymerization employs a metal catalyst such as copper to immobilize hydrophilic polymers on different surfaces.[56] Grafting utilizes the active site on the surface of the channels to covalently bond hydrophilic polymer or ligand on UV-activated microfluidic channel surfaces.[57-59] These modification processes remain stable at varying pH and over multiple runs. However, the tedious processes employed in stable surface modification spur the exploration of different dynamic coatings.

1.5.2.2 Dynamic Coating

Polymer microfluidic devices are hindered by the problem of sample adsorption.[60] This non-specific adsorption results in reduced reproducibility and separation efficiency.[61] Different water-soluble surfactants such as sodium dodecyl sulfate (SDS),[62] cellulose-based polymers,[63] and PEG[64] have been used as buffer additives that act as dynamic coatings. Increasing the concentration of the polymers to their entanglement point can also provide a sieving matrix that can improve separation efficiency.[64-66] The ease of this method decreases the device preparation time and still produces acceptable separation efficiency and reproducibility.

1.6 MONOLITHS

Monoliths are a single piece of a porous particle that are widely being studied as solid supports for liquid chromatography[67] and for miniaturized systems such as capillary electrophoresis and ME.[68] The advantages of low back pressure, ease of fabrication, lower dead volume and faster mass transfer make monoliths an attractive alternative to columns made of packed beads.[69] Monoliths have been developed into affinity columns using various substrates such as agarose,[70] methacrylates,[71] and silica.[72] Detailed optimization of fabrication processes for monolithic columns in microchips will be discussed in chapter 4.

1.7 IMMUNOASSAYS

Immunoassays are commonly used in clinical diagnostics and rely on the formation of an antigen-antibody complex to determine the presence or absence of the antigen of interest. The principles regarding immunoassays are the same in the traditional 96-well plate enzyme linked immunosorbent assay (ELISA) (see Figure 1.5) or in the microarray immunoassays. First, antigens are immobilized on the solid support. Primary antibodies conjugated to enzymes are used to probe for the presence of antigens. The most commonly used enzyme to visualize bound antibodies is horseradish peroxidase (HRP). The HRP/peroxide system oxidizes 3,5,3′,5′-tetramethylbenzidine (TMB), to 3,5,3′,5′-tetramethylbenzidine diimine, and subsequently the reaction can be halted by addition of acidic buffer.[73]

Antibodies contain antigen binding sites (F_{ab}) that bind to specific or multiple epitopes on the antigen. This complex formation is reversible. According to the law of mass action (see equation 1.4), at equilibrium, the ratio between the concentration of the product ([*complex*]) and

the reactants ([*antigen*] and [*antibody*]) is constant. The equilibrium constant, K_{eq}, is equal to the ratio between the association (k_a) and dissociation (k_d) rate constants.

$$\frac{[complex]}{[antigen]*[antibody]} = \frac{k_a}{k_d} = K_{eq} \qquad (1.4)$$

From the equation, complex formation can be improved by increasing the concentrations of the antigen and antibody, or increasing the equilibrium constant; for example, a stronger bond results in a higher equilibrium constant. The forces that govern the interaction of F_{ab} and epitope include Van der Waals, electrostatic, ion dipole, and hydrophobic interactions.[74] Antigen-antibody complex formation is affected by several factors such as pH, temperature, and ionic strength.

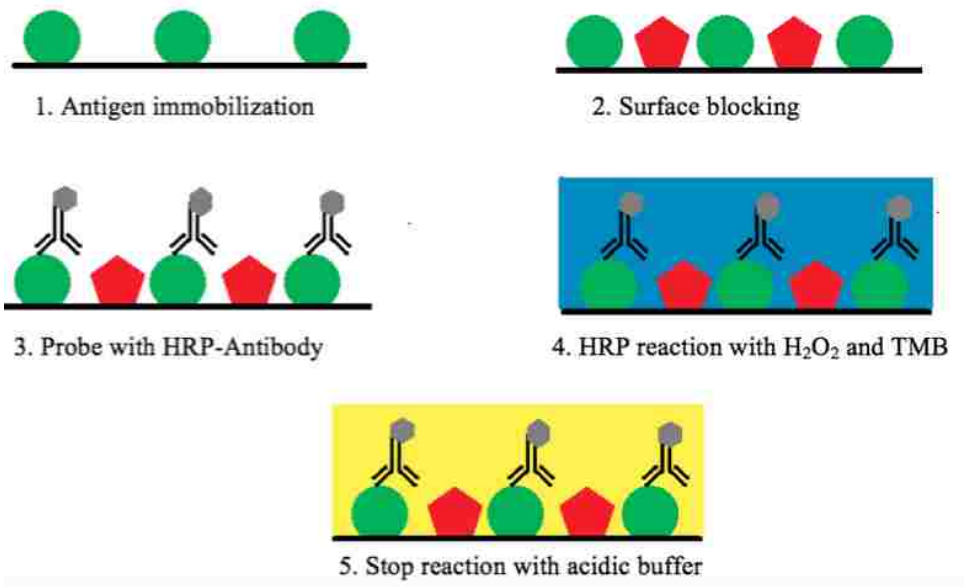

Figure 1.5 Direct ELISA.

The amino acids involved in antigen-antibody interaction can be protonated or deprotonated depending on their isoelectric point. Extreme pH values induce conformational changes to the antibody or the antigen that destroy the complementarity of the antigen and

antibody binding sites.[75] The optimum temperature depends on the weak bonds involved in the interaction as well as the chemical nature of the epitope and the paratope, which is the part of the F_{ab} region that recognizes the antigen. For example, hydrogen bonds are more stable at low temperature.[76] At increasing temperature, the protein conformation changes and more hydrophobic regions are exposed; therefore, hydrophobic interaction increases with temperature.[77] Ionic strength, the concentration of ions in a solution, can affect the availability of the paratopes and epitope to interact due to the interaction of ions with the charged groups of the proteins. A study on an antibody against blood group antigen D revealed that decreasing the ionic strength of the buffer resulted in increased rate of association.[78] These factors have to be considered carefully when designing immunoassays, and condition optimization for each antibody used in an experiment must be done to ensure reliable results.

1.8 CANCER BIOMARKERS

1.8.1 Introduction

Biomarkers are measurable molecular indicators of normal biological processes, pathological processes or a pharmacological response to a therapeutic agent. Biomarkers are obtained from tissue samples and biological fluids such as blood, urine, and saliva. For a biomarker to be accepted for clinical use, several characteristics must be assessed. It should have high sensitivity, accurately-a high true positive rate, and specificity, accurately-a high true negative rate. Two potential biomarkers I studied were thymidine kinase 1 (TK1) and interleukin 8 (IL8).

1.8.2 Thymidine Kinase 1

Thymidine kinase is an enzyme involved in the DNA salvage pathway. There are two isoenzymes of thymidine kinase, cytosolic TK (TK1) and mitochondrial TK (TK2). TK1 is cell-cycle dependent while TK2 is constitutively expressed.[79] Thymidine kinase 1 has been reported to be elevated in serum of cancer patients.[80] TK1 activity is regulated by post-transcriptional and post-translational mechanisms. The precise function of TK1 is still not fully understood since many TK1 deficient cells grow normally in culture, though research suggests that TK1 is important for precise fine-tuning of the pool size of dTTP, an allosteric regulator of the mammalian ribonucleotide reductase.[79,81] It also catalyzes the phosphorylation of deoxythymidine, coverting it to deoxythymidine monophosphate (dTMP). The monomer of human TK1 has a reported molecular weight of 25-30 kD and the oligomeric form has a molecular weight of up to 96 kD.[82] It has been found in breast cancer patients that the serum level of TK1 has no correlation with the TK1 activity,[83] and others have reported that different isoforms of TK1 have different activity.[84] Therefore, analysis of TK1 is not straightforward. The enzymatic activity at different isoforms could be used to better understand the diagnostic value of TK1 for cancer detection.

1.8.3 Interleukin 8

IL8 is a chemokine associated with chemotaxis and degranulation of neutrophils.[85] It activates multiple signaling pathways downstream of two G-protein coupled receptors, CXCR1 and CXCR2.[86] One of the results of the activation of these receptors is the increased activation of Akt, a serine/threonine-specific protein kinase, which has a role in modulating cell survival, angiogenesis and cell migration.[87] In 2005, IL8 was first reported to be elevated in saliva, 86 pM,

of oropharyngeal squamous cell carcinoma cases compared to healthy individuals, 30 pM.[88] Analysis of biomarkers from saliva could offer a non-invasive solution for routine diagnosis and would be compatible with point-of-care diagnostics.

1.9 OVERVIEW OF DISSERTATION

The focus of my dissertation is on development of immunoassays for cancer markers in microfluidic devices. This dissertation is divided into six chapters. In this chapter, I have discussed microfluidic device fabrication, principles of ME, including operation and detection; recent advancements in the last five years in ME of potential clinical biomarkers; surface modification; monolith columns; principles of immunoassays; and cancer biomarkers, TK1 and IL8.

In chapter 2, I describe development of a microchip immunoassay for detection of recombinant thymidine kinase 1 in microchip devices. I describe the selection of appropriate buffer conditions for immune complex formation and separation. I also explore the effects of different molecular weights of methylcellulose as a dynamic coating and sieving matrix.

Chapter 3 focuses on determining the appropriate protein depletion method to concentrate low concentrations of endogenous TK1 in serum. Two candidate monoclonal antibodies, mouse anti-TK1 and rabbit anti-TK1, which both exhibit specificity to purified recombinant TK1, were tested for binding to endogenous TK1 in cancer and normal serum samples. I verified my results using several biochemical techniques such as native and denatured western blots, ELISA and kinase activity assay. The results showed that, under conditions described in the analyses,

rabbit-TK1 bound to both endogenous and purified recombinant TK1 (pTK1) while the mouse-TK1 exhibited detectable binding only to pTK1.

Chapter 4 describes a strategy for optimization of monolith composition using bulk polymerization and scanning electron microscopy. The addition of Tween-20 in the monolith solution resulted in more porous monolithic columns that are compatible with electrokinetic injection and integration with ME. This method allowed multiple monolith solution comparisons without the need to initially in situ fabricate the monolith in microchip devices as was previously done. Other students have successfully adapted this process to develop reverse phase monolithic columns.[89, 90]

Chapter 5 describes the development of the optimized monolithic columns into affinity columns. I also detail the processes involved to immobilize active antibody in integrated monolithic columns. Preliminary results showed the ability of an integrated monolithic column to extract IL8 from buffer and spiked-saliva samples.

Conclusions and future work will be discussed in Chapter 6.

1.10 REFERENCES

1. Harrison, D. J.; Manz, A.; Fan, Z. H.; Ludi, H.; Widmer, H. M., Capillary Electrophoresis and Sample Injection Systems Integrated on a Planar Glass Chip. *Anal Chem* **1992,** *64* (17), 1926-1932.

2. Gordon, J.; Michel, G., Discerning trends in multiplex immunoassay technology with potential for resource-limited settings. *Clinical chemistry* **2012,** *58* (4), 690-8.

3. van der Meel, R.; Krawczyk-Durka, M.; van Solinge, W. W.; Schiffelers, R. M., Toward routine detection of extracellular vesicles in clinical samples. *International journal of laboratory hematology* **2014,** *36* (3), 244-53.

4. Yang, Z.; Sweedler, J. V., Application of capillary electrophoresis for the early diagnosis of cancer. *Analytical and bioanalytical chemistry* **2014,** *406* (17), 4013-31.

5. Jokerst, J. C.; Emory, J. M.; Henry, C. S., Advances in microfluidics for environmental analysis. *The Analyst* **2012,** *137* (1), 24-34.

6. Kenyon, S. M.; Meighan, M. M.; Hayes, M. A., Recent developments in electrophoretic separations on microfluidic devices. *Electrophoresis* **2011,** *32* (5), 482-93.

7. Kelly, R. T.; Woolley, A. T., Thermal bonding of polymeric capillary electrophoresis microdevices in water. *Anal Chem* **2003,** *75* (8), 1941-1945.

8. Wang, Y.; Lin, Q.; Mukherjee, T., A model for Joule heating-induced dispersion in microchip electrophoresis. *Lab Chip* **2004,** *4* (6), 625-631.

9. Guihen, E., Recent advances in miniaturization-The role of microchip electrophoresis in clinical analysis. *Electrophoresis* **2014,** *35* (1), 138-146.

10. Henry, C. S., Microchip Capillary Electrophoresis: An Introduction. In *Microchip Capillary Electrophoresis: Methods and Protocols*, Henry, C. S., Ed. Humana Press: Totowa, New Jersey, 2006; Vol. 339, pp 1-9.

11. Kirby, B. J.; Hasselbrink, E. F., Zeta potential of microfluidic substrates: 1. Theory, experimental techniques, and effects on separations. *Electrophoresis* **2004,** *25* (2), 187-202.

12. Fernandez-Abedul, M. T.; Alvarez-Martos, I.; Alonso, F. J. G.; Costa-Gracia, A., Improving the Separation in Microchip Electrophoresis by Surface Modification. In *Capillary Electrophoresis and Microchip Capillary Electrophoresis Principles Applications and Limitations*, Garcia, C. D.; Chumbimuni-Torres, K. Y.; Carrilho, E., Eds. John Wiley & Sons, Inc: Hoboken, New Jersey, 2013; pp 95-120.

13. Fu, L. M.; Yang, R. J.; Lee, G. B.; Liu, H. H., Electrokinetic injection techniques in microfluidic chips. *Anal Chem* **2002,** *74* (19), 5084-5091.

14. Yu, M.; Wang, Q. S.; Patterson, J. E.; Woolley, A. T., Multilayer Polymer Microchip Capillary Array Electrophoresis Devices with Integrated On-Chip Labeling for High-Throughput Protein Analysis. *Anal Chem* **2011,** *83* (9), 3541-3547.

15. Gong, M. J.; Wehmeyer, K. R.; Stalcup, A. M.; Limbach, P. A.; Heineman, W. R., Study of injection bias in a simple hydrodynamic injection in microchip CE. *Electrophoresis* **2007,** *28* (10), 1564-1571.

16. Jacobson, S. C.; Hergenroder, R.; Koutny, L. B.; Warmack, R. J.; Ramsey, J. M., Effects of Injection Schemes and Column Geometry on the Performance of Microchip Electrophoresis Devices. *Anal Chem* **1994,** *66* (7), 1107-1113.

17. Slentz, B. E.; Penner, N. A.; Regnier, F., Sampling BIAS at channel junctions in gated flow injection on chips. *Anal Chem* **2002,** *74* (18), 4835-4840.

18. Mohammed, M. I.; Desmulliez, M. P., Lab-on-a-chip based immunosensor principles and technologies for the detection of cardiac biomarkers: a review. *Lab Chip* **2011,** *11* (4), 569-95.

19. Berneis, K.; Jeanneret, C.; Muser, E.; Felix, B.; Miserez, A. R., Low-density lipoprotein size and subclasses are markers of clinically apparent and non-apparent atherosclerosis in type 2 diabetes. *Metabolism* **2005,** *54* (2), 227-234.

20. Hopewell, J. C.; Seedorf, U.; Farrall, M.; Parish, S.; Kyriakou, T.; Goel, A.; Hamsten, A.; Collins, R.; Watkins, H.; Clarke, R.; Consortium, P., Impact of lipoprotein(a) levels and apolipoprotein(a) isoform size on risk of coronary heart disease. *J Intern Med* **2014,** *276* (3), 260-268.

21. DeFilippis, A. P.; Blaha, M. J.; Martin, S. S.; Reed, R. M.; Jones, S. R.; Nasir, K.; Blumenthal, R. S.; Budoff, M. J., Nonalcoholic fatty liver disease and serum lipoproteins: The Multi-Ethnic Study of Atherosclerosis. *Atherosclerosis* **2013,** *227* (2), 429-436.

22. Llanos, A. A.; Makambi, K. H.; Tucker, C. A.; Wallington, S. F.; Shields, P. G.; Adams-Campbell, L. L., Cholesterol, Lipoproteins, and Breast Cancer Risk in African American Women. *Ethnic Dis* **2012,** *22* (3), 281-287.

23. Williams, P. T.; Zhao, X. Q.; Marcovina, S. M.; Otvos, J. D.; Brown, B. G.; Krauss, R. M., Comparison of four methods of analysis of lipoprotein particle subfractions for their association with angiographic progression of coronary artery disease. *Atherosclerosis* **2014,** *233* (2), 713-720.

24. Garber, D. W.; Kulkarni, K. R.; Anantharamaiah, G. M., A sensitive and convenient method for lipoprotein profile analysis of individual mouse plasma samples. *J Lipid Res* **2000,** *41* (6), 1020-1026.

25. Otvos, J. D.; Jeyarajah, E. J.; Bennett, D. W.; Krauss, R. M., Development of a Proton Nuclear-Magnetic-Resonance Spectroscopic Method for Determining Plasma-Lipoprotein

Concentrations and Subspecies Distributions from a Single, Rapid Measurement. *Clinical chemistry* **1992,** *38* (9), 1632-1638.

26. Ruecha, N.; Siangproh, W.; Chailapakul, O., A fast and highly sensitive detection of cholesterol using polymer microfluidic devices and amperometric system. *Talanta* **2011,** *84* (5), 1323-1328.

27. Wang, H.; Wang, D. X.; Wang, J. C.; Wang, H. M.; Gu, J.; Han, C. X.; Jin, Q. H.; Xu, B. J.; He, C.; Cao, L.; Wang, Y.; Zhao, J. L., Application of poly(dimethylsiloxane)/glass microchip for fast electrophoretic separation of serum small, dense low-density lipoprotein. *J Chromatogr A* **2009,** *1216* (35), 6343-6347.

28. Tyurin, V. A.; Tyurina, Y. Y.; Borisenko, G. G.; Sokolova, T. V.; Ritov, V. B.; Quinn, P. J.; Rose, M.; Kochanek, P.; Graham, S. H.; Kagan, V. E., Oxidative stress following traumatic brain injury in rats: Quantitation of biomarkers and detection of free radical intermediates. *J Neurochem* **2000,** *75* (5), 2178-2189.

29. Cracowski, J. L.; Ormezzano, O., Isoprostanes, emerging biomarkers and potential mediators in cardiovascular diseases. *European heart journal* **2004,** *25* (19), 1675-8.

30. Gibson, L. R.; Bohn, P. W., Non-aqueous microchip electrophoresis for characterization of lipid biomarkers. *Interface Focus* **2013,** *3* (3), 20120096.

31. Leymarie, N.; Griffin, P. J.; Jonscher, K.; Kolarich, D.; Orlando, R.; McComb, M.; Zaia, J.; Aguilan, J.; Alley, W. R.; Altmann, F.; Ball, L. E.; Basumallick, L.; Bazemore-Walker, C. R.; Behnken, H.; Blank, M. A.; Brown, K. J.; Bunz, S. C.; Cairo, C. W.; Cipollo, J. F.; Daneshfar, R.; Desaire, H.; Drake, R. R.; Go, E. P.; Goldman, R.; Gruber, C.; Halim, A.; Hathout, Y.; Hensbergen, P. J.; Horn, D. M.; Hurum, D.; Jabs, W.; Larson, G.; Ly, M.; Mann, B. F.; Marx,

K.; Mechref, Y.; Meyer, B.; Moginger, U.; Neusubeta, C.; Nilsson, J.; Novotny, M. V.; Nyalwidhe, J. O.; Packer, N. H.; Pompach, P.; Reiz, B.; Resemann, A.; Rohrer, J. S.; Ruthenbeck, A.; Sanda, M.; Schulz, J. M.; Schweiger-Hufnagel, U.; Sihlbom, C.; Song, E.; Staples, G. O.; Suckau, D.; Tang, H.; Thaysen-Andersen, M.; Viner, R. I.; An, Y.; Valmu, L.; Wada, Y.; Watson, M.; Windwarder, M.; Whittal, R.; Wuhrer, M.; Zhu, Y.; Zou, C., Interlaboratory study on differential analysis of protein glycosylation by mass spectrometry: the ABRF glycoprotein research multi-institutional study 2012. *Molecular & cellular proteomics : MCP* **2013,** *12* (10), 2935-51.

32. Morelle, W.; Michalski, J. C., Analysis of protein glycosylation by mass spectrometry. *Nature protocols* **2007,** *2* (7), 1585-602.

33. Mitra, I.; Alley, W. R.; Goetz, J. A.; Vasseur, J. A.; Novotny, M. V.; Jacobson, S. C., Comparative Profiling of N-Glycans Isolated from Serum Samples of Ovarian Cancer Patients and Analyzed by Microchip Electrophoresis. *J Proteome Res* **2013,** *12* (10), 4490-4496.

34. Zhuang, Z.; Starkey, J. A.; Mechref, Y.; Novotny, M. V.; Jacobson, S. C., Electrophoretic analysis of N-glycans on microfluidic devices. *Anal Chem* **2007,** *79* (18), 7170-7175.

35. Nagata, H.; Itoh, T.; Baba, Y.; Ishikawa, M., Highly Sensitive Detection of Monosaccharides on Microchip Electrophoresis Using pH Discontinuous Solution System. *Anal Sci* **2010,** *26* (7), 731-736.

36. Sadee, W.; Dai, Z. Y., Pharmacogenetics/genomics and personalized medicine. *Hum Mol Genet* **2005,** *14*, R207-R214.

37. Pirmohamed, M., Warfarin: almost 60 years old and still causing problems. *Brit J Clin Pharmaco* **2006,** *62* (5), 509-511.

38. Poe, B. L.; Haverstick, D. M.; Landers, J. P., Warfarin Genotyping in a Single PCR Reaction for Microchip Electrophoresis. *Clinical chemistry* **2012,** *58* (4), 725-731.

39. Madsen, B. E.; Villesen, P.; Wiuf, C., Short tandem repeats in human exons: A target for disease mutations. *Bmc Genomics* **2008,** *9* (410 doi:10.1186/1471-2164-9-410).

40. Le Roux, D.; Root, B. E.; Hickey, J. A.; Scott, O. N.; Tsuei, A.; Li, J.; Saul, D. J.; Chassagne, L.; Landers, J. P.; de Mazancourt, P., An integrated sample-in-answer-out microfluidic chip for rapid human identification by STR analysis. *Lab Chip* **2014,** *14* (22), 4415-25.

41. Jin, S.; Anderson, G. J.; Kennedy, R. T., Western Blotting Using Microchip Electrophoresis Interfaced to a Protein Capture Membrane. *Anal Chem* **2013,** *85* (12), 6073-6079.

42. Wang, D. J.; Bodovitz, S., Single cell analysis: the new frontier in 'omics'. *Trends Biotechnol* **2010,** *28* (6), 281-290.

43. Hughes, A. J.; Spelke, D. P.; Xu, Z. C.; Kang, C. C.; Schaffer, D. V.; Herr, A. E., Single-cell western blotting. *Nat Methods* **2014,** *11* (7), 749-U94.

44. Kang, C. C.; Lin, J. M. G.; Xu, Z. C.; Kumar, S.; Herr, A. E., Single-Cell Western Blotting after Whole-Cell Imaging to Assess Cancer Chemotherapeutic Response. *Anal Chem* **2014,** *86* (20), 10429-10436.

45. Murphy, M. P.; LeVine, H., 3rd, Alzheimer's disease and the amyloid-beta peptide. *Journal of Alzheimer's disease : JAD* **2010,** *19* (1), 311-23.

46. Mohamadi, M. R.; Svobodova, Z.; Verpillot, R.; Esselmann, H.; Wiltfang, J.; Otto, M.; Taverna, M.; Bilkova, Z.; Viovy, J. L., Microchip electrophoresis profiling of A beta peptides in the cerebrospinal fluid of patients with Alzheimer's disease. *Anal Chem* **2010,** *82* (18), 7611-7.

47. Soejima, M.; Koda, Y., TaqMan-Based Real-Time PCR for Genotyping Common Polymorphisms of Haptoglobin (HP1 and HP2). *Clinical chemistry* **2008,** *54* (11), 1908-1913.

48. Maes, M.; Delanghe, J.; Bocchio Chiavetto, L.; Bignotti, S.; Tura, G. B.; Pioli, R.; Zanardini, R.; Altamura, C. A., Haptoglobin polymorphism and schizophrenia: genetic variation on chromosome 16. *Psychiatry research* **2001,** *104* (1), 1-9.

49. Hochberg, I.; Roguin, A.; Nikolsky, E.; Chanderashekhar, P. V.; Cohen, S.; Levy, A. P., Haptoglobin phenotype and coronary artery collaterals in diabetic patients. *Atherosclerosis* **2002,** *161* (2), 441-6.

50. Huang, B.; Huang, C.; Liu, P.; Wang, F.; Na, N.; Ouyang, J., Fast haptoglobin phenotyping based on microchip electrophoresis. *Talanta* **2011,** *85* (1), 333-8.

51. Whiteaker, J. R.; Zhao, L.; Anderson, L.; Paulovich, A. G., An Automated and Multiplexed Method for High Throughput Peptide Immunoaffinity Enrichment and Multiple Reaction Monitoring Mass Spectrometry-based Quantification of Protein Biomarkers. *Molecular & Cellular Proteomics* **2010,** *9* (1), 184-196.

52. Kalish, H.; Phillips, T. M., Assessment of chemokine profiles in human skin biopsies by an immunoaffinity capillary electrophoresis chip. *Methods* **2012,** *56* (2), 198-203.

53. Doherty, E. A. S.; Meagher, R. J.; Albarghouthi, M. N.; Barron, A. E., Microchannel wall coatings for protein separations by capillary and chip electrophoresis. *Electrophoresis* **2003,** *24* (1-2), 34-54.

54. Currie, C. A.; Shim, J. S.; Lee, S. H.; Ahn, C.; Limbach, P. A.; Halsall, H. B.; Heineman, W. R., Comparing polyelectrolyte multilayer-coated PMMA microfluidic devices and glass microchips for electrophoretic separations. *Electrophoresis* **2009,** *30* (24), 4245-4250.

55. Prakash, S.; Long, T. M.; Selby, J. C.; Moore, J. S.; Shannon, M. A., "Click" modification of silica surfaces and glass microfluidic channels. *Anal Chem* **2007,** *79* (4), 1661-1667.

56. Sun, X. F.; Liu, J. K.; Lee, M. L., Surface modification of polymer microfluidic devices using in-channel atom transfer radical polymerization. *Electrophoresis* **2008,** *29* (13), 2760-2767.

57. Kovach, K. M.; Capadona, J. R.; Sen Gupta, A.; Potkay, J. A., The effects of PEG-based surface modification of PDMS microchannels on long-term hemocompatibility. *J Biomed Mater Res A* **2014,** *102* (12), 4195-4205.

58. Jackson, J. M.; Witek, M. A.; Hupert, M. L.; Brady, C.; Pullagurla, S.; Kamande, J.; Aufforth, R. D.; Tignanelli, C. J.; Torphy, R. J.; Yeh, J. J.; Soper, S. A., UV activation of polymeric high aspect ratio microstructures: ramifications in antibody surface loading for circulating tumor cell selection. *Lab Chip* **2014,** *14* (1), 106-117.

59. Hu, S. W.; Ren, X. Q.; Bachman, M.; Sims, C. E.; Li, G. P.; Allbritton, N., Surface modification of poly(dimethylsiloxane) microfluidic devices by ultraviolet polymer grafting. *Anal Chem* **2002,** *74* (16), 4117-4123.

60. Le, N. C. H.; Gubala, V.; Gandhiraman, R. P.; Daniels, S.; Williams, D. E., Evaluation of Different Nonspecific Binding Blocking Agents Deposited Inside Poly(methyl methacrylate) Microfluidic Flow-Cells. *Langmuir* **2011,** *27* (14), 9043-9051.

61. Bi, H. Y.; Meng, S.; Li, Y.; Guo, K.; Chen, Y. P.; Kong, J. L.; Yang, P. Y.; Zhong, W.; Liu, B. H., Deposition of PEG onto PMMA microchannel surface to minimize nonspecific adsorption. *Lab Chip* **2006,** *6* (6), 769-775.

62. Nagata, H.; Tabuchi, M.; Hirano, K.; Baba, Y., Microchip electrophoretic protein separation using electroosmotic flow induced by dynamic sodium dodecyl sulfate-coating of uncoated plastic chips. *Electrophoresis* **2005,** *26* (11), 2247-2253.

63. Mohamadi, M. R.; Mahmoudian, L.; Kaji, N.; Tokeshi, M.; Baba, Y., Dynamic coating using methylcellulose and polysorbate 20 for nondenaturing electrophoresis of proteins on plastic microchips. *Electrophoresis* **2007,** *28* (5), 830-836.

64. Takahashi, T.; Kawana, J.; Tamura, Y.; Hoshino, H., Dynamic Coating Capillary Electrophoresis for Separation of Humic Acid Using Mixture Solution of Non-ionic Polymers both as Coating Agent and Separation Medium. *Anal Sci* **2013,** *29* (11), 1099-1102.

65. Sanders, J. C.; Breadmore, M. C.; Kwok, Y. C.; Horsman, K. M.; Landers, J. P., Hydroxypropyl cellulose as an adsorptive coating sieving matrix for DNA separations: Artificial neural network optimization for microchip analysis. *Anal Chem* **2003,** *75* (4), 986-994.

66. Mohamadi, M. R.; Kaji, N.; Tokeshi, M.; Baba, Y., Online preconcentration by transient isotachophoresis in linear polymer on a poly(methyl methacrylate) microchip for separation of human serum albumin immunoassay mixtures. *Anal Chem* **2007,** *79* (10), 3667-3672.

67. Guiochon, G., Monolithic columns in high-performance liquid chromatography. *J Chromatogr A* **2007,** *1168* (1-2), 101-168.

68. Faure, K.; Bias, M.; Yassine, O.; Delaunay, N.; Cretier, G.; Albert, M.; Rocca, J. L., Electrochromatography in poly(dimethyl)siloxane microchips using organic monolithic stationary phases. *Electrophoresis* **2007,** *28* (11), 1668-1673.

69. Moliner-Martinez, Y.; Molins-Legua, C.; Verdu-Andres, J.; Herraez-Hernandez, R.; Campins-Falco, P., Advantages of monolithic over particulate columns for multiresidue analysis of organic pollutants by in-tube solid-phase microextraction coupled to capillary liquid chromatography. *J Chromatogr A* **2011,** *1218* (37), 6256-6262.

70. Sun, S. J.; Tang, Y. H.; Fu, Q.; Liu, X.; Du, W.; Guo, L. A.; Zhao, Y. D., Preparation of agarose/chitosan composite supermacroporous monolithic cryogels for affinity purification of glycoproteins. *J Sep Sci* **2012,** *35* (7), 893-900.

71. Uzun, L.; Say, R.; Denizli, A., Porous poly(hydroxyethyl methacrylate) based monolith as a new adsorbent for affinity chromatography. *React Funct Polym* **2005,** *64* (2), 93-102.

72. Li, Q. J.; Lu, C. C.; Li, H. Y.; Liu, Y. C.; Wang, H. Y.; Wang, X.; Liu, Z., Preparation of organic-silica hybrid boronate affinity monolithic column for the specific capture and separation of cis-diol containing compounds. *J Chromatogr A* **2012,** *1256*, 114-120.

73. Josephy, P. D.; Eling, T.; Mason, R. P., The Horseradish Peroxidase-Catalyzed Oxidation of 3,5,3',5'-Tetramethylbenzidine - Free-Radical and Charge-Transfer Complex Intermediates. *J Biol Chem* **1982,** *257* (7), 3669-3675.

74. Reverberi, R.; Reverberi, L., Factors affecting the antigen-antibody reaction. *Blood transfusion = Trasfusione del sangue* **2007,** *5* (4), 227-40.

75. Barnes, A. E., The specificity of pH and ionic strength effects on the kinetics of the Rh (D)-anti-Rh (D) system. *Journal of immunology* **1966,** *96* (5), 854-64.

76. Chaplin, M. Water's hydrogen bond strength, cond-mat/0706.1355 2007.

77. Chen, W. Y.; Huang, H. M.; Lin, C. C.; Lin, F. Y.; Chan, Y. C., Effect of temperature on hydrophobic interaction between proteins and hydrophobic adsorbents: Studies by isothermal titration calorimetry and the van't Hoff equation. *Langmuir* **2003,** *19* (22), 9395-9403.

78. Hunges-Jones, N. C.; Gardner, B.; Telford, R., The Effect of pH and Ionic Strength on the Reaction between Anti-D and Erythrocytes. *Immunology* **1964,** *7* (1), 72-81.

79. Munch-Petersen, B.; Cloos, L.; Jensen, H. K.; Tyrsted, G., Human Thymidine Kinase-1 - Regulation in Normal and Malignant-Cells. *Adv Enzyme Regul* **1995,** *35*, 69-89.

80. Konoplev, S. N.; Fritsche, H. A.; O'Brien, S.; Wierda, W. G.; Keating, M. J.; Garnet, T. G.; St Romain, S.; Wang, X. M.; Inamdar, K.; Johnson, M. R.; Medeiros, L. J.; Bueso-Ramos, C. E., High Serum Thymidine Kinase 1 Level Predicts Poorer Survival in Patients With Chronic Lymphocytic Leukemia. *Am J Clin Pathol* **2010,** *134* (3), 472-477.

81. Thelander, L.; Reichard, P., Reduction of Ribonucleotides. *Annu Rev Biochem* **1979,** *48*, 133-158.

82. Tsukifuji-Nabeya, R.; Yusa, T.; Kuroiwa, N.; Kumazawa, T.; Tamiya, N.; Moriyama, Y.; Okamoto, S.; Yamaguchi, Y.; Fujimura, S., Characterization of the purified cytosolic thymidine kinase from murine Ehrlich ascites tumor: Interconversion of two different relative molecular weight forms. *Biochem Mol Biol Int* **1996,** *40* (2), 379-388.

83. He, Q.; Zou, L.; Zhang, P. A.; Liu, J. X.; Skog, S.; Fornander, T., The clinical significance of thymidine kinase 1 measurement in serum of breast cancer patients using anti-TK1 antibody. *Int J Biol Marker* **2000,** *15* (2), 139-146.

84. Munch-Petersen, B.; Tyrsted, G.; Cloos, L., Reversible Atp-Dependent Transition between 2 Forms of Human Cytosolic Thymidine Kinase with Different Enzymatic-Properties. *J Biol Chem* **1993,** *268* (21), 15621-15625.

85. Harada, A.; Sekido, N.; Akahoshi, T.; Wada, T.; Mukaida, N.; Matsushima, K., Essential Involvement of Interleukin-8 (IL8) in Acute-Inflammation. *J Leukocyte Biol* **1994,** *56* (5), 559-564.

86. Waugh, D. J. J.; Wilson, C., The Interleukin-8 Pathway in Cancer. *Clin Cancer Res* **2008,** *14* (21), 6735-6741.

87. Knall, C.; Worthen, G. S.; Johnson, G. L., Interleukin 8-stimulated phosphatidylinositol-3-kinase activity regulates the migration of human neutrophils independent of extracellular signal-regulated kinase and p38 mitogen-activated protein kinases. *P Natl Acad Sci USA* **1997,** *94* (7), 3052-3057.

88. Yang, C. Y.; Brooks, E.; Li, Y.; Denny, P.; Ho, C. M.; Qi, F. X.; Shi, W. Y.; Wolinsky, L.; Wu, B.; Wong, D. T. W.; Montemagno, C. D., Detection of picomolar levels of interleukin-8 in human saliva by SPR. *Lab Chip* **2005,** *5* (10), 1017-1023.

89. Nge, P. N.; Pagaduan, J. V.; Yu, M.; Woolley, A. T., Microfluidic chips with reversed-phase monoliths for solid phase extraction and on-chip labeling. *J Chromatogr A* **2012,** *1261*, 129-135.

90. Yang, R.; Pagaduan, J. V.; Yu, M.; Woolley, A. T., On chip preconcentration and fluorescence labeling of model proteins by use of monolithic columns: device fabrication, optimization, and automation. *Analytical and bioanalytical chemistry* **2015,** *407* (3), 737-747.

CHAPTER 2: MICROCHIP IMMUNOAFFINITY ELECTROPHORESIS OF ANTIBODY-THYMIDINE KINASE 1 COMPLEX*

2.1 INTRODUCTION

Molecular diagnostics focuses on the accurate detection of biochemical markers of diseases. Often, blood samples are drawn from the patient and biomarkers are measured to identify the disease state. The usage of biomarkers can be a more effective way of detecting cancer at an early stage compared to tissue biopsy alone.[1] Cancer biomarkers often indicate disruption of the regular cell-signaling pattern resulting in resistance to cell death, uncontrolled proliferation, invasion, metastasis, and activation of angiogenesis.[2]

Thymidine kinase is an important nucleotide salvage pathway enzyme involved specifically in the conversion of thymidine to thymidine monophosphate.[3] There are two types of thymidine kinase in the cell: thymidine kinase-1 (TK1) is found in the cytosol and is cell cycle regulated; the other, thymidine kinase-2, is found in the mitochondria and is constitutively expressed.[4] The mechanism of release of TK1 into the serum is not fully understood, but TK1 concentration in serum is higher in cancer patients than in healthy individuals.[5-7]

Typically, radioimmunoassay is used to detect TK1 activity in serum,[8] and enzyme-linked immunoassay (ELISA) is used to determine TK1 concentration.[5] Previous reports indicate that TK1 activity and TK1 concentration are not closely correlated.[6] Another finding showed that

---

* This chapter is reproduced with permission from Pagaduan, J.V.; Ramsden, M.; O'Neill, K.; Woolley, A.T. *Electrophoresis* **2015**, 36, 813-817

TK1 was commonly expressed in its dimeric form and that addition of ATP to the solution resulted in tetramer formation.[9] The tetrameric TK1 also had more catalytic activity than the dimeric form, which is a possible explanation for the discrepancy in TK1 activity and concentration in cancer patients.[6]

A novel antibody that specifically targets TK1 was developed, tested and reported by O'Neill et al.[10] They demonstrated through ELISA, immunohistochemistry and western blot results that the antibody has the ability to detect purified recombinant TK1 (pTK1) and cytosolic TK1 in clinical samples. These classical techniques are sensitive (ng/mL to pg/mL); however, they are time consuming. A possible alternative to detecting TK1 activity (to eliminate the use of radioactive material) is through determining the quantity of each isoform of TK1 since the isoforms correlate with enzymatic activity. Development of an inexpensive, fast, and accurate diagnostic assay for TK1 isoforms and concentration could thus hasten the accurate detection of disease state.

Microchip electrophoresis has been used in separation of different clinically relevant biomolecules because it has many advantages over traditional methods such as use of small sample volumes, fast analysis, low cost, portability and disposability. Virtually all fluorescent tags used in on-plate immunoassays can be used in microchip electrophoresis to improve sensitivity if appropriate laser wavelengths and filters are also incorporated in the detection system. Microchip electrophoresis can be high throughput by changing the design to include multiple lanes but still maintain low sample and reagent consumption and faster analysis compared to on-plate immunoassay.[11] Integration of photopolymerized cross-linked polyacrylamide gels in microfluidic devices has been used for separation of immune

complexes.[12, 13] As an alternative to photopolymerization of gels, buffers with cellulose-based polymers or linear polyacrylamide as dynamic coatings and sieving matrices have been developed.[14-16] Different cellulose sieving matrices were successfully used for genomic and proteomic analysis.[17] The ability of methylcellulose to effectively suppress electroosmotic flow and stabilize the pH gradient allowed efficient isoelectric focusing on a microchip.[18] Electrophoresis in microdevices with hydrophilic polymer sieving matrices and coatings is thus an attractive potential platform for quantifying TK1.

In the present study I report the use of a monoclonal anti-TK1 antibody[10] to detect immune complexes with as low as 80 nM TK1 using microchip electrophoresis. I used FITC-labeled anti-TK1 antibodies to monitor the formation of the immune complex. I explored the effect of commonly used buffers on immune complex formation and found a strong buffer dependence. I also studied the effect of buffer viscosity on the separation and peak shape. After identifying an appropriate buffer and sieving matrix I was able to develop an easy to perform microchip electrophoresis assay of Ab-TK1 complexes. This approach could potentially be adapted for detecting TK1 in serum for early diagnosis of cancer or its recurrence.

2.2 EXPERIMENTAL SECTON

2.2.1 Materials and Reagents.

Methylcellulose (MC) of different molecular weights (14000, 41000, and 88000 Da) was purchased from Sigma-Aldrich (St Louis, MO). Tween 20 was acquired from Mallinckrodt Baker (Paris KY). Sodium chloride came from Columbus Chemical (Columbus, WI). Tris-base

and 10x phosphate buffer saline were from Fisher Scientific (Fair Lawn, NJ). Boric acid, glycine and hydrochloric acid were obtained from EMD Chemical (Gibbstown, NJ). Fluorescein isothiocyanate (FITC) and ethylenediaminetetraacetic acid (EDTA) were purchased from Life Technologies (Carlsbad, CA). Centrifugal filters were from Millipore (Billerica, MA). Poly(methyl methacrylate) (PMMA) substrates were purchased from Evonik (Parsippany, NJ). All solutions were made using deionized water, 18.3 MΩ.

2.2.2 Buffer preparation. 1% MC solutions were prepared as recommended by the manufacturer. Briefly, MC was first dissolved in deionized water at 80°C, and then the corresponding buffer volume was added to the solution. Cold deionized water (~4°C) was next added up to the required volume and the solution was stored at 4°C for 1 hour. The buffer was then agitated at room temperature for at least 1 hour, resulting in a clear and viscous solution. All buffer solutions had Tween-20 added to 0.01% and were stored at room temperature after preparation.

2.2.3 Device Fabrication. PMMA microchips were fabricated using adaptations of protocols reported previously.[19] Silicon templates were made in the BYU Integrated Microfabrication Lab using standard photolithography techniques to provide elevated channel features (20 μm tall, 50 μm wide) in a T design**.** Microchannel features were hot embossed onto 1.5 mm thick PMMA sheets (2 x 5 cm^2) for 30 minutes at 138°C. 3-mm thick PMMA sheets (2 x 5 cm^2) with laser-cut reservoirs were thermally bonded as cover plates for 27 minutes at 110°C to enclose the microfluidic channels.

2.2.4 Sample Preparation. Mouse anti-human TK1 monoclonal antibodies[10] were conjugated with FITC as described previously.[20] Excess FITC was removed using Amicon Ultra-0.5 centrifugal filters (30 kDa). Concentrations of the stock antibody were measured to be 1 mg/mL using a Nanodrop ND-1000 spectrophotometer (Nanodrop Technologies, Wilmington, DE). FITC-conjugated antibodies were tested for TK1 binding using dot blots on nitrocellulose membranes. Labeled antibodies were stored in 1X PBS at 4°C. Human recombinant purified TK1 was obtained from Genscript (Piscataway, NJ). Full length human TK1 was expressed with a histidine tag, which was used for purification and then subsequently cleaved.

2.2.5 Contact Angle Measurement. MC (1% w/v) was prepared in 20 mM Tris-HCl buffer. PMMA sheets (2 x 2 cm^2) were washed with deionized water and dried with nitrogen. MC solutions (1 mL) were then placed on one side of a PMMA sheet and incubated for 30 minutes; then excess solution was completely removed by blowing using nitrogen flow. A 10 µL drop of deionized water was placed on the surface, and the static contact angle was immediately measured using a goniometer (Rame-Hart, Succasunna, NJ). Three contact angle measurements were used to measure standard deviation and average.

2.2.6 Device Operation. Separations were done with "pinched" injection,[20] using +350 V as the intermediate potential and +850 V as the high voltage. A laser-induced fluorescence system coupled with an inverted confocal microscope and a photomultiplier tube was used for detection, as reported previously.[21] The data were collected at 20 Hz using software written in LabView.

2.3 RESULTS AND DISCUSSION

One of the challenges in using PMMA for microfluidics is its hydrophobicity that affects reproducibility in separation of proteins.[22] Cellulose-based polymer dynamic coatings are effective at inhibiting the nonspecific adsorption of proteins in polymer microfluidic devices by increasing the hydrophilicity of the surface.[23] Three different molecular weight MCs were evaluated as dynamic coatings. As shown in Table 2.1, treatment of the surface with buffer containing 1% MC of all molecular weights decreased the PMMA contact angle. PMMA treatment with the lowest molecular weight MC (14000 Da) increased the hydrophilicity of the surface the most as indicated by the least contact angle.

Table 2.1 Effect of 1% w/v MC treatment on PMMA surface contact angle.

MC mol wt. (Da)	Contact Angle
No MC	$71.5 \pm 0°$
14000	$16.6 \pm 2.5°$
41000	$30.5 \pm 0.9°$
88000	$33.2 \pm 0.9°$

The choice of buffer affects the formation and stability of immune complexes. Theoretically, the best separation can be achieved by applying high voltage in a buffer having low conductivity. For example Tris-glycine buffer is commonly used for capillary electrophoresis because it has low conductivity and current under high voltage.[24, 25] I tested several common electrophoresis buffers for sample flow by positioning the laser at the channel intersection point and measuring the fluorescence over time when voltage was applied (see Table 2.2). I also observed the current during this process as noted in Table 2.2, with low currents <30 μA and high currents greater than this value. Although the current was low, no sample flow

was observed in channels when Tris-glycine buffer was used, even at potentials up to +1450 V. This could be due to effects of this buffer and/or MC on the mobility. Moreover, I observed that when 1X PBS was used, the current was high and particles were seen under microscope observation inside the microchannels, perhaps due to Joule heating that partially evaporated the solvent, resulting in buffer salt or MC deposits. Both 0.5X PBS and 1X Tris-borate EDTA (TBE, 90 mM) yielded the desirable combination of low current and sample flow when voltage was applied.

Table 2.2 Current and sample flow for different buffers.

Buffer	Sample Flow	Current
1X PBS, pH 7.4	Yes	High
0.5X PBS, pH 7.4	Yes	Low
25 mM Tris-192 mM glycine, pH 8.3	No	Low
90 mM Tris-borate EDTA, pH 8.0	Yes	Low

I noted that separation distance affects the protein peak height and shape. Electropherograms of the anti-TK1 antibody by itself showed that increasing the separation distance to the detection point resulted in peak broadening and a decrease in peak height. Background-subtracted peak height increased as separation distance was decreased from 15 to 10 and 5 mm (Figure 2.1A-C; 0.14, 0.16, and 0.21 units). Peak full width at half maximum (FWHM) also decreased (7.2, 5.5, and 4.7 s) with these same decreasing separation distances.

Previously it has been shown that the choice of buffer can affect immune complex formation.[26] I tested separations in 1X TBE, pH 8.0 with 1% w/v MC-88000. TBE buffer resulted in sharper peaks, but resolution between the anti-TK1 antibody peak and the immune complex peak was not observed (see Figure 2.2). The inability to separate or detect the immune complex under this condition may be due to the instability of the complex at pH 8. As in Figure

2.1, peak broadening was observed with increased separation distance, with FWHMs of 0.15, 0.20, and 0.25 s for 5, 10 and 15 mm separation distances, respectively. Peak height also decreased with increased separation distance (2.4, 0.9, and 0.6 units for 5, 10 and 15 mm, respectively) as was observed in 0.5X PBS (Fig. 2.1). In Figs. 2.1 and 2.2 band broadening with incraseased separation distance is caused by longitudinal diffusion during the longer separation times. In subsequent immunoaffinity separations, where Ab and antigen-Ab complexes are resolved (e.g. Fig. 2.3), additional broadening could occur from greater dissociation of formed antigen-Ab complexes with longer separation times or distances, although these conditions were not studied.

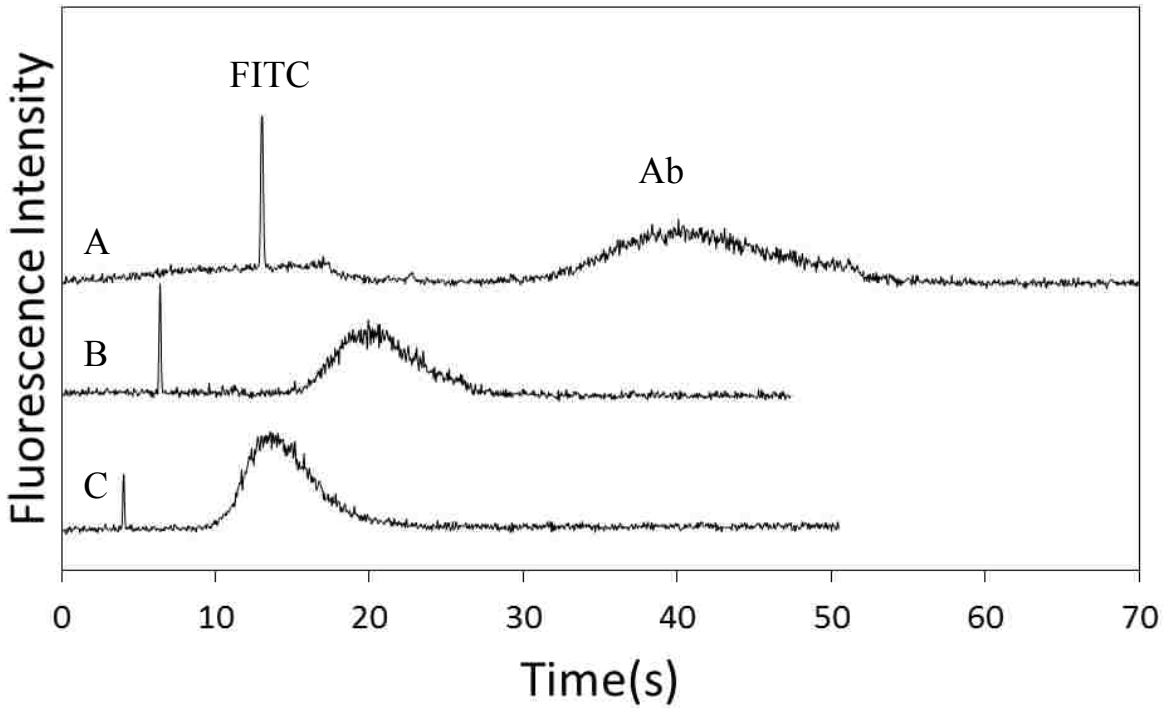

Figure 2.1 Effect of separation distance on peak shape. A decrease in peak intensity and increase in peak broadening were observed as separation distance was increased. Injection was at +350V and separation was at +850V; separation distances are (A) 15, (B) 10, and (C) 5 mm. Electropherograms were offset for clarity.

I observed that 0.5X PBS buffer containing 1% MC-14000 or MC-41000 failed to resolve free anti-TK1 antibody from immune complex (Figure 2.3 A and B), but buffer with 1% MC-88000 resulted in separation of the unbound anti-TK1 antibody from the immune complex (Figure 2.3C). These observations agree with other studies where higher molecular weight MC resulted in better separation.[14, 15, 23] However, with the increased solution viscosity, I had to inject for 60 seconds in MC 41000 and MC 88000 to obtain adequate fluorescence signal, while 30 second injection was enough for buffer with MC 14000. A separation distance of 5 mm was sufficient to resolve the free antibody from the immune complex when 0.5X PBS buffer with 1% MC 88000 was used; moreover, these separations were faster, so I utilized a 5 mm separation

distance in subsequent experiments. Increasing the MC concentration above 1% made it difficult to load the solution into the channel and sometimes resulted in delaminated devices because of backpressure during filling.

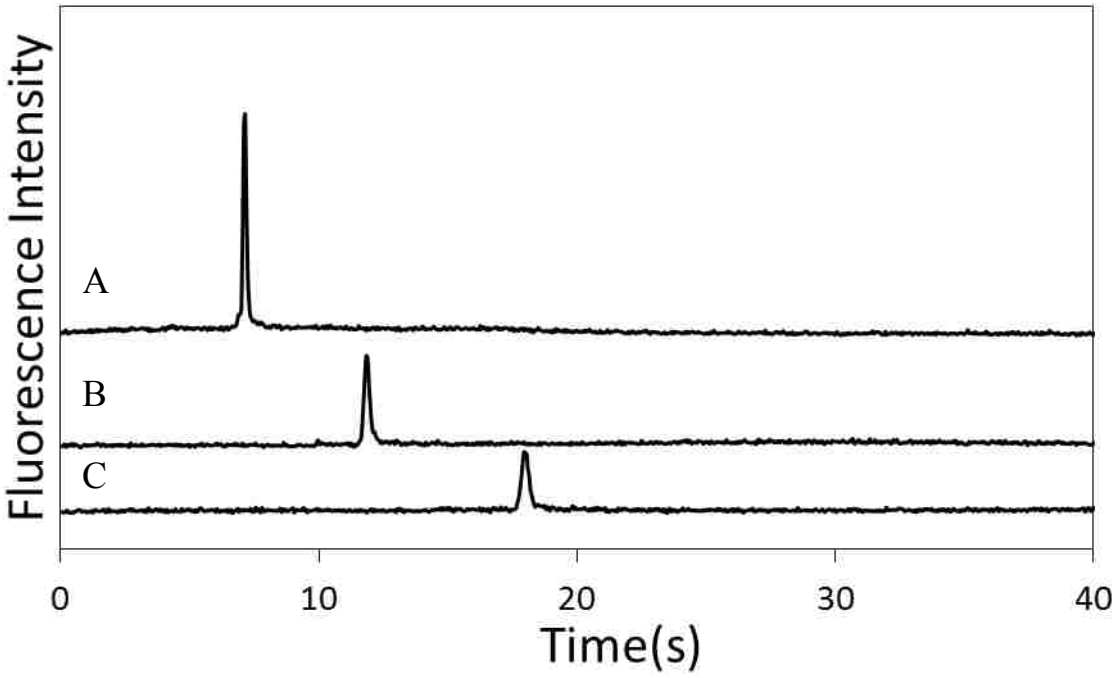

Figure 2.2 Attempted separation of Ab-TK1 complex from free Ab in 1X TBE buffer with different separation distances. A) 5 mm B) 10 mm C) 15 mm. Sample was 25 µg/mL (156 nM) Ab incubated with 25 µg/mL (1 µM) TK1; injection and separation conditions were the same as in Fig. 2.1; electropherograms are offset for clarity.

Using the optimized conditions, I performed microchip electrophoresis of anti-TK1 solutions with increasing pTK1 concentration. Figure 2.4A shows the electropherograms of anti-TK1 incubated with different pTK1 concentrations; I found that the immune complex peak increased as pTK1 concentration was increased. A plot of peak area of the immune complex

correlated with pTK1 concentration (Figure 2.4B). The immune complex peak was observed at pTK1 concentrations above 2 µg/mL (80 nM); I was not able to observe the complex peak when the concentration of pTK1 was lower.

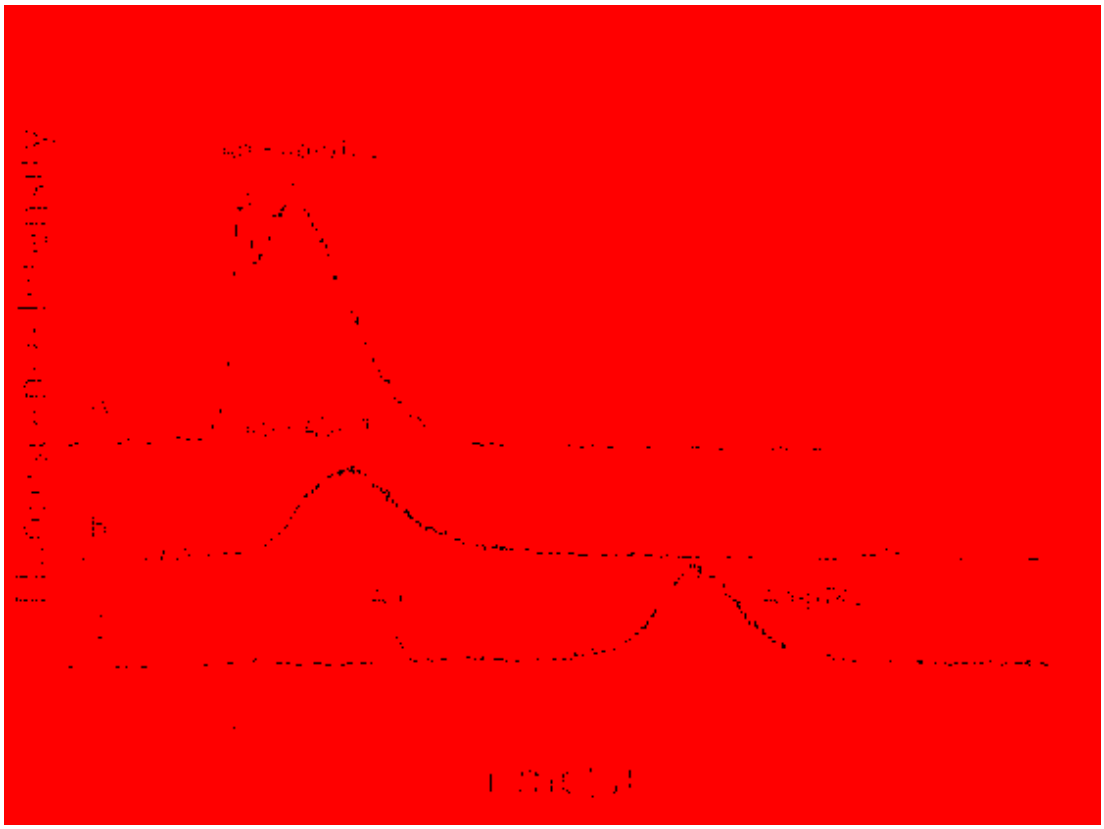

Figure 2.3 Separation of Ab-TK1 complex with different 1% w/v MC additives in 0.5X PBS. A) MC-14000, 30 s injection B) MC-41000, 60 s injection and C) MC-88000, 60 s injection. Samples were 25 µg/mL (156 nM) Ab incubated with 25 µg/mL (1 µM) TK1. injection and separation conditions were the same as in Fig. 2.1; electropherograms are offset for clarity.

The clinical concentration of TK1 in serum of cancer patients varies depending on the type of cancer and can be as low as 2 pM or as high as 50 pM, while the TK1 concentration in healthy individuals is lower than 2 pM,[6] so the detection limit has to be improved for this approach to be used in cancer screening. Several factors that could be explored to lower

detection limits by improving antigen-antibody binding are ionic strength, temperature, and pH. Neutral pH is commonly used for immunoaffinity assays, although research suggests that immobilized monoclonal antibody to antigen binding capacity may improve as pH decreases to ~3.[27] However, not all immune complexes are stable at low pH; further work would be required to investigate this possibility more fully, which is beyond the scope of this paper. I note that fluorescence quenching occurs at low pH with FITC, but other dyes with high quantum yield in low pH solutions could be used.[28] Another important factor to consider when analyzing serum sample is sample processing. Serum is replete with high abundance proteins such as immunoglobulins and human serum albumin that may interfere with antigen-antibody binding. Depletion of these high abundance proteins using a commercial serum depletion kit could be employed prior to microchip electrophoresis. This depletion step could also be incorporated in the design of microchip device to develop a completely automated analysis of serum.

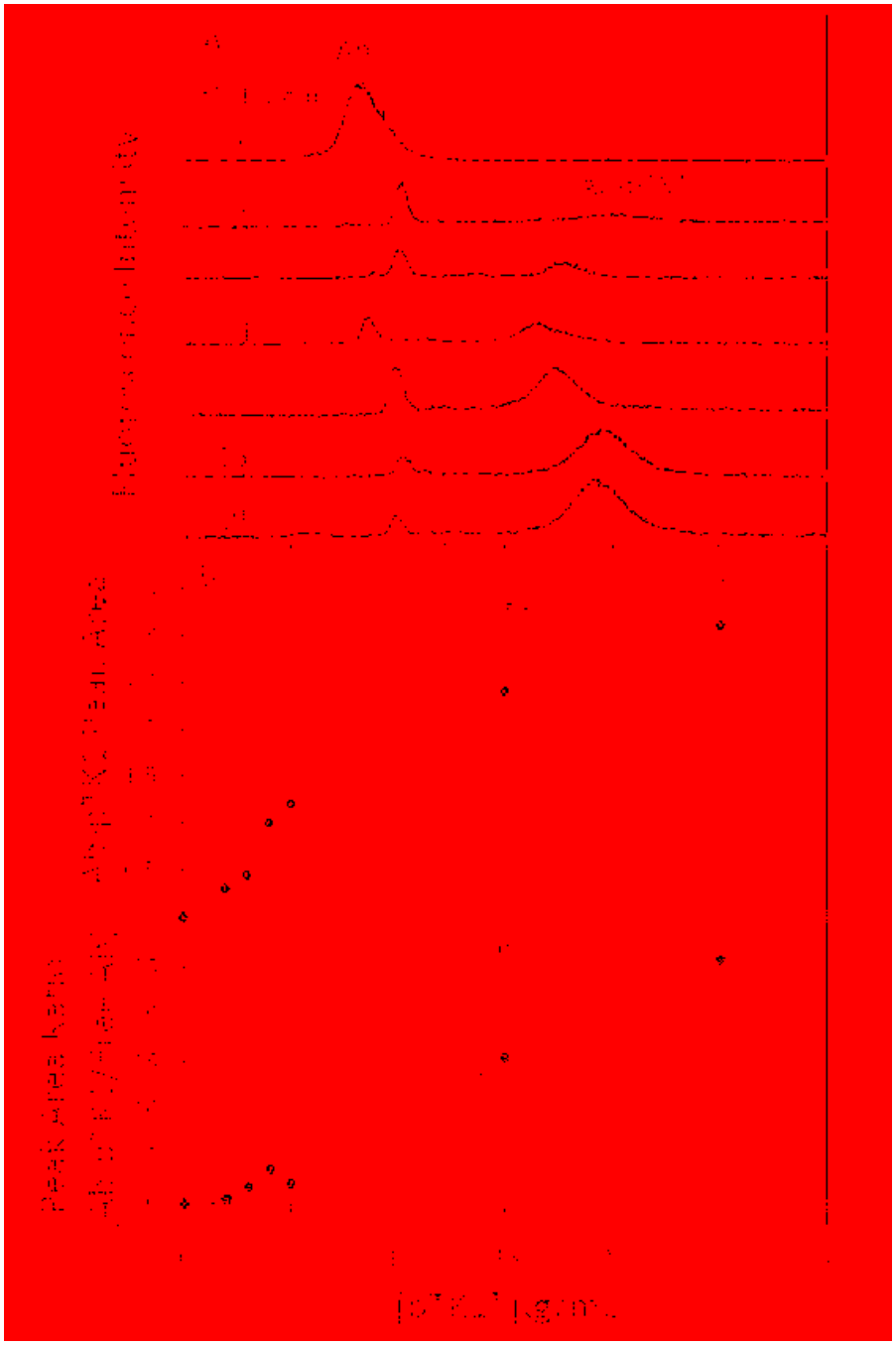

Figure 2.4 Microchip immunoaffinity electrophoresis of pTK1. (A) Increasing pTK1 concentration resulted in increasing immune complex peak size, going from 2-25 μg/mL (0.080-1 μM) pTK1. Injection and separation conditiones are the same as in Figure 2.3 (B) Plot of Ab-pTK1 peak area as a function of pTK1 concentration. Best line fit is $y = 0.123x + 0.26$, $R^2 = 0.94$, $s_m = 0.014$, $s_b = 0.15$ (C) Peak area ratio of complex and free Ab (which accounts for injection differences) $y = 1.085x-1.30$, $R^2 = 0.988$ $s_m = 0.053$ $s_b = 0.60$.

2.4 CONCLUSIONS

I developed a microchip electrophoresis immunoaffinity assay for measuring thymidine kinase-1 using a monoclonal antibody. I have shown that buffer composition and additives affect sample flow, formation of immune complexes, and separation of unbound antibodies from immune complexes. The separation of Ab and Ab-TK1 complex was achieved in 0.5X PBS with 1% methylcellulose (88000 Da). Using optimized conditions I was able to separate the immune complex from free antibody within a 5-mm separation length.

I am currently working on using the optimized conditions to detect TK1 in clinical serum samples. Since I monitor the formation of antibody-antigen complex I may be able to detect the form of TK1, (i.e., dimeric vs tetrameric), based on the electrophoretic mobility of the immune complex. If I can identify TK1 forms in a simple and rapid test, it would be an attractive alternative to RIA.

2.5 REFERENCES

1. Goggins, M., Markers of pancreatic cancer: working toward early detection. *Clinical cancer research : an official journal of the American Association for Cancer Research* **2011,** *17* (4), 635-7.

2. Hanahan, D.; Weinberg, R. A., Hallmarks of cancer: the next generation. *Cell* **2011,** *144* (5), 646-74.

3. Tolson, J.; Bogumil, R.; Brunst, E.; Beck, H.; Elsner, R.; Humeny, A.; Kratzin, H.; Deeg, M.; Kuczyk, M.; Mueller, G. A.; Mueller, C. A.; Flad, T., Serum protein profiling by SELDI

mass spectrometry: detection of multiple variants of serum amyloid alpha in renal cancer patients. *Lab Invest* **2004,** *84* (7), 845-856.

4. Munch-Petersen, B., Enzymatic regulation of cytosolic thymidine kinase 1 and mitochondrial thymidine kinase 2: a mini review. *Nucleos Nucleot Nucl* **2010,** *29* (4-6), 363-9.

5. O'Neill, K. L.; Buckwalter, M. R.; Murray, B. K., Thymidine kinase: diagnostic and prognostic potential. *Expert review of molecular diagnostics* **2001,** *1* (4), 428-33.

6. He, Q.; Zou, L.; Zhang, P. A.; Lui, J. X.; Skog, S.; Fornander, T., The clinical significance of thymidine kinase 1 measurement in serum of breast cancer patients using anti-TK1 antibody. *Int J Biol Markers.* **2000,** *15* (2), 139-46.

7. O'Neill, K. L.; Zhang, F.; Li, H.; Fuja, D. G.; Murray, B. K., Thymidine kinase 1--a prognostic and diagnostic indicator in ALL and AML patients. *Leukemia* **2007,** *21* (3), 560-3.

8. He, Q.; Zhang, P.; Zou, L.; Li, H.; Wang, X.; Zhou, S.; Fornander, T.; Skog, S., Concentration of thymidine kinase 1 in serum (S-TK1) is a more sensitive proliferation marker in human solid tumors than its activity. *Oncology reports* **2005,** *14* (4), 1013-9.

9. Munchpetersen, B.; Tyrsted, G.; Cloos, L., Reversible Atp-Dependent Transition between 2 Forms of Human Cytosolic Thymidine Kinase with Different Enzymatic-Properties. *J. Biol. Chem.* **1993,** *268* (21), 15621-15625.

10. Zhang, F.; Shao, X.; Li, H.; Robison, J. G.; Murray, B. K.; O'Neill, K. L., A monoclonal antibody specific for human thymidine kinase 1. *Hybridoma* **2001,** *20* (1), 25-34.

11. Nge, P. N.; Rogers, C. I.; Woolley, A. T., Advances in microfluidic materials, functions, integration, and applications. *Chemical reviews* **2013,** *113* (4), 2550-83.

12. Herr, A. E.; Hatch, A. V.; Throckmorton, D. J.; Tran, H. M.; Brennan, J. S.; Giannobile, W. V.; Singh, A. K., Microfluidic immunoassays as rapid saliva-based clinical diagnostics. *Proceedings of the National Academy of Sciences of the United States of America* **2007,** *104* (13), 5268-73.

13. Herr, A. E.; Throckmorton, D. J.; Davenport, A. A.; Singh, A. K., On-chip native gel electrophoresis-based immunoassays for tetanus antibody and toxin. *Anal. Chem.* **2005,** *77* (2), 585-90.

14. Mohamadi, M. R.; Mahmoudian, L.; Kaji, N.; Tokeshi, M.; Baba, Y., Dynamic coating using methylcellulose and polysorbate 20 for nondenaturing electrophoresis of proteins on plastic microchips. *Electrophoresis* **2007,** *28* (5), 830-6.

15. Mohamadi, M. R.; Kaji, N.; Tokeshi, M.; Baba, Y., Online preconcentration by transient isotachophoresis in linear polymer on a poly(methyl methacrylate) microchip for separation of human serum albumin immunoassay mixtures. *Anal. Chem.* **2007,** *79* (10), 3667-72.

16. Sun, M.; Lin, J. S.; Barron, A. E., Ultrafast, efficient separations of large-sized dsDNA in a blended polymer matrix by microfluidic chip electrophoresis: a design of experiments approach. *Electrophoresis* **2011,** *32* (22), 3233-40.

17. Jabasini, M.; Murakami, Y.; Kaji, N.; Tokeshi, M.; Baba, Y., Low viscous separation media for genomics and proteomics analysis on microchip electrophoresis system. *Biological & pharmaceutical bulletin* **2006,** *29* (4), 595-604.

18. Cui, H.; Horiuchi, K.; Dutta, P.; Ivory, C. F., Isoelectric focusing in a poly(dimethylsiloxane) microfluidic chip. *Anal. Chem.* **2005,** *77* (5), 1303-9.

19. Yang, W.; Sun, X.; Pan, T.; Woolley, A. T., Affinity monolith preconcentrators for polymer microchip capillary electrophoresis. *Electrophoresis* **2008,** *29* (16), 3429-35.

20. Nge, P. N.; Yang, W.; Pagaduan, J. V.; Woolley, A. T., Ion-permeable membrane for on-chip preconcentration and separation of cancer marker proteins. *Electrophoresis* **2011,** *32* (10), 1133-40.

21. Yu, M.; Wang, H. Y.; Woolley, A. T., Polymer microchip CE of proteins either off- or on-chip labeled with chameleon dye for simplified analysis. *Electrophoresis* **2009,** *30* (24), 4230-6.

22. Nagata, H.; Tabuchi, M.; Hirano, K.; Baba, Y., Microchip electrophoretic protein separation using electroosmotic flow induced by dynamic sodium dodecyl sulfate-coating of uncoated plastic chips. *Electrophoresis* **2005,** *26* (11), 2247-53.

23. Yasui, T.; Reza Mohamadi, M.; Kaji, N.; Okamoto, Y.; Tokeshi, M.; Baba, Y., Characterization of low viscosity polymer solutions for microchip electrophoresis of non-denatured proteins on plastic chips. *Biomicrofluidics* **2011,** *5* (4), 44114-441149.

24. Bean, S. R.; Lookhart, G. L., Faster capillary electrophoresis separation of wheat proteins through modifications to buffer composition and sample handling. *Electrophoresis* **1998,** *19* (18), 3190-8.

25. Gong, M.; Nikcevic, I.; Wehmeyer, K. R.; Limbach, P. A.; Heineman, W. R., Protein-aptamer binding studies using microchip affinity capillary electrophoresis. *Electrophoresis* **2008,** *29* (7), 1415-22.

26. Babar, S. M.; Song, E. J.; Hasan, M. N.; Yoo, Y. S., Experimental design optimization of the capillary electrophoresis separation of leucine enkephalin and its immune complex. *Journal of separation science* **2007,** *30* (14), 2311-9.

27. Tarakanova Iu, N.; Dmitriev, D. A.; Massino Iu, S.; Smirnova, M. B.; Segal, O. L.; Fartushnaia, O. V.; Iakovleva, D. A.; Koliaskina, G. I.; Lavrov, V. F.; Dmitriev, A. D., [Effect of conditions of monoclonal antibody adsorption on antigen-binding activity]. *Appl. Biochem. Microbiol.* **2012,** *48* (5), 557-63.

28. Miksa, M.; Komura, H.; Wu, R.; Shah, K. G.; Wang, P., A novel method to determine the engulfment of apoptotic cells by macrophages using pHrodo succinimidyl ester. *Journal of immunological methods* **2009,** *342* (1-2), 71-7.

CHAPTER 3: COMPARISON OF DIFFERENT PROTEIN DEPLETION METHODS TO IMPROVE THYMIDINE KINASE 1 DETECTION

3.1 INTRODUCTION

Serum contains biomarkers important for diagnostic purposes. However, it is also replete with abundant proteins such as albumin and immunoglobulin that can hinder the detection of low abundance biomarkers. Removal of high abundance proteins before sample analysis is often required to improve detection of low concentrations of biomarkers.[1] Thymidine kinase 1 (TK1) is an enzyme important for the DNA salvage pathway and is elevated in serum of cancer patients. The concentration of thymidine kinase 1 in serum of cancer patients has been reported to have a range of 2 pM to 50 pM, whereas non-cancer patients have no detectable TK1 concentration above 2 pM.[2] Conventional methods such as precipitation and affinity chromatography are commonly used sample processing steps to obtain quasi-pure sample with enriched low abundance proteins.

Precipitation either by salt or solvent takes advantage of the solubility of proteins at different ionic strengths.[3] Choosing the appropriate precipitating agent is important, especially if the activity or preservation of the protein's native form is important after processing. Ammonium sulfate precipitation has been commonly used to precipitate out proteins from complex samples and yet maintain the proteins' native form and activity.[4] Affinity columns can be specific by using antibodies or ligands, such as protein A, protein G or cibacron blue. Proteins A and G have been used to specifically bind Fc regions of immunoglobulins while cibacron dye was used to

bind human serum albumin.[5, 6] Immunoglobulin and albumin make up 60-80% of serum protein concentration,[7] hence removal of these abundant proteins can increase detection sensitivity of TK1 in serum.

Integration of necessary sample processing steps such as pre-concentration of target analyte is necessary to develop an automated analysis of complex biological fluids in microfluidic platforms. Therefore, identification of sample processing steps is necessary to effectively design automated microfluidic devices. In this chapter, I compared three different protein depletion methods; ammonium sulfate precipitation, albumin depletion and combined albumin and immunoglobulin depletion to concentrate purified recombinant thymidine kinase 1 (pTK1) from pTK1-spiked serum. The best method to concentrate pTK1 from serum was determined to be ammonium sulfate precipitation. Further, I applied ammonium sulfate precipitation to concentrate endogenous TK1 from cancer and normal serum. The precipitate was also tested using ELISA to quantify TK1 and kinase assay to determine the difference in activity of TK1 between cancer and normal serum. ELISA and kinase assay indicated that the concentration and activity of TK1 was higher in cancer than in normal serum.

3.2 MATERIALS AND METHODS

3.2.1 Serum Preparation. 300 μL of serum from a normal donor obtained after informed consent under an institutional review board approved protocol was used to prepare the stock serum sample. 10 μL of pTK1 (1 mg/mL) was added to 300 μL of serum before adding 150 μL

of 25 mM Tris, 75 mM NaCl, pH 7.5 into the solution. The sample was quickly vortexed, and 150 μL of the spiked sample solution was used for each process described below.

3.2.2 Ammonium Sulfate Precipitation. Ammonium sulfate purchased from Sigma (St. Louis, MO) was used to make an 80% w/v saturated ammonium sulfate solution. After 1 hour in a shaker (SCILOGEX, Rocky Hill, CT), the solution was centrifuged at 14 000 rpm for 5 minutes. The supernatant was transferred into a clean microcentrifuge tube. The volume of saturated ammonium sulfate used was equal to half of the volume of serum being processed. The solution was incubated for 30 minutes with mild shaking at 4°C and then centrifuged to separate the precipitate from the supernatant. The supernatant and the precipitate samples were desalted using a spin filter with 3 kDa MW cut-off. The precipitate was reconstituted in 150 μL of 25 mM Tris, 75 mM NaCl, pH 7.5.

3.2.3 Albumin Depletion. A Pierce Albumin Depletion Kit was purchased from Thermo Scientific (Rockford, IL). This kit contained agarose resin with cibacron blue as the affinity ligand. Briefly, columns were equilibrated with 200 μL of provided wash/binding buffer twice. 150 μL of the prepared serum was incubated in the column for 10 minutes before centrifuging at 12 000 rpm for 1 minute. The depleted serum was again incubated in the column for 5 minutes before centrifuging the column. The twice-depleted sample was kept at -20°C until use.

3.2.4 Albumin and IgG Depletion. A ProteoPrep Immunoaffinity Albumin and IgG Depletion Kit was purchased from Sigma-Aldrich (St. Louis, MO). The manufacturer's protocol for using the kit was followed. Briefly, columns were equilibrated with 200 μL of 25 mM Tris, 75 mM NaCl, pH 7.5 twice. 300 μL of serum spiked with 10 μL of pTK1 (1 mg/mL) was prepared. 155 μL of 25 mM Tris, 75 mM NaCl, pH 7.5 was then added into the spiked serum. 150 μL of the

prepared serum was loaded on a column. The flow-through was again incubated with the same column, so it was protein depleted twice.

3.2.5 Dot Blot. After protein depletion, the presence of TK1 was assessed qualitatively using direct dot blot of 3 μL on a nitrocellulose membrane purchased from Bio-Rad (Hercules, CA). After the samples had dried, the membrane was blocked for 1 hour with 5% w/v non-fat dry milk (NFDM) dissolved in PBS (Hyclone, Logan, UT). The membrane was probed with a 1:1000 dilution of monoclonal anti-human TK1 or 1:1000 monoclonal rabbit-anti TK1 in 5% NFDM solution for 1 hour with gentle shaking at room temperature. After washing with PBS three times, the membrane was probed with a secondary antibody labeled with IRDye 680RD from LI-COR (Lincoln, NE) for 1 hour. The membrane was washed with PBS and imaged with a LI-COR Odyssey near-IR fluorescence scanner (Lincoln, NE).

3.2.6 ELISA. To quantitatively compare the amount of TK1 obtained after processing, 50 μg of serum was incubated overnight in 96-well plates purchased from Corning (Tewksbury, MA). Nonspecific binding was minimized by blocking the well surfaces with 300 μL of 20 μg/mL BSA dissolved in Pierce Protein-Free T 20 PBS (Rockford, IL) for one hour at room temperature with gentle shaking. Each well was washed 4 times with 400 μL of PBS buffer after incubation. 50 μL of 1 μg/mL primary antibody conjugated to horseradish peroxidase (HRP) diluted in 20 μg/mL BSA solution was used to probe for the presence of TK1. For rabbit anti-TK1 antibody, indirect ELISA was performed using a goat-anti rabbit secondary antibody conjugated to HRP from Millipore (Temecula, CA). Before addition of HRP substrate, 3,3′,5,5′-tetramethylbenzidine (TMB) from Thermo Scientific (Rockford, IL), each well was washed 4 times with 300 μL of PBS buffer. The reaction was allowed to proceed for 30 minutes and the

reaction was stopped using 50 μL of 2 M H_2SO_4. Absorbance was measured at 450 nm using a Biotek Synergy H4 Hybrid Microplate Reader (Winooski, VT).

3.2.7 Denaturing Polyacrylamide Gel Electrophoresis (PAGE). NuPAGE 10% BisTris Gel from Novex (Carlsbad, CA) was used for SDS PAGE. Samples were separated using 1X SDS MOPS buffer at 120 V and 4°C for about 1 hour.

3.2.8 Native PAGE. 6% Tris boric acid gel, pH 8.7 was prepared with 6% Tris-HCl stacking gel, pH 8.0. Samples were separated using 1X Tris boric acid buffer, pH 8.7 at 200 V and 4°C for 2 hours.

3.2.9 Western Blot. A nitrocellulose membrane was used for western blots. Protein transfer was performed for 1 hour at 100 V using 25 mM Tris, 250 mM glycine buffer with 20% v/v methanol. The membrane was blocked with 5% w/v NFDM in PBS for 1 hour and then incubated with a 1:1000 dilution in 5% w/v NFDM in PBS of rabbit anti-TK1 purchased from Epitomics (Burlingame, CA) and mouse anti-TK1 overnight at 4°C. The membrane was then washed three times with PBS. The two secondary antibodies purchased from LI-COR were IR Dye 800CW labeled donkey anti-rabbit and goat anti-mouse. After 1 hour of secondary antibody incubation at room temperature, the membranes were washed with PBS and imaged using a LI-COR Odyssey (Lincoln, NE) near-IR fluorescence scanner.

3.2.10 Kinase Assay. A universal kinase kit assay from R&D Systems (Minneapolis, MN) was used to analyze kinase activity in 15 μg of protein per sample. The instructions as recommended by the manufacturer were followed. Briefly, samples were loaded into a 96-well plate and the reagents were added as directed. After the reaction, the sample absorbance was measured at 620 nm using a Biotek Synergy H4 Hybrid Microplate Reader.

3.3 RESULTS AND DISCUSSION

Protein content of processed serum samples was measured using a ND-1000 spectrophotometer (Nanodrop Technologies, Wilmington, DE) and compared with unprocessed serum as reported in table 3.1. Protein content decreased the most using ProteoPrep Immunoaffinity Albumin and IgG Depletion Kit which resulted in retention of 24.6% of protein in the flow-through while Pierce Albumin Depletion Kit and precipitate from ammonium sulfate contained 51.5% and 46.3% of protein, respectively, compared to unprocessed pTK1 spiked serum. A dot blot was performed to qualitatively assess if the pTK1 was retained after processing, and results shown in Figure 3.1 indicated that both albumin depletion and immunoaffinity depletion kits confirmed presence of pTK1 in the flow-through after serum processing. Also, precipitate from ammonium sulfate processing indicated more concentrated pTK1 as indicated by the darker spot compared to the supernatant.

.

Table 3.1 Protein concentration after protein depletion. Average of 3 measurements of total protein after processing of pTK1-spiked serum

Sample Processing	Average Protein Concentration (mg/mL)	% Protein after processing
ammonium sulfate precipitation (precipitate)	31.0	46.3
ProteoPrep Immunoaffinity Albumin and IgG Depletion Kit	16.5	24.6
Pierce Albumin Depletion Kit	34.5	51.5
Unprocessed serum	67.0	100

Since it was difficult to quantitatively analyze the results of dot blots, ELISA was utilized to measure the presence of pTK1 in each processed serum sample, based on the absorbance at 450 nm. ELISA results in Figure 3.2 indicated that ammonium sulfate precipitation had the highest concentration of pTK1 per 50 μg of total protein while albumin depletion resulted in the

least concentration of pTK1. The Pierce Albumin Depletion Kit used cibacron dye to bind human serum albumin. It has been reported that cibacron dye binds non-specifically,[8] which may explain the low concentration of pTK1 in the processed serum. On the other hand, ProteoPrep Immunoaffinity Albumin and IgG Depletion Kit uses antibody ligands, which specifically bind to human albumin and IgG.

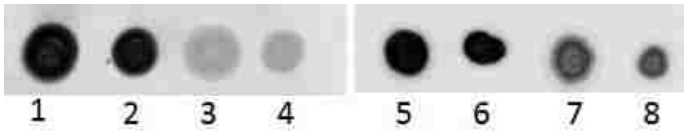

Figure 3.1 Dot blot analysis for presence of pTK1 after processing of spiked serum samples. Mouse monoclonal anti-TK1 was used to probe for presence of TK1. 3 μL of each sample was blotted twice on a nitrocellulose membrane. Dark spots indicate presence of pTK1 in the sample. 1,2) Precipitate after ammonium sulfate precipitation. 3,4) Supernatant after ammonium sulfate precipitation. 5,6) Flow-through after processing with ProteoPrep Immunoaffinity Albumin and IgG Depletion Kit. 7,8) Flow-through after processing with Pierce Albumin Depletion Kit.

Because ammonium sulfate precipitation contained the most pTK1, cancer serum was also processed using this method. Figure 3.3 shows the ELISA results that indicate successful concentration of endogenous TK1 in the precipitate. The average (n=3) calculated amount of TK1 per 50 μg of total protein in cancer serum precipitate was 8.5 ± 0.02 ng compared to 6.1 ± 0.1 ng in normal serum precipitate. For 5 μg of total protein, TK1 concentrations were 5.8 ± 0.02 ng and 4.8 ± 0.03 ng for cancer and normal serum, respectively. The decrease in total protein (from 50 μg to 5 μg) is expected to result in lower TK1 concentration, as observed. This was done to determine if the signal obtained in the ELISA was dependent on the concentration of TK1.

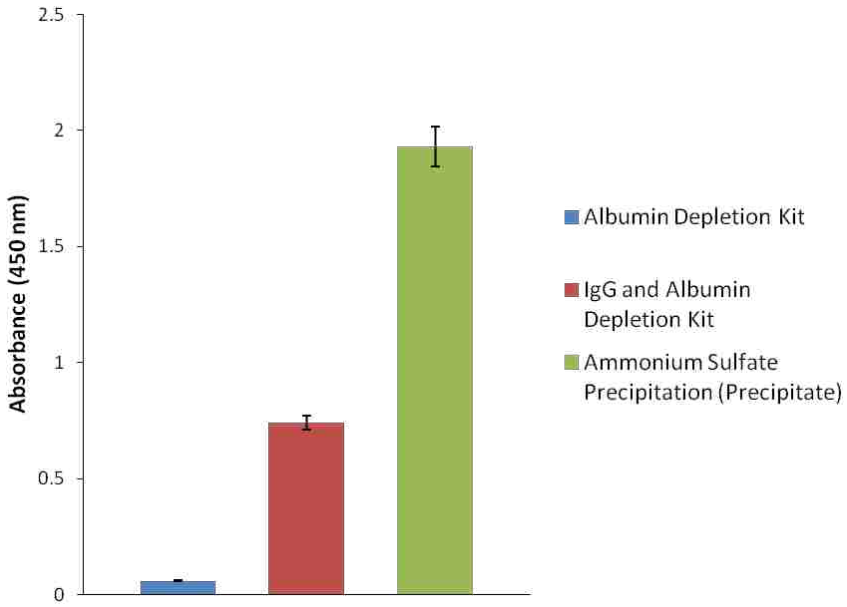

Figure 3.2 Comparison of ELISA results after protein depletion of pTK1-spiked serum. Ammonium sulfate treatment precipitate retained the most pTK1 followed by ProteoPrep Immunoaffinity Albumin and IgG Depletion Kit, while Pierce Albumin Depletion Kit retained the least pTK1 after protein depletion. 50 µg of total protein was used for each sample analysis. The error bars represent the standard error of the mean (SEM) (n=3).

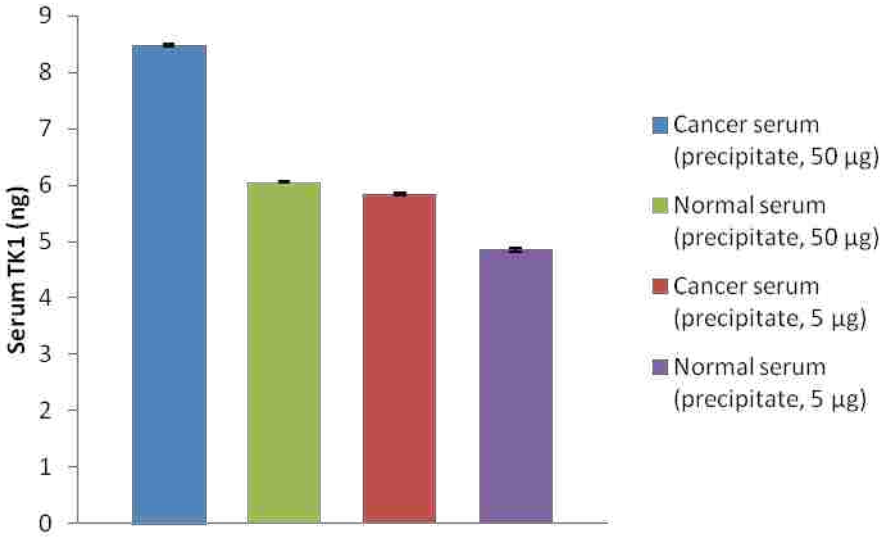

Figure 3.3 ELISA of ammonium sulfate precipitation of cancer serum and normal serum. Endogenous TK1 was effectively concentrated in the precipitate. An increase in signal was observed in the precipitate compared to the unprocessed serum. Error bars represent the SEM (n=3).

To verify that that the ELISA results correspond to TK1 in serum and not non-specific binding, western blots were performed. Western blots of denatured proteins were probed together with the novel mouse anti-TK1 and commercial rabbit anti-TK1 (Figure 3.4). Rabbit antibody (see Figure 3.4A) bound to proteins in all lanes, including normal serum precipitate and cancer serum precipitate. Multiple protein bands were present in pTK1, pTK1-spiked, and cancer serum precipitate, while only one band (>50 kD, corresponds to dimer form) was present in normal serum precipitate (Figure 3.4A, lane 1). Cancer serum was postive for ~120 kD band that corresponds to the tetrameric form of TK, which has higher kinase activity than the dimer form (Figure 3.4A, lane 3). As expected, pTK1-spiked normal serum precipitate (Figure 3.4A-C, lane 5) showed the most binding when probed with both antibodies. These results indicate that serum processing is important to detect other possible TK1 isoforms. On the other hand, the novel mouse anti-TK1 bound less protein and also exhibited more nonspecific binding as shown by the presence of random red fluorescence on the membrane (Figure 3.4C). It also only showed strong binding in pTK1 and ammonium sulfate processed pTK1-spiked protein (lanes 5 and 6, respectively, Figure 3.4B).

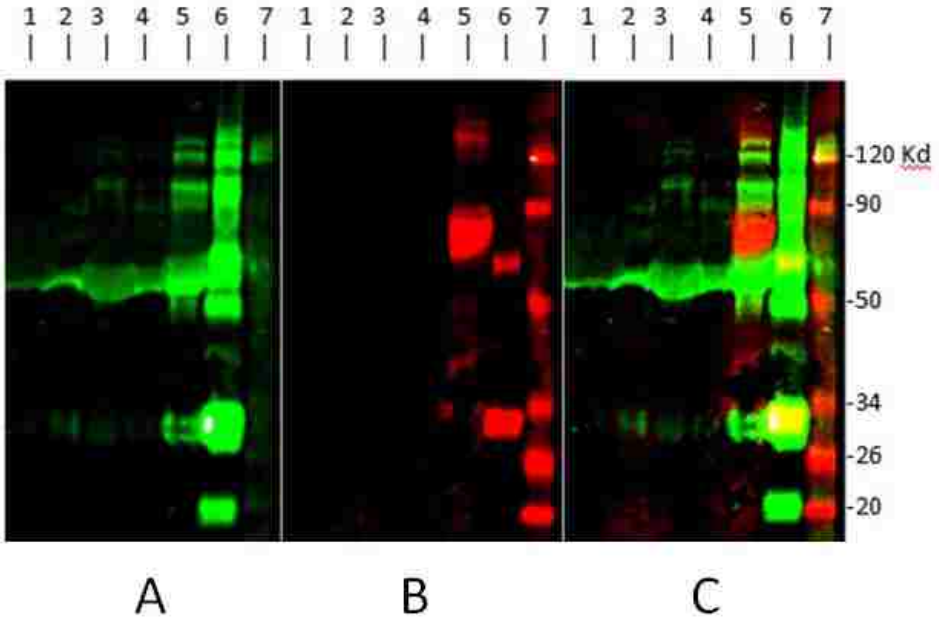

Figure 3.4 Western blot analysis of processed serum samples after SDS PAGE. 1) Normal serum precipitate, 2) IgG and albumin depleted spiked normal serum, 3) precipitate from cancer serum, 4) albumin depleted spiked normal serum, 5) precipitate from pTK1-spiked normal serum, 6) pTK1 sample and 7) protein ladder. Blots were probed with A) monoclonal rabbit anti-TK1 and B) monoclonal mouse anti-TK1; intensity was adjusted to emphasize the faint bands. C) Merged image; yellow indicates both antibodies bind to the protein. 50 μg of total protein was loaded for each serum sample, while 2 μg of pTK1 was used as positive control.

I performed western blot analysis of native PAGE to determine if the mouse anti-TK1 could only recognize endogenous TK1 in its native form because of the absence of binding to endogenous TK1 in the denatured western blots. Figure 3.5A shows binding of rabbit antibody to pTK1 (lane 1) and endogenous TK1 from serum cancer. In contrast, mouse anti-TK1 still bound only to pTK1 (Figure 3.5B, lane 1) but did not bind to endogenous TK1 in processed cancer serum (lane 2). The difference in migration distance suggests that pTK1 has different physical characteristics than the endogenous TK1.

The observed difference between binding patterns in denatured and native TK1 could also suggest that the antibodies have different binding affinities. To answer that question, ELISA

was performed to determine the dissociation constant, Kd, of the two antibodies. The antigen used to calculate the dissociation constant was pTK1. Using the equation y = x*Bmax/(x+Kd) the calculated Kd's were 4.88 $\pm$ 0.98 nM and 1.38 $\pm$ 0.16 nM for mouse and rabbit antibodies, respectively (Figure 3.6). The Kd values suggest that the rabbit antibody is more sensitive than the mouse antibody. However, the calculated Kd values were only about a factor of 3 different, which should not result in dramatic differences in the binding pattern. Therefore, the non-binding of mouse anti-TK1 to endogenous TK1 and the presence of non-specific binding as observed in both native (Figure 3.4) and denatured (Figure 3.5) western blots suggest that the ELISA could be a false positive. Another factor that could result in no binding in the western blot would be the change in structure of TK1 in any of the stages of the western blot, such as the protein transfer step where 20% methanol was included in the buffer, resulting in loss of the epitope conformation identified by mouse anti-TK1.

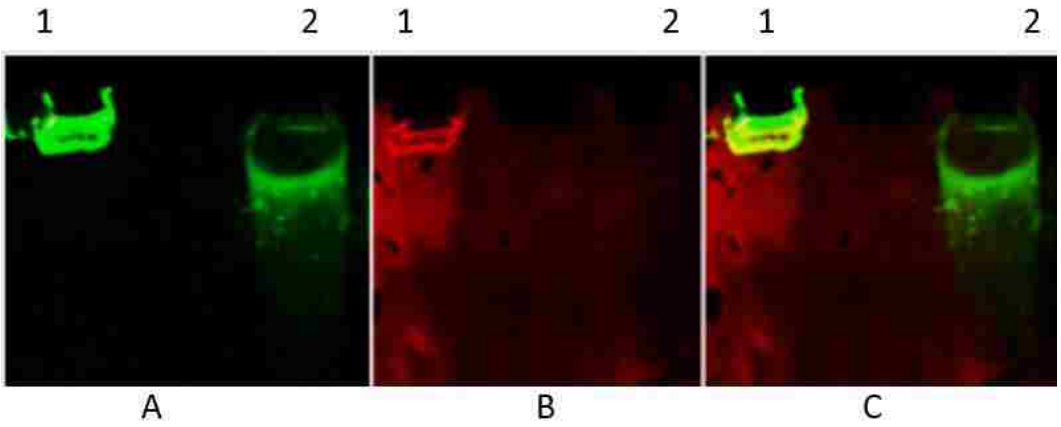

Figure 3.5 Native PAGE of pTK1 and endogenous TK1. 1) pTK1. 2) Precipitate from cancer serum. Blot probed with A) rabbit anti-TK1 and B) mouse anti-TK1 antibody. C) Merged image of A and B; yellow color in lane 1 indicates binding of both mouse and rabbit antibodies.

Finally, to ensure that the rabbit antibody was indeed binding pTK1, kinase activity was tested in the precipitate of cancer and normal serum and unprocessed counterparts. Kinase activity was detected in cancer serum samples before and after ammonium sulfate precipitation, but activity was detected above the noise level in normal serum only after ammonium sulfate precipitation (Figure 3.7). From the obtained absorbance values, TK1 activity was calculated based on the amount of adenosine diphosphate produced as described by the manufacturer. The calculated TK1 activity in unprocessed serum was 1.6 pmol/min/µg of total protein but increased to 19.2 pmol/min/µg of total protein in the ammonium sulfate precipitate. In normal serum, kinase activity was undetected in unprocessed serum, increasing to 1.5 pmol/min/µg of total protein in the ammonium sulfate precipitate. The increase in activity indicated that TK1 was concentrated after processing. I can also infer from this result that the positive binding of rabbit antibody in western blot results for the cancer serum precipitate was due to the presence of TK1.

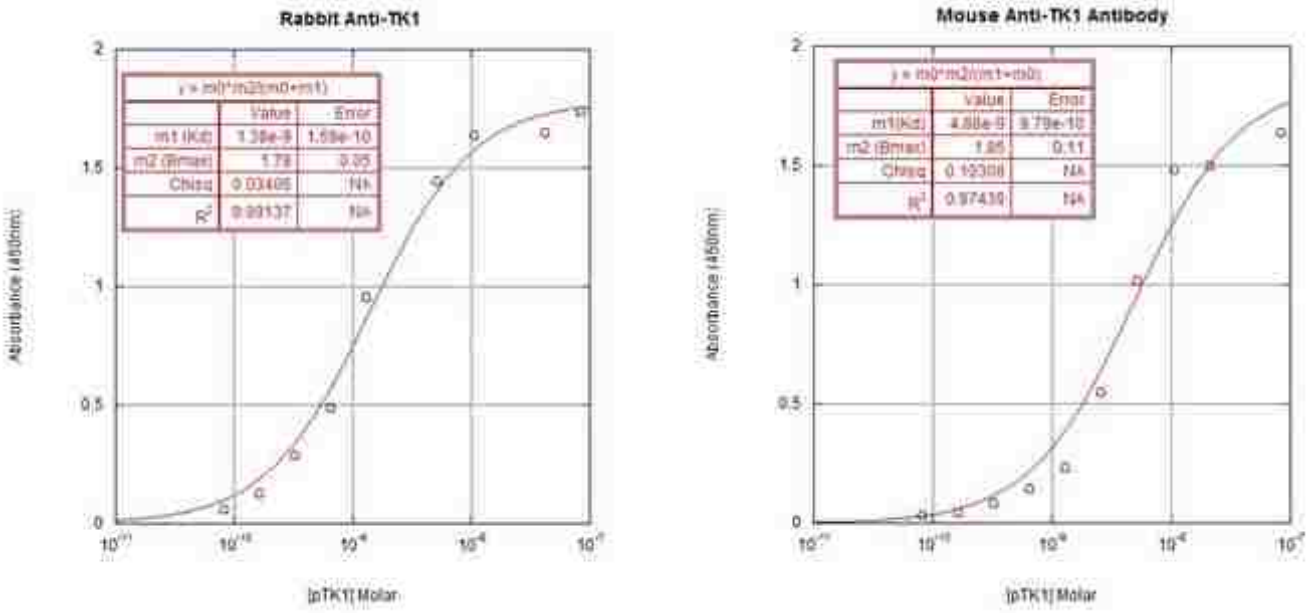

Figure 3.6 Kd curve fitting. Equation used was x*Bmax/(x+Kd). Antigen used was pTK1.

After having established that rabbit anti-TK1 binds TK1 in western blots, endogenous TK1 from cancer and normal serum samples was measured using indirect ELISA with the rabbit antibody. Figure 3.8 shows that TK1 concentration was higher in cancer than in normal serum, and the difference was more pronounced at 50 μg of total protein (0.98 $\pm$ 0.01 ng in cancer and 0.61 $\pm$ 0.01 ng normal serum) than in 5 μg of total protein (0.59 $\pm$ 0.00 ng in cancer and 0.44 $\pm$ 0.00 ng in normal). The same trend as in direct ELISA was observed with mouse anti-TK1 though the measured concentrations of TK1 were different from each other. The similar trend of concentrations suggest that the earlier assumption that the presence of methanol in the transfer buffer may have affected the TK1 conformation resulting in negative binding of mouse anti TK1.

If this is the case, then mouse anti-TK1 is quite sensitive to conformational changes of endogenous TK1, and it may be difficult to use on different platforms. Therefore, it is important to determine what conformation of endogenous TK1 the mouse anti-TK1 binds, perhaps by immunoprecipitation and mass spectrometry analysis.

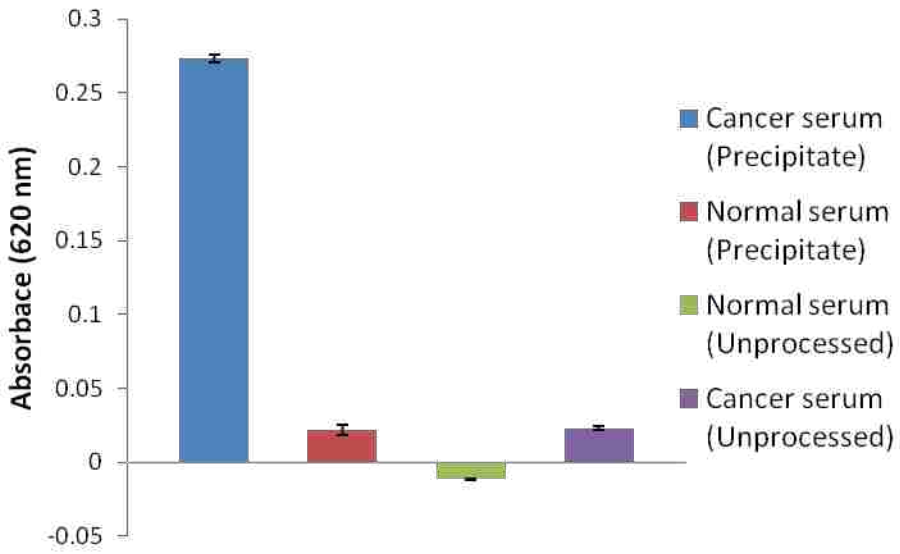

Figure 3.7 Comparison of kinase activity. Kinase activity before and after ammonium sulfate precipitation of cancer and normal serum samples. Error bars represent SEM (n=3).

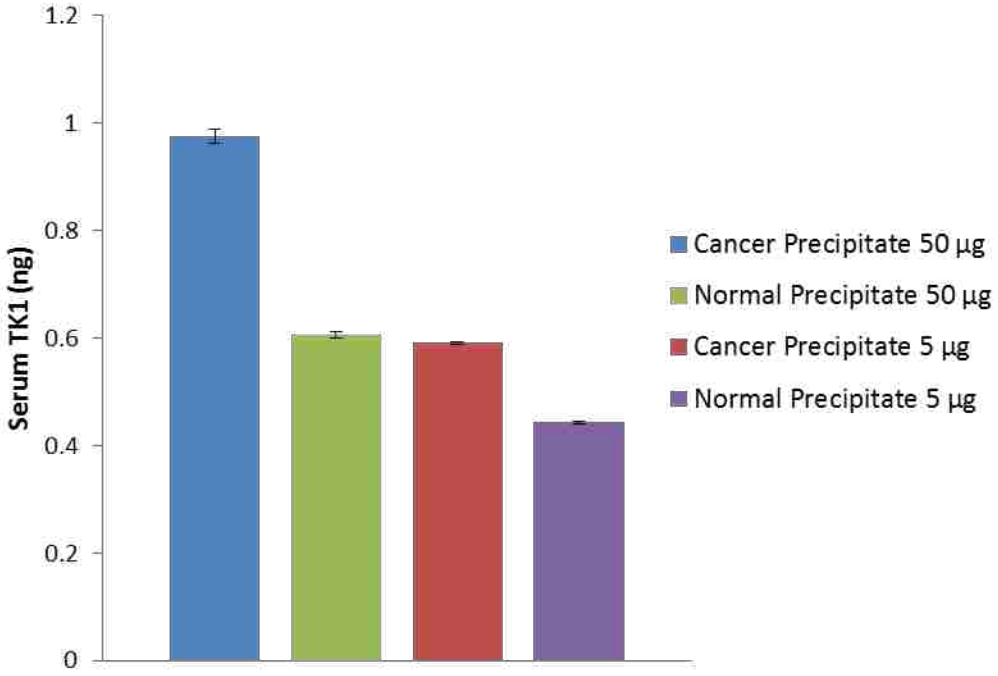

Figure 3.8 Indirect ELISA of ammonium sulfate precipitate from cancer and normal serum using rabbit anti-TK1. Error bars represent SEM (n=3).

3.4 CONCLUSIONS

Choosing the appropriate commercial kit for protein depletion must be carefully studied to determine if the target analyte will be lost or retained during the process. I have demonstrated that ammonium sulfate precipitation retained the most pTK1 followed by Proteo Prep Immunoaffinity Albumin and IgG Depletion Kit, while Pierce Albumin Depletion Kit retained the least pTK1 among the three processes. Ammonium sulfate precipitation was also effective at concentrating endogenous TK1 from serum while maintaining its activity.

ELISA, western blot and kinase assay results showed that processing was important to clearly differentiate cancer from normal serum. Though the samples tested here were limited, these results give direction on how to process serum samples for future work. I also determined that rabbit anti-TK1 binds to both pTK1 and endogenous TK1 while the mouse anti-TK1 binds only to pTK1 in the conditions used in these experiments. The difference in migration time in native PAGE of endogenous TK1 from pTK1 indicates that the two proteins have different physical properties. This result agrees with the early studies of recombinant TK1 reported by Munch-Petersen et al.[9] where they attributed the differences in TK1 physical properties to different post-translational modifications that may take place depending on the type of cell used in cloning the recombinant protein. Furthermore, the presence of higher molecular weight bands in cancer serum in denaturing PAGE hints that the different isoforms of TK1 are worth further investigation.

Processed serum samples showed about 13 fold more activity in cancer than in normal serum. It is interesting to note that the concentration of TK1 in cancer serum was only about 1.4 fold higher than normal. These findings solidify the previous reports that the difference in activity of TK1 is dependent on its isoform, where higher molecular weight TK1 have higher activity than low molecular weight TK1. Recent findings by Jagarlamudi et al[10] also indicated that at early stage of cancer, particularly prostate and breast, had higher fractions of less active dimer form of TK1. Therefore, for future studies, serum processing and profiling of the different isoforms of TK1 at different stages could be helpful in developing a TK1 assay for early detection of cancer.

3.5 REFERENCES

1. Bjorhall, K.; Miliotis, T.; Davidsson, P., Comparison of different depletion strategies for improved resolution in proteomic analysis of human serum samples. *Proteomics* **2005,** *5* (1), 307-317.

2. He, Q.; Zhang, P.; Zou, L.; Li, H.; Wang, X.; Zhou, S.; Fornander, T.; Skog, S., Concentration of thymidine kinase 1 in serum (S-TK1) is a more sensitive proliferation marker in human solid tumors than its activity. *Oncology reports* **2005,** *14* (4), 1013-9.

3. Jiang, L.; He, L.; Fountoulakis, M., Comparison of protein precipitation methods for sample preparation prior to proteomic analysis. *J Chromatogr A* **2004,** *1023* (2), 317-320.

4. Kanwar, L.; Gogoi, B. K.; Goswami, P., Production of a Pseudomonas lipase in n-alkane substrate and its isolation using an improved ammonium sulfate precipitation technique. *Bioresource Technol* **2002,** *84* (3), 207-211.

5. Ruckenstein, E.; Zeng, X. F., Albumin separation with Cibacron Blue carrying macroporous chitosan and chitin affinity membranes. *J Membrane Sci* **1998,** *142* (1), 13-26.

6. Bergmann-Leitner, E. S.; Mease, R. M.; Duncan, E. H.; Khan, F.; Waitumbi, J.; Angov, E., Evaluation of immunoglobulin purification methods and their impact on quality and yield of antigen-specific antibodies. *Malaria J* **2008,** *7*.

7. Anderson, N. L.; Anderson, N. G., The human plasma proteome: History, character, and diagnostic prospects (vol 1, pg 845, 2002). *Mol Cell Proteomics* **2003,** *2* (1), 50-50.

8. Steel, L. F.; Trotter, M. G.; Nakajima, P. B.; Mattu, T. S.; Gonye, G.; Block, T., Efficient and specific removal of albumin from human serum samples. *Mol Cell Proteomics* **2003,** *2* (4), 262-270.

9. Munch-Petersen, B.; Cloos, L.; Jensen, H. K.; Tyrsted, G., Human Thymidine Kinase-1 - Regulation in Normal and Malignant-Cells. *Adv Enzyme Regul* **1995,** *35*, 69-89.

10. Jagarlamudi, K. K.; Hansson, L. O.; Eriksson, S., Breast and prostate cancer patients differ significantly in their serum Thymidine kinase 1 (TK1) specific activities compared with those hematological malignancies and blood donors: implications of using serum TK1 as a biomarker. *Bmc Cancer* **2015,** *15*.

CHAPTER 4: OPTIMIZATION OF MONOLITHIC COLUMNS FOR MICROFLUIDIC DEVICES*

4.1 INTRODUCTION

Disease-specific biomarkers are important for proper diagnoses and treatments of diseases. For example, a panel of biomarkers such as proteins, metabolites, or nucleic acids can be probed to diagnose or monitor treatments of some diseases. Proteins and metabolite biomarkers are heavily studied because they are relatively easy to obtain in different biological fluids. Protein biomarkers are generally detected contingent on the availability of the corresponding antibody. Extracellular nucleic acid biomarkers of diseases have also been found in urine,[1, 2] serum[3], milk,[4] cerebrospinal fluid,[5] and saliva[6]. However, detection of nucleic acid in biological fluids is hindered by low concentration. Additionally, short nucleic acid fragments such as miRNA are difficult to detect because they are almost the same size as primers used in PCR. Therefore it should be beneficial to develop sensitive and easy assays that can analyze these panels of biomarkers for point-of-care diagnostics.

Analysis of panels of biomarkers is desirable for point-of-care diagnostics, potentially enabling routine tests to be performed easily and inexpensively. Assessment of tumors for example, currently requires aseptic techniques and expensive personnel time to obtain a tissue sample to confirm disease.[7] Also, tissue sample size is limited to reduce discomfort to the

---

* This chapter is reproduced with permission from Pagaduan J.V.; Yang, W.; Woolley, A.T.; *Proc. SPIE* 8031 Micro- and Nanotechnology Sensors, Systems, and Applications III, 80311V (May 13, 2011)

patient. Blood contains important biomarkers. Although less invasive compared to biopsy, sterile needles and aseptic techniques are still required. On the other hand, biological fluids such as urine and saliva can be obtained non-invasively and multiple times to obtain sample in a day if needed. An assay that can analyze small volumes of biological fluids, produce rapid results, and be easy to use is necessary for point-of-care diagnostics.

Some methods of detecting biomarkers are immunoassays,[8] PCR,[9] and mass spectrometry.[10, 11] These methods are sensitive and high throughput but are expensive and tedious, requiring multistep sample preparations and specialized machines. Immunoassays are also dependent on the availability of antibodies for the target antigens. PCR for detecting nucleic acids requires expensive reagents and sample purification. Mass spectrometry instruments are expensive and incompatible with samples containing particulates, high salt, and surfactants, thus requiring sample pre-treatments. Therefore, there is a need for fast, simple, and cheap assays for point-of-care applications.

Microfluidic devices are useful in handling nanoliter to picoliter biological fluid samples, with strong potential to decrease analysis time. Some applications of microfluidic systems are for genomic sequencing,[12] protein analysis,[13] cell sorting,[14] and PCR.[15] Because microfluidics are effective in analyzing small volumes, reagent usage is also dramatically reduced. Such devices are generally small, enabling portability, while microfabrication technology facilitates mass production. The desire for automated sample analyses has led to integration of different sample treatment methods on the devices such as on-column labeling,[16] pre-concentration,[17, 18] and target extraction using solid phase extractors.[19] These integrated functions in microfluidics devices are promising applications in point-of-care diagnostics.

Here I describe the integration of functionalizable monoliths as affinity columns in microfluidic devices. Typical monolithic columns in chromatography separations require pressure[20, 21] to flow the samples through. Applied voltages offer a simplified way to flow the sample through the monolithic columns. However, bubble entrapment in monoliths is a frequent problem when electric fields are applied across monolithic columns. Therefore it is necessary to make monolithic columns that are porous enough that air bubbles are not trapped during capillary flow. Here I show an optimized process for making glycidyl metharcylate-ethylene glycol dimethacrylate monolithic columns. I used cyclohexanol and 1-dodecanol as porogens, with the surfactant Tween 20, which increased the pore size. The amount of porogens affected the nodule morphology and size of pores. The monoliths formed are very porous as water and buffer can flow through the monoliths by capillary action.

4.2 MATERIALS AND METHODS

4.2.1 Materials and Reagents. Polyethylene glycol dimethacrylate (PEGDMA), ethylene glycol dimethacrylate (EGDMA, 98%), glycidyl methacrylate (GMA, 97%), 2,2-dimethoxy-2-phenylacetophenone (DMPA, 98%), and 1-dodecanol (98%), were from Aldrich (Milwaukee, WI). Cyclohexanol was from J. T. Baker (Phillipsburg, NJ). Tween 20 was from Mallinckrodt Baker (Paris, KY).

4.2.2 Monolith preparation in glass vials. Porogens, monomers, and photoinitiator were weighed according to the amounts indicated in Table 4.1, mixed together and ultrasonicated until the photoinitiator was completely dissolved. The total weight of the mixture was 1 g. 0.5 g of

the mixture was transferred into another clear clean glass vial and 0.2 g of Tween 20 was added into the mixture. The solutions with and without Tween 20 were sonicated again for five minutes before photopolymerization in the glass vials under UV exposure using a Sunray 400 lamp (Intelligent Dispensing Systems, Encino, CA) for 12-15 minutes at 200 W. Higher porogen levels resulted in increased in polymerization time. After polymerization, monoliths were cooled to room temperature. Immediately after cooling, the monoliths were placed in separate thimbles and cleaned using Soxhlet extraction apparatus overnight using 2-propanol as solvent. The monolith was then gently washed with deionized water several times and air dried before scanning electron microscope imaging.

Table 4.1 Monolith composition

	Monomer (g)	Crosslinker (g)	Porogens (g)		Photoinitiator (mg)	Surfactant (g) per 0.5g of mixture
Monolith	GMA	EGDMA	cyclohexanol	1-dodecanol	DMPA	Tween 20
A	0.25	0.25	0.25	0.25	20	0
B	0.25	0.25	0.25	0.25	20	0.2
C	0.20	0.20	0.30	0.30	20	0
D	0.20	0.20	0.30	0.30	20	0.2
E	0.2	0.1	0.30	0.40	20	0
F	0.2	0.1	0.30	0.40	20	0.2

4.2.3 Microfabrication of microfluidic devices. The fabrication process for making microfluidic devices has been previously described.[22,23] Briefly, photolithography was used to transfer the channel design on oxidized silicon which had been spin coated with SPR 1805 photoresist (MicroChem Corp., Newton, MA). After development, the silicon was etched with HF until the silicon wafer became hydrophobic, followed by a KOH etch to achieve a channel

depth of about 20 μm. The microfluidic design was transferred onto PMMA by hot embossing. PMMA with laser cut holes was then thermally bonded to enclose the channels.

4.2.4 In-situ polymerization of monoliths in microfluidic channels. The initial procedure for preparing the solutions was similar to that described for monolith preparation in glass vials except the solution was purged with nitrogen gas after ultrasonication. Then, the solution was flowed by capillary action into the microfluidic channel. Excess solution in the reservoir was removed to limit hydrodynamic flow during polymerization. Black tape was used to mask other parts of the channel to contain polymerization of the solution in target area only. The device was then exposed to UV light using a PRX 1000 (Tamarack Scientific, Corona, CA) lamp with power of 1 kW for about 12 minutes. The monoliths were immediately washed with 2-propanol until the monolith became white in color, then washed with deionized water several times and dried at room temperature.

4.2.5 Scanning electron microscopy imaging. The channel containing the monolith was laser cut and glued on plastic stubs. The edge that contained the end of the channel with monolith was cut using a manual microtome with a glass knife until the monolith was exposed. The surface was cleaned using scotch tape to remove debris. Samples were mounted on aluminum stubs using carbon tape and coated with gold using a Polaron Gold Sputtter for 3 minutes to decrease charging. The samples were coated under 0.1 Torr, with an applied potential of 2.5 kV and current maintained at 18-20 mA. The gold coating under these conditions was about 20 nm. All images were taken using a Philips XL30 ESEM FEG in low vacuum mode using a gaseous secondary electron detector. Voltage applied varied from 10-12 kV since the monoliths charged

differently. However, the magnifications and working distances were similar for each set to make comparison easier.

4.3. RESULTS

4.3.1 PEGDMA vs. EGDMA Crosslinkers. Figure 4.1 compares SEM data for GMA-PEGDMA and GMA-EGDMA monoliths. The GMA-PEGDMA monolith has smaller nodules than the GMA-EGDMA monolith. Smaller nodules mean more surface area for immobilizing probes. The smaller nodule of GMA-PEGDMA is due to the poorer cross-linking efficiency of PEGDMA.[24] Also with GMA-PEGDMA, the SEM image shows smaller pores; hence, more pressure would be needed to flow the liquid through the monolith. Water did not flow through in-situ polymerized GMA-PEGDMA, while partial flow was observed in GMA-EGDMA monoliths. Thus, no other formulation was tried using PEGDMA crosslinker. Instead, I decided to optimize GMA-EGDMA monolith formulation targeting irregular large through pores, high surface area, mechanical stability, and surface amenable for functionalization. High surface area increases diffusion mass transport and irregular pores enhance convective transport as liquid flows through the monolith.[25]

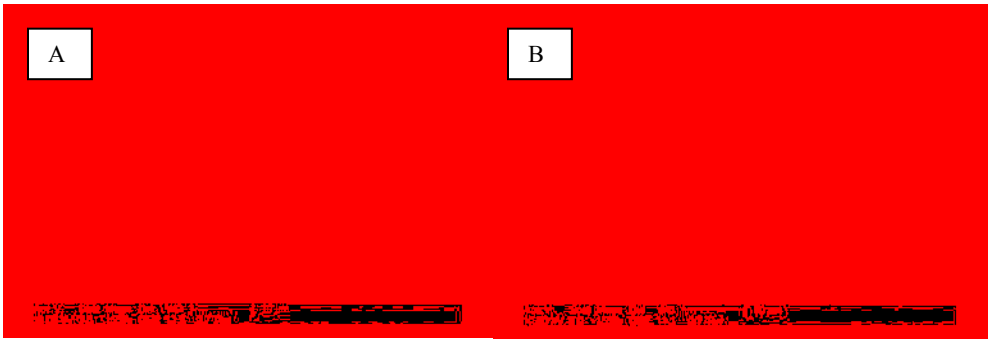

Figure 4.1 SEM images of (A) GMA-PEGDMA and (B) GMA-EDGDMA monoliths show different globule formations. Both monoliths were made by mixing 0.3 g cyclohexanol, 0.4 g 1-dodecanol, 10 mg DMPA, 0.1 g GMA, and 0.25 g EGDMA or PEGDMA.

4.3.2 Comparison of morphology of GMA-EGDMA monoliths. One way of controlling the pore size is by changing the porogen concentration. I observed that a total porogen of mass 0.80 g resulted in a soft monolith when exposed for 12-15 minutes. Therefore, I selected a maximum total porogen of 0.7 g. Monolith solution with surfactant content more than 0.2 g produced bubbles after ultrasonication and during nitrogen purging; these bubbles hindered flow of solution through the microchannels. Thus, surfactant content ≤0.20 g was used.

SEM images in Figure 4.2 show the effects on the morphology of the nodules and pore size by varying two parameters: porogen content (A, C and E) and presence or absence of Tween 20 surfactant (B, D, and F). Increasing only the total porogen resulted in larger nodule size but at 70% (wt/wt) the globular nodules became somewhat fused. The monoliths without Tween 20 (A, C and E) have through pores that range from ~1 μm (A) to ~2.5 μm (C). However, in the solution with 60% porogen (C), only increased size of the globular nodules was observed. Mechanically weak monoliths were produced when total porogen was greater than 70% (wt/wt) under the same polymerization conditions. Addition of surfactant also increased pore size.

Adding 0.2 g of Tween 20 increased the pore size from ~2.5 µm (E) to ~ 4 µm (F). It has been suggested that surfactants in emulsions affect phase separation during polymerization.[26] I tested the following surfactants: sodium dodecyl sulfate, polystyrene sulfonate sodium salt, and Tween 20. Tween 20 gave the best result in terms of homogeneity of solution.

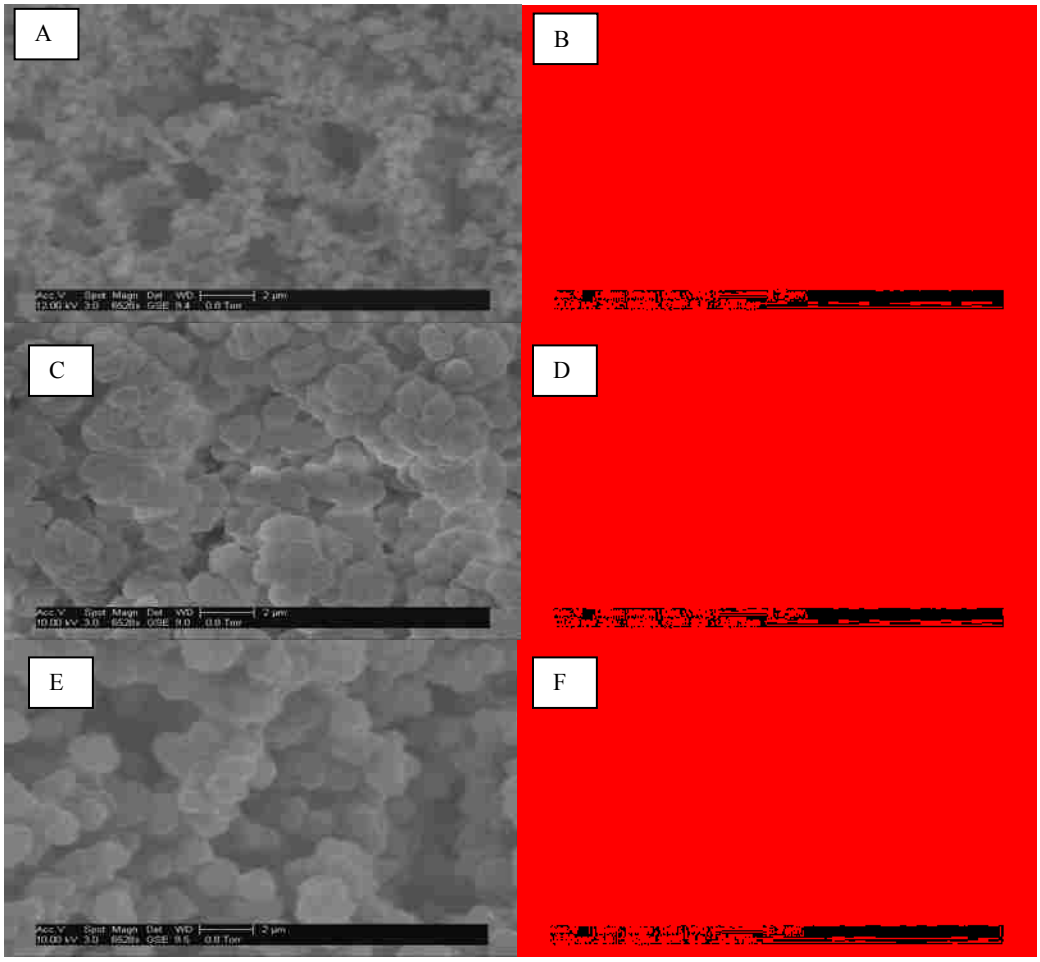

Figure 4.2 SEM images of GMA-EGDMA monoliths under different compositions. A, C, and E are GMA-EGDMA monoliths while B, D, and F are the corresponding monoliths with 0.2 g of Tween 20 as well. See Table 4.1 for detailed information for each monolith. Increasing the total porogen concentration results in an increase in size of the nodules (A, C, E). Addition of Tween 20 increases the size of through-pores.

4.3.3 Optimal monolith formation in microdevices. Because of the large pore size, the monolith with 70% porogen (F) was in-situ polymerized in a microchip (Figure 4.3), and capillary flow was observed. In an in-situ polymerized monolith without the surfactant (E), air bubbles formed in the monolith when water flowed through were difficult to remove. In contrast, the addition of surfactant to 70% porogen monolith resulted in less bubble trapping and water flowed through the monolith by capillary action.

This optimized formulation is advantageous for integrating monolithic columns in microfluidic devices. The monoliths formed, though porous, exhibit high surface area with functionalizable surface. Also, because the liquid solutions can flow through the optimized monolith by capillary action, surface modification of the monolith will be easier, and electrophoretic flow can be used to move fluid through the monolith instead of pumps.

Figure 4.3 SEM image of in-situ polymerized monolithic column in a microfluidic device.

4.4 CONCLUSION

I have optimized in-situ polymerized GMA-EGDMA monolithic columns in microfluidic devices. Nodule size and through-pore dimensions increased with increasing porogen content and addition of the surfactant, Tween 20. Capillary action was sufficient to flow water through a monolith with a composition of 70% porogen and added surfactant. The presence of epoxy groups on the surface can be utilized for immobilizing single-stranded DNA probes for on-line extraction of single stranded nucleic acid biomarkers in biological fluids.

4.5 REFERENCES

1. Schepetiuk, S.; Kok, T.; Martin, L.; Waddell, R.; Higgins, G., Detection of Chlamydia trachomatis in urine samples by nucleic acid tests: Comparison with culture and enzyme immunoassay of genital swab specimens. *Journal of Clinical Microbiology* **1997,** *35* (12), 3355-3357.

2. Hessels, D.; Klein Gunnewiek, J. M. T.; van Oort, I.; Karthaus, H. F. M.; van Leenders, G. J. L.; van Balken, B.; Kiemeney, L. A.; Witjes, J. A.; Schalken, J. A., DD3PCA3-based Molecular Urine Analysis for the Diagnosis of Prostate Cancer. *European Urology* **2003,** *44* (1), 8-16.

3. Lavon, I.; Refael, M.; Zelikovitch, B.; Shalom, E.; Siegal, T., Serum DNA can define tumor-specific genetic and epigenetic markers in gliomas of various grades. *Neuro-Oncology* **2010,** *12* (2), 173-180.

4. O'Driscoll, L., Extracellular nucleic acids and their potential as diagnostic, prognostic and predictive biomarkers. *Anticancer Research* **2007,** *27* (3A), 1257-1265.

5. Cogswell, J. P.; Ward, J.; Taylor, I. A.; Waters, M.; Shi, Y. L.; Cannon, B.; Kelnar, K.; Kemppainen, J.; Brown, D.; Chen, C.; Prinjha, R. K.; Richardson, J. C.; Saunders, A. M.; Roses, A. D.; Richards, C. A., Identification of miRNA changes in Alzheimer's disease brain and CSF yields putative biomarkers and insights into disease pathways. *J Alzheimers Dis* **2008,** *14* (1), 27-41.

6. Michael, A.; Bajracharya, S. D.; Yuen, P. S. T.; Zhou, H.; Star, R. A.; Illei, G. G.; Alevizos, I., Exosomes from human saliva as a source of microRNA biomarkers. *Oral Dis* **2010,** *16* (1), 34-38.

7. Epstein, J. I.; Walsh, P. C.; Carter, H. B., Importance of posterolateral needle biopsies in the detection of prostate cancer. *Urology* **2001,** *57* (6), 1112-1116.

8. Park, J.-E.; Li, L.; Park, J.; Knecht, R.; Strebhardt, K.; Yuspa, S. H.; Lee, K. S., Direct quantification of polo-like kinase 1 activity in cells and tissues using a highly sensitive and specific ELISA assay. *Proceedings of the National Academy of Sciences* **2009,** *106* (6), 1725-1730.

9. Zuo, Z.; Chen, S. S.; Chandra, P. K.; Galbincea, J. M.; Soape, M.; Doan, S.; Barkoh, B. A.; Koeppen, H.; Medeiros, L. J.; Luthra, R., Application of COLD-PCR for improved detection of KRAS mutations in clinical samples. *Mod Pathol* **2009,** *22* (8), 1023-1031.

10. Radulovic, D.; Jelveh, S.; Ryu, S.; Hamilton, T. G.; Foss, E.; Mao, Y.; Emili, A., Informatics Platform for Global Proteomic Profiling and Biomarker Discovery Using Liquid Chromatography-Tandem Mass Spectrometry. *Molecular & Cellular Proteomics* **2004,** *3* (10), 984-997.

11. Tolson, J.; Bogumil, R.; Brunst, E.; Beck, H.; Elsner, R.; Humeny, A.; Kratzin, H.; Deeg, M.; Kuczyk, M.; Mueller, G. A.; Mueller, C. A.; Flad, T., Serum protein profiling by SELDI mass spectrometry: detection of multiple variants of serum amyloid alpha in renal cancer patients. *Lab Invest* **2004,** *84* (7), 845-856.

12. Kartalov, E. P.; Quake, S. R., Microfluidic device reads up to four consecutive base pairs in DNA sequencing-by-synthesis. *Nucleic Acids Research* **2004,** *32* (9), 2873-2879.

13. Armenta, J. M.; Dawoud, A. A.; Lazar, I. M., Microfluidic chips for protein differential expression profiling. *Electrophoresis* **2009,** *30* (7), 1145-1156.

14. Takahashi, K.; Hattori, A.; Suzuki, I.; Ichiki, T.; Yasuda, K., Non-destructive on-chip cell sorting system with real-time microscopic image processing. *Journal of Nanobiotechnology* **2004,** *2* (1), 5.

15. Ottesen, E. A.; Hong, J. W.; Quake, S. R.; Leadbetter, J. R., Microfluidic Digital PCR Enables Multigene Analysis of Individual Environmental Bacteria. *Science* **2006,** *314* (5804), 1464-1467.

16. Yu, M.; Wang, H.-Y.; Woolley, A. T., Polymer microchip CE of proteins either off- or on-chip labeled with chameleon dye for simplified analysis. *Electrophoresis* **2009,** *30* (24), 4230-4236.

17. Wainright, A.; Williams, S. J.; Ciambrone, G.; Xue, Q.; Wei, J.; Harris, D., Sample pre-concentration by isotachophoresis in microfluidic devices. *J Chromatogr A* **2002,** *979* (1-2), 69-80.

18. Foote, R. S.; Khandurina, J.; Jacobson, S. C.; Ramsey, J. M., Preconcentration of Proteins on Microfluidic Devices Using Porous Silica Membranes. *Analytical Chemistry* **2004,** *77* (1), 57-63.

19. Shaw, K. J.; Joyce, D. A.; Docker, P. T.; Dyer, C. E.; Greenman, J.; Greenway, G. M.; Haswell, S. J., Simple practical approach for sample loading prior to DNA extraction using a silica monolith in a microfluidic device. *Lab on a Chip* **2009,** *9* (23), 3430-3432.

20. Nema, T.; Chan, E. C. Y.; Ho, P. C., Application of silica-based monolith as solid phase extraction cartridge for extracting polar compounds from urine. *Talanta* **2010,** *82* (2), 488-494.

21. Li, Y.; Tolley, H. D.; Lee, M. L., Preparation of Polymer Monoliths That Exhibit Size Exclusion Properties for Proteins and Peptides. *Analytical Chemistry* **2009,** *81* (11), 4406-4413.

22. Sun, X.; Farnsworth, P. B.; Woolley, A. T.; Tolley, H. D.; Warnick, K. F.; Lee, M. L., Poly(ethylene glycol)-functionalized devices for electric field gradient focusing. *Analytical Chemistry* **2008,** *80* (2), 451-460.

23. Kelly, R. T.; Woolley, A. T., Thermal bonding of polymeric capillary electrophoresis microdevices in water. *Analytical Chemistry* **2003,** *75* (8), 1941-1945.

24. Deb, S.; Vazquez, B.; Bonfield, W., Effect of crosslinking agents on acrylic bone cements based on poly(methylmethacrylate). *Journal of Biomedical Materials Research* **1997,** *37* (4), 465-473.

25. Svec, F., Organic polymer monoliths as stationary phases for capillary HPLC. *J Sep Sci* **2004,** *27* (17-18), 1419-30.

26. Wang, J.; Zhang, C.; Du, Z.; Xiang, A.; Li, H., Formation of porous epoxy monolith via concentrated emulsion polymerization. *Journal of Colloid and Interface Science* **2008,** *325* (2), 453-458.

CHAPTER 5: MONOLITH AFFINITY EXTRACTION OF INTERLEUKIN-8, A POTENTIAL CANCER MARKER, FROM SALIVA IN MICROFLUIDIC DEVICES

5.1 INTRODUCTION

Oral squamous cell carcinoma (OSCC) of the head and neck is one of the most common cancers worldwide characterized by high morbidity and mortality rate.[1] The survival rate is about 50%, 5 years after detection, because it is often diagnosed at the late stage of the disease.[2] The known risk factors of oral cancer are tobacco use and alcohol consumption. Human papilloma virus has also been linked to oral and oropharyngeal cancer.[3, 4] The standard for diagnosing OSCC is through biopsy and immunohistochemistry testing of lesions found in mucosal surfaces.[2] However, the unrealiability of histologic grading spurs increased interest in identifying molecular markers that will be useful for accurate and early stage diagnosis.[5]

Interleukin 8 (IL8) is a chemokine implicated in the tumorigenesis and metastasis in OSCC.[6] It has been reported that IL8 in saliva was detected at higher concentrations in cancer, 86 pM, than in normal patients, 30 pM.[5, 7, 8] A saliva-based test could be a cost-effective and non-invasive early diagnosis or follow-up in conjunction with conventional diagnostic methods.

In this chapter, I describe a process of integrating monolith affinity columns in poly(methyl methacrylate) (PMMA) devices. I also test the ability of these affinity columns to extract IL8 in buffer and in spiked saliva. Preliminary results show successful immobilization of active antibody and extraction of IL8 from buffer and saliva. However, decreased extraction efficiency of IL8 from saliva compared to IL8 in buffer is observed. These results are

encouraging to pursue further development of microchip immunoaffinity assays for detecting potential disease markers in saliva.

5.2 MATERIALS AND METHODS

5.2.1 Reagents. Ethylene glycol dimethacrylate (EGDMA, 98%), glycidyl methacrylate (GMA, 97%), 2,2-dimethoxy-2-phenylacetophenone (DMPA, 98%), and 1-dodecanol (98%), were obtained from Aldrich (Milwaukee, WI). Cyclohexanol was from J. T. Baker (Phillipsburg, NJ). Tween 20, sulfuric acid and acetic acid were purchased from Mallinckrodt Baker (Paris, KY). Sodium periodate was obtained from Fisher Scientific (Waltham, MA).

5.2.2 Device fabrication. An offset T-design with two extra reservoirs was used in the experiments (see Figure 5.1).[9] Silicon templates were fabricated in the BYU Integrated Microfabrication Lab using standard photolithography techniques to provide elevated channel features (20 μm tall, 50 μm wide). Microchannel features were hot embossed onto 1.5 mm-thick PMMA sheets (2 x 5 cm^2) for 30 minutes at 138°C. 3-mm thick PMMA sheets (2 x 5 cm^2) with laser-cut reservoirs were thermally bonded as cover plates for 27 minutes at 110°C to enclose the microfluidic channels.

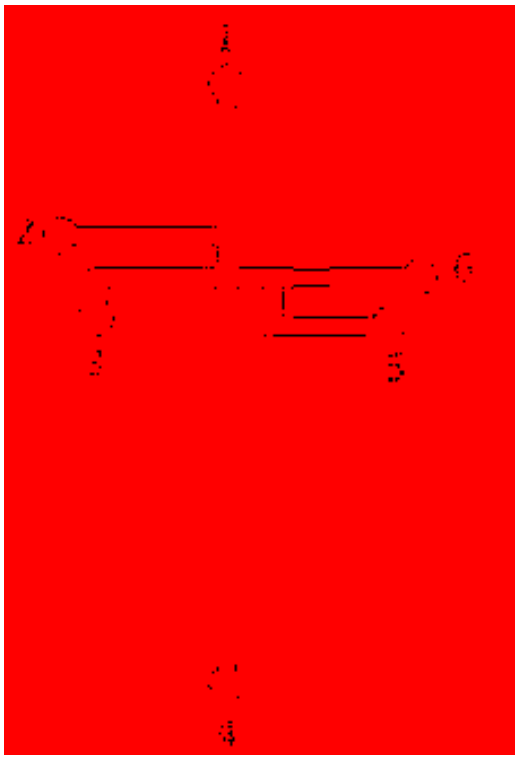

Figure 5.1 Schematic of a six-reservoir microfluidic device. 1) Buffer reservoir, 2) injection waste reservoir, 3) titration reservoir, 4) separation waste reservoir, 5) extra channel for monolith fabrication, and 6) sample reservoir.

5.2.3 Monolith integration. Monolith fabrication was previously described[10] in chapter 4 and adapted with some changes in the composition of the monolith. Briefly, monolith solution was made by mixing 0.30 g GMA, 0.10 g EGDMA, 0.20 g Tween-20, 0.20 g cyclohexanol, 0.2 g 1-dodecanol and 8 mg DMPA in a glass vial. The solution was vortexed until DMPA was completely dissolved. Then the solution was immediately loaded into the microfluidic device and exposed to UV light using a Sun Ray 600 Lamp (Uvitron, West Springfield, MA) for 12 minutes under a chrome photomask with a 2-mm window. Immediately after polymerization, the unpolymerized solution was quickly flushed with 2-propanol until the monolith turned white and then washed with a copious amount of water until 2-propanol was completely removed. The

monolith columns were dried under vacuum overnight before immobilization of antibody. Figure 5.2 illustrates the schematic of monolith fabrication.

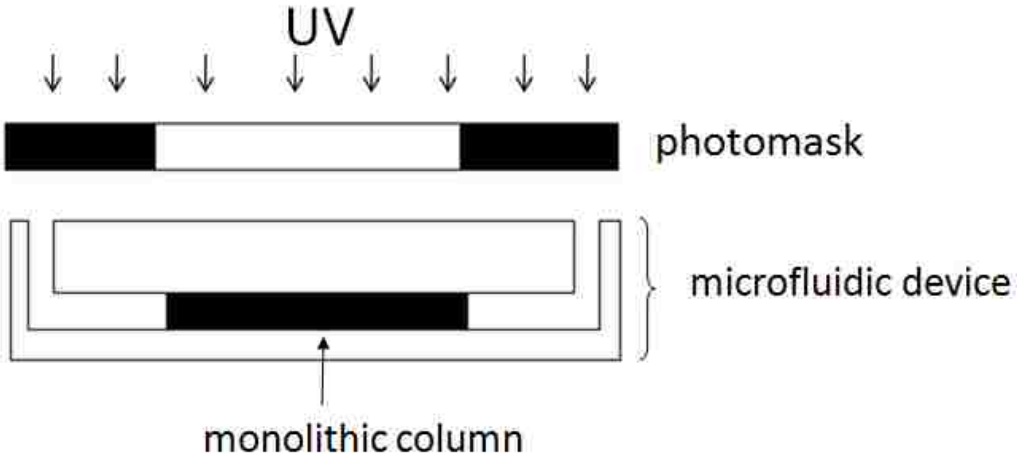

Figure 5.2 Schematic of in-situ monolith fabrication (cross sectional view)**.**

5.2.4 Antibody Immobilization. An immobilization method previously reported[11] was implemented with some modifications (see Figure 5.3). Briefly, the GMA epoxy groups were hydrolyzed to form diols by incubating the monolith in 0.5 M sulfuric acid at 60 °C for 4 hours. After flushing the column with water, the monolith was incubated in sodium periodate (1 g/mL in 90% acetic acid) solution for 4 hours at room temperature in the dark to convert diols into aldehydes. The aldehyde containing column was then reacted with 5 mg/mL mouse anti-human IL8 (R&D Systems, McKinley Place, NE) diluted in 0.5X PBS with 100 mg/mL sodium cyanoboroydride (Sigma, St. Louis, MO) overnight at 4 °C. Fresh antibody solution was pumped into the column every day for 3 days. The column was washed with 1X PBS buffer to remove unbound antibodies. The devices were kept at 4 °C and used within 1 week. Figure 5.2 illustrates the process of antibody immobilization.

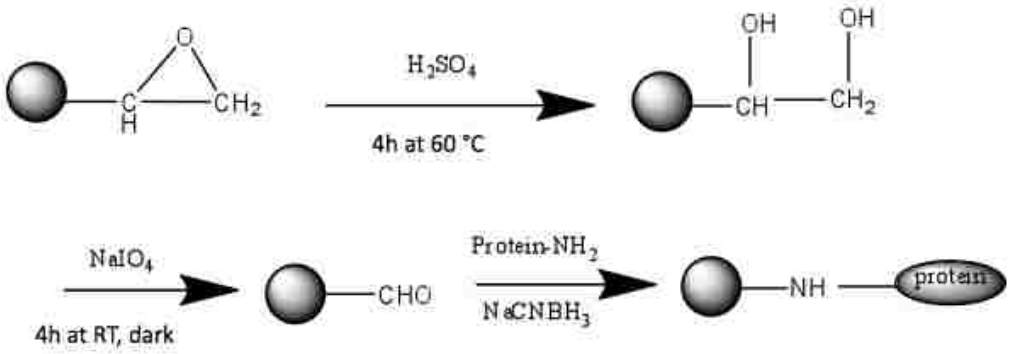

Figure 5.3 Schiff base antibody immobilization on GMA-EGDMA monolithic column.

5.2.5 Sample labeling. Human IL8 protein (Sigma, St. Louis, MO) in a stock solution of 1 mg/mL in carbonate buffer pH 9.2 was labeled with Alexafluor 488 TFP ester (Invitrogen) as previously reported.[9] The dye was first dissolved in dimethyl sulfoxide (Sigma, St. Louis, MO) to a concentration of 10 mg/mL. 5 μL of the solution was added to 250 μL of IL8 stock solution and incubated in the dark for 1 hr at room temperature. Excess unconjugated dye was removed by diafiltration, using an Amicon Ultra-0.5 (Millipore, centrifugal filter (3K MWCO) and 0.5X PBS, pH 7.4. The amount of filtered IL8 was measured and the sample was stored in the dark at 4 °C until use.

5.2.6 Device Operation. Figure 5.4 illustrates the voltage configuration to manipulate the flow of sample and solutions in the device. First, the channels were filled with 0.5X PBS. Labeled IL8 was diluted in binding buffer, 0.5X PBS, pH 7.4. For the spiked-saliva sample, the desired IL8 concentration was added to 50% v/v saliva diluted in PBS. Sample was loaded in reservoir 6 and injected into the column for 5 minutes (see Figure 5.4A). After 5 minutes, the current was turned off and the sample was allowed to incubate in the column for another 5 minutes.

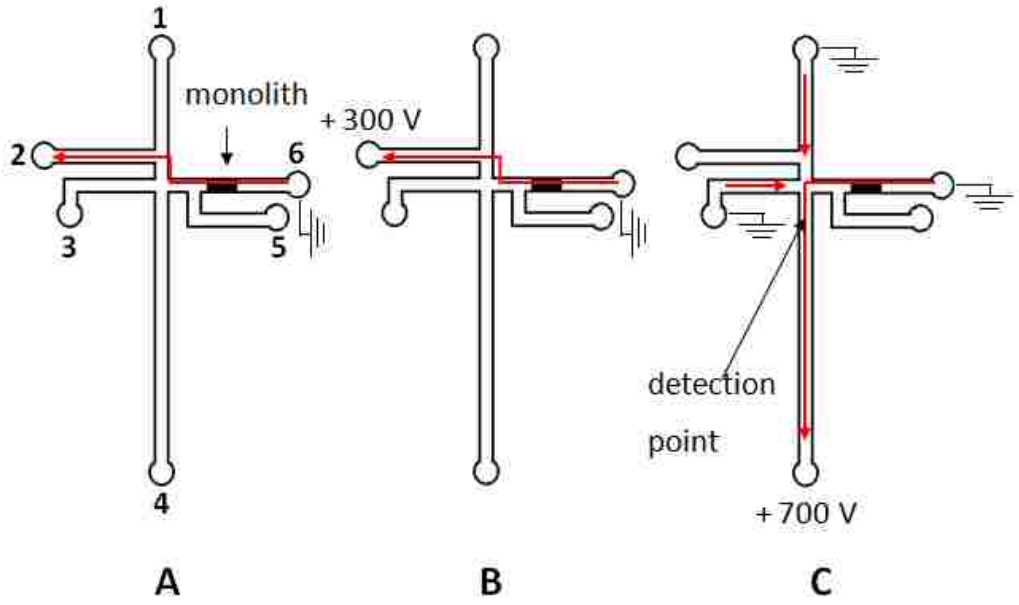

Figure 5.4 Device layout and voltage configuration for A) loading, B) washing, and C) elution. 1) Buffer reservoir, 2) injection waste reservoir, 3) titration reservoir, 4) separation waste reservoir, 5) extra channel for monolith fabrication, and 6) sample reservoir.

After incubation, the column was thoroughly washed with 0.5X PBS (see Figure 5.3B). Then, the reservoirs were emptied and cleaned. Elution buffer, 100 mM acetic acid, pH 3, was loaded into the sample reservoir (6). Buffer (1), titration (3) and separation waste (4) reservoirs were loaded with 10 mM carbonate-bicarbonate buffer pH 10. The rest of the reservoirs were loaded with 0.5X PBS. Fluorescence was detected using a photomultiplier tube and the electrochromatogram was recorded using LabView.

5.2.5 Saliva processing. Saliva samples were obtained by drooling and collected in cold, sterile conical tubes. About 5 mL of saliva was collected and immediately centrifuged at 14 000 rpm for 10 minutes at room temperature to remove debris. The saliva was immediately frozen unless

used immediately. Saliva was spiked with fluorescently labeled IL8 immediately before use and then vortexed prior to loading in the reservoir.

5.3 RESULTS AND DISCUSSION

Monolithic columns were successfully integrated in PMMA microfluidic devices. Figure 5.5A shows a photomicrograph of an integrated monolithic column showing a continuous column and Figure 5.5B shows a porous monolith with high surface area imaged using an electron microscope (Philips FEI XL30 ESEM).

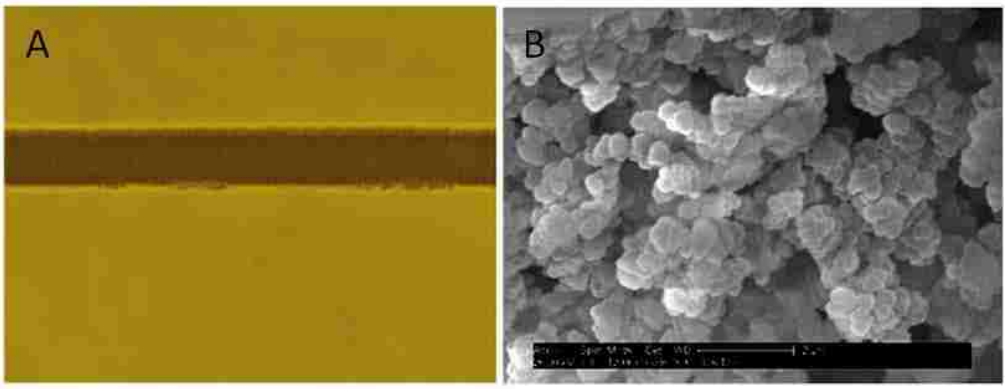

Figure 5.5 A) Photomicrograph of a continuous monolithic column in a PMMA device, B) SEM image of a monolith column showing a high surface area, porous monolith.

Monolithic columns were fabricated in-situ without prior modification of PMMA. The methacrylate on the surface of PMMA was compatible with the GMA-EGDMA monolith and showed mechanical stability over several runs. However, one of the problems encountered was bubble formation when the channels were being filled with buffer. Using pressure to push the bubbles out of the column can solve this problem but sometimes resulted in delaminated microfluidic devices. Bubbles also formed when voltage was continuously applied longer than 10 minutes; for this reason, 5-minute injection and lower voltages were used.

Immobilization of mouse anti-IL8 was verified by probing the column with an anti-mouse secondary antibody conjugated to an infrared fluorescent dye. The column was then scanned for fluorescence using a LI-COR Odyssey near IR fluorescence scanner (Lincoln, NE). Figure 5.6A shows the column modified with mouse anti-IL8 probed with anti-mouse secondary antibody fluorescing indicating the presence of immobilized antibodies, while the column blocked with non-fat dry milk only showed no fluorescence (see Figure 5.6B).

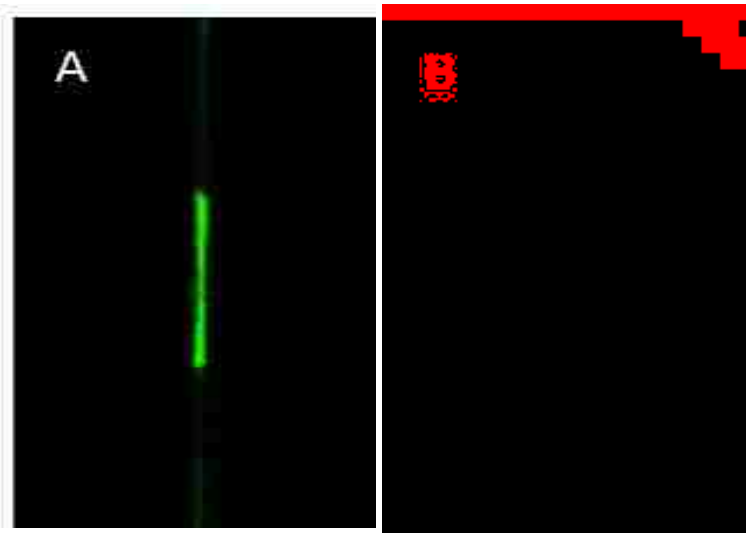

Figure 5.6 LI-COR image of monolith columns modified with A) anti-human IL8 and B) non-fat dry milk. Green color indicates presence of anti-human IL8.

The binding of the immobilized antibodies to IL8 was tested by electrochromatography. Low pH quenches the fluorescence of Alexa Flour so a high pH buffer was used to titrate the eluted stream to bring back fluorescence, a technique previously described by Wang et al.[12] Figure 5.7 shows the electrochromatogram of elution of IL8 extracted from buffer. A single

sharp peak at ~100 s was observed when Alexafluor dye was loaded onto the column (see Figure 5.7A). An extra peak that eluted at ~150 s was obtained when labeled IL8 was loaded onto the column (see Figure 5.7B) and the intensity of this peak increased when the IL8 concentration was increased from 1 ng/mL to 5 ng/mL (see Figure 5.7C).

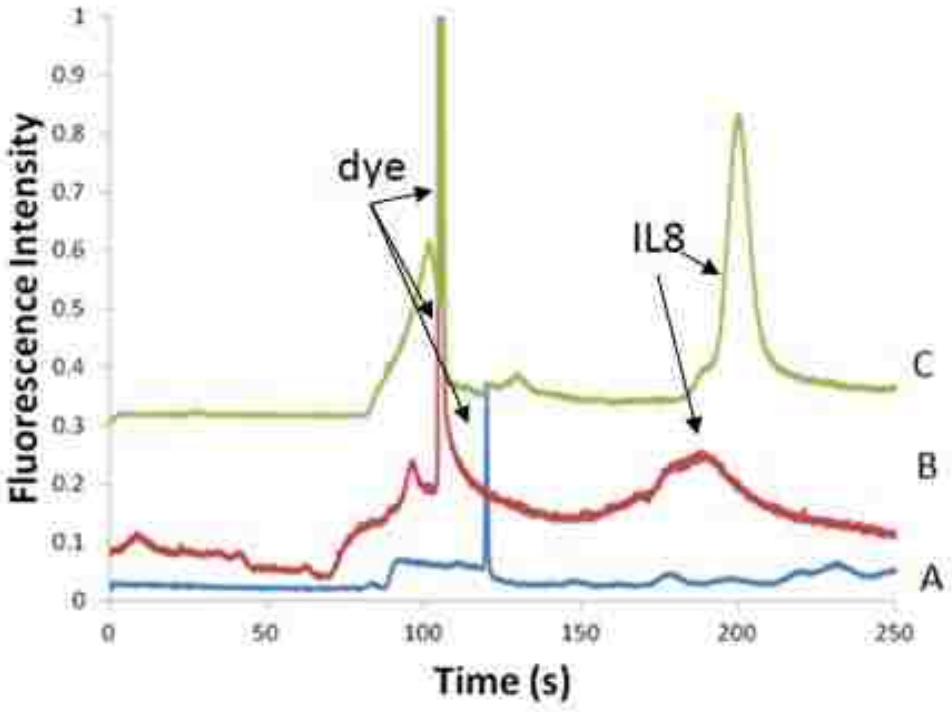

Figure 5.7 Affinity electrochromatograms of IL8 in buffer. A) Dye, B) 1 ng/mL IL8, and C) 5 ng/ mL.

I then tested the extraction of IL8 from 50% saliva. 100% saliva was viscous, so 50% saliva in buffer was used. A similar electrochromatogram was observed with IL8-spiked saliva (see Figure 5.8B-C). However, no IL8 peak was observed at IL8 concentrations lower than 10 ng/mL, which may be due to interference by other salivary proteins. The electrochromatogram of labeled unspiked saliva also only showed a peak that corresponded to the dye (compare Figure 5.8A with Figure 5.7A). The absence of an IL8 peak may be because the saliva from the healthy

donor had low IL8 that was not detectable using this method. Furthermore, using the same column for more than three complete runs failed to extract of IL8, which may be due to the loss of activity of the antibodies after exposure to extreme pH conditions. For point-of-care application, devices are meant for one time use. Loss of activity would be a problem if the column were to be used multiple times like in research settings or optimization processes. For multiple uses, either a competitor to elute bound proteins or a different antibody with good stability at extreme pH conditions would be a good alternative.

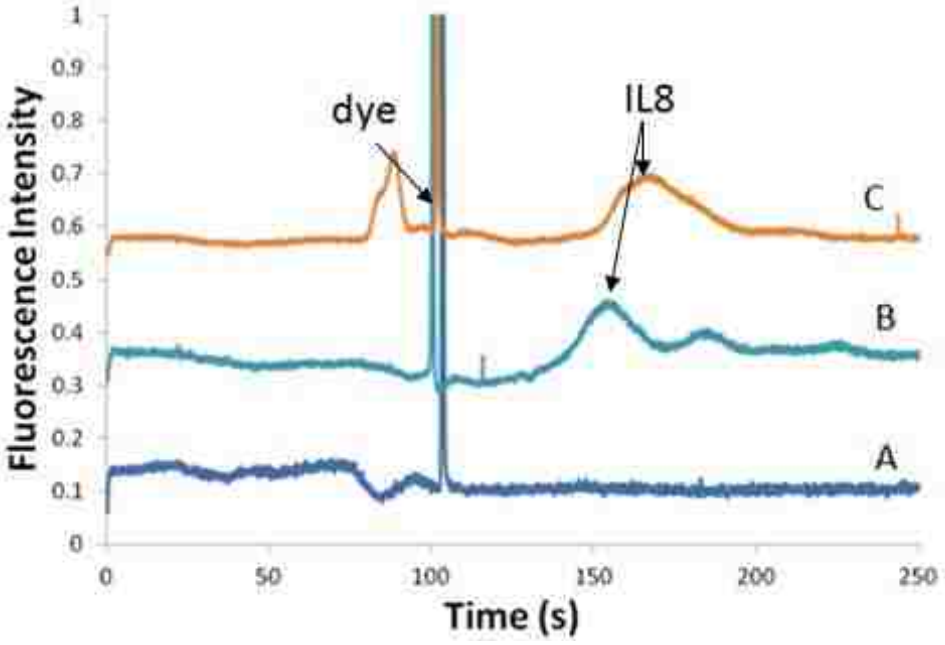

Figure 5.8 Affinity electrochromatograms of IL8-spiked saliva. A) Labeled saliva and B-C) 10 ng/mL IL8 spiked saliva.

5.4 CONCLUSIONS

I have demonstrated a working microfluidic device with integrated IL8 monolith affinity column. The columns were easily fabricated in-situ without the need to modify the surface of

PMMA prior to fabrication. I have also successfully extracted, eluted, and detected human IL8 from buffer and from spiked saliva at concentrations as low as 1 ng/mL and 10 ng/mL, respectively. Clinically relevant concentrations of IL8 were reported to be in the pg/mL range so there is a need to improve the limit of detection. Increasing the column volume and surface area would increase loading capacity. Forming a monolith with smaller nodules that still maintains low backpressure could increase surface area. Furthermore, increasing the density of antibody in the column would help increase the loading capacity. Increasing the antibody concentration during surface attachment or optimizing the immobilization conditions such as temperature and time could improve the density of the immobilized antibody. Therefore, further optimization of the immobilization procedure should be conducted. Depleting abundant proteins to improve detection could also help to better detection of low abundance IL8 in saliva.

5.5. REFERENCES

1. Rothenberg, S. M.; Ellisen, L. W., The molecular pathogenesis of head and neck squamous cell carcinoma. *J Clin Invest* **2012,** *122* (6), 1951-1957.

2. Silverman, S., Early Diagnosis of Oral-Cancer. *Cancer* **1988,** *62* (8), 1796-1799.

3. Ndiaye, C.; Mena, M.; Alemany, L.; Arbyn, M.; Castellsague, X.; Laporte, L.; Bosch, F. X.; de Sanjose, S.; Trottier, H., HPV DNA, E6/E7 mRNA, and p16(INK4a) detection in head and neck cancers: a systematic review and meta-analysis. *Lancet Oncol* **2014,** *15* (12), 1319-1331.

4. Herrero, R.; Castellsague, X.; Pawlita, M.; Lissowska, J.; Kee, F.; Balaram, P.; Rajkumar, T.; Sridhar, H.; Rose, B.; Pintos, J.; Fernandez, L.; Idris, A.; Sanchez, M. J.; Nieto, A.; Talamini, R.; Tavani, A.; Bosch, F. X.; Reidel, U.; Snijders, P. J. F.; Meijer, C. J. L. M.; Viscidi, R.; Munoz, N.; Franceschi, S.; G, I. M. O. C. S., Human papillomavirus and oral cancer: The international agency for research on cancer multicenter study. *J Natl Cancer I* **2003,** *95* (23), 1772-1783.

5. Punyani, S. R.; Sathawane, R. S., Salivary level of interleukin-8 in oral precancer and oral squamous cell carcinoma. *Clin Oral Invest* **2013,** *17* (2), 517-524.

6. Watanabe, H.; Iwase, M.; Ohashi, M.; Nagumo, M., Role of interleukin-8 secreted from human oral squamous cell carcinoma cell lines. *Oral Oncol* **2002,** *38* (7), 670-679.

7. St John, M. A. R.; Li, Y.; Zhou, X. F.; Denny, P.; Ho, C. M.; Montemagno, C.; Shi, W. Y.; Qi, F. X.; Wu, B.; Sinha, U.; Jordan, R.; Wolinsky, L.; Park, N. H.; Liu, H. H.; Abemayor, E.; Wong, D. T. W., Interleukin 6 and interleukin 8 as potential biomarkers for oral cavity and oropharyngeal squamous cell carcinoma. *Arch Otolaryngol* **2004,** *130* (8), 929-935.

8. Yang, C. Y.; Brooks, E.; Li, Y.; Denny, P.; Ho, C. M.; Qi, F. X.; Shi, W. Y.; Wolinsky, L.; Wu, B.; Wong, D. T. W.; Montemagno, C. D., Detection of picomolar levels of interleukin-8 in human saliva by SPR. *Lab Chip* **2005,** *5* (10), 1017-1023.

9. Nge, P. N.; Yang, W. C.; Pagaduan, J. V.; Woolley, A. T., Ion-permeable membrane for on-chip preconcentration and separation of cancer marker proteins. *Electrophoresis* **2011,** *32* (10), 1133-1140.

10. Pagaduan, J. V.; Yang, W.; Woolley, A. T., Optimizationn of monolithic columns for microfluidic devices. *Proc. SPIE* **2011,** *8031*, 80311V/80311-80311V/80317.

11. Mallik, R.; Tao, J.; Hage, D. S., High-performance affinity monolith chromatography: Development and evaluation of human serum albumin columns. *Anal Chem* **2004,** *76* (23), 7013-7022.

12. Yang, W.; Sun, X.; Pan, T.; Woolley, A. T., Affinity monolith preconcentrators for polymer microchip capillary electrophoresis. *Electrophoresis* **2008,** *29* (16), 3429-35.

CHAPTER 6. SUMMARY AND FUTURE WORK

6.1 SUMMARY

I have demonstrated fabrication of PMMA microfluidic devices and developed immunoassays for detecting two potential cancer biomarkers, thymidine kinase 1 (TK1) and interleukin 8 (IL8).

1% w/v methylcellulose in buffer acts as a dynamic coating and sieving matrix and demonstrated a simple yet effective method to separate large proteins such as IgG and its immune complex. Other dynamic coatings could be explored to improve separation efficiency of the antigen-antibody complex from free antibody. The struggle to detect endogenous TK1 in serum was determined to be due to the inability of the novel mouse anti-TK1 to form a complex with TK1 under the conditions used in the experiments. This finding can be applied to future assay development by using the commercial rabbit anti-TK1 antibody. Immunoassays depend on the ability of the antibody to specifically determine the target antigen. The ability of the antibody to bind the target antigen must be first established or any attempt to optimize other parameters such as pH, ionic strength, etc. would be futile, as was the case in my attempt to detect endogenous TK1 prior to characterization of the novel mouse anti-TK1.

I have also described a method to batch process multiple monolith formulations using SEM that led to faster optimization of monolithic columns for microfluidic devices. Batch processing made it possible to qualitatively assess the effect of Tween-20 on the morphology of the monolith column before its integration on-chip. This saved time and resources by not using

devices for early stage monolith optimization. I have integrated monolithic columns in PMMA devices and successfully immobilized active antibodies for affinity extraction of interleukin 8 from buffer and saliva. The lowest IL8 concentration detected was 1 ng/mL in buffer and 10 ng/mL in spiked saliva. The higher detection limit in spiked saliva may be due to the interference by other high abundance proteins. Protein depletion described in Chapter 3 could be used for testing endogenous IL8 to further this work.

6.2 FUTURE WORK

6.2.1 Integrated blood plasma separation and protein immunodepletion for immune complex detection in microfluidics.

Blood analysis often requires removal of interfering cells such as red blood cells, white blood cells, and platelets. Blood is usually drawn and processed using conventional methods such as centrifugation to extract plasma for analysis. Another method used to remove cells is through cell lysis. However, this technique results in release of proteins and nucleic acids into the plasma thus contaminating it. Integration of plasma isolation processes on chip would decrease sample contamination and sample preparation time.

Several groups have utilized the Zweifach-Fung effect or bifurcation law to isolate plasma from blood cells in microfluidic devices.[1, 2] The bifurcation law describes that a particle, in this case blood cells, at a bifurcation region has a tendency to move towards a channel with higher flow rate, leaving very few cells flowing into the lower flow rate channel.[2] Obtaining cell-free plasma is affected by the geometry of the bifurcating channels.[3]

Plasma is replete with proteins that can interfere with immunoassays. As described in Chapter 2, depletion of immunoglobulin and serum albumin can enrich low-abundance protein biomarkers. Even though ammonium sulfate precipitation is a cheap and effective method to enrich low-abundance proteins it requires a desalting step to make the protein depleted sample compatible with microchip electrophoresis. For this reason, an immunodepletion monolith column would be more suitable. Figure 6.1 shows the schematic of a microfluidic device with the capability to isolate plasma analyze protein markers by immunoaffinity microchip electrophoresis. Blood can be loaded into the device using integrated pumps.[4] At the bifurcation point, the plasma will be collected in the plasma reservoir and the blood cells will exit the other channel. Valves will also be used to prevent sample leakage during loading and microchip electrophoresis. The collected plasma will then be depleted of immunoglobulin and albumin for better detection of low-abundance markers. The plasma sample can be loaded into the column by pumping. The serpentine design of the reaction channel will enhance mixing of fluorescently tagged antibody with the antigen, and hence should decrease reaction time. Gated injection could be used to load a larger sample volume for detection of low-abundance markers.

This integrated device will eliminate the need to process the blood off-chip thus decreasing sample analysis time and contamination. A multilayer device could be designed for parallel analysis of biomarkers without increasing the footprint of the device.

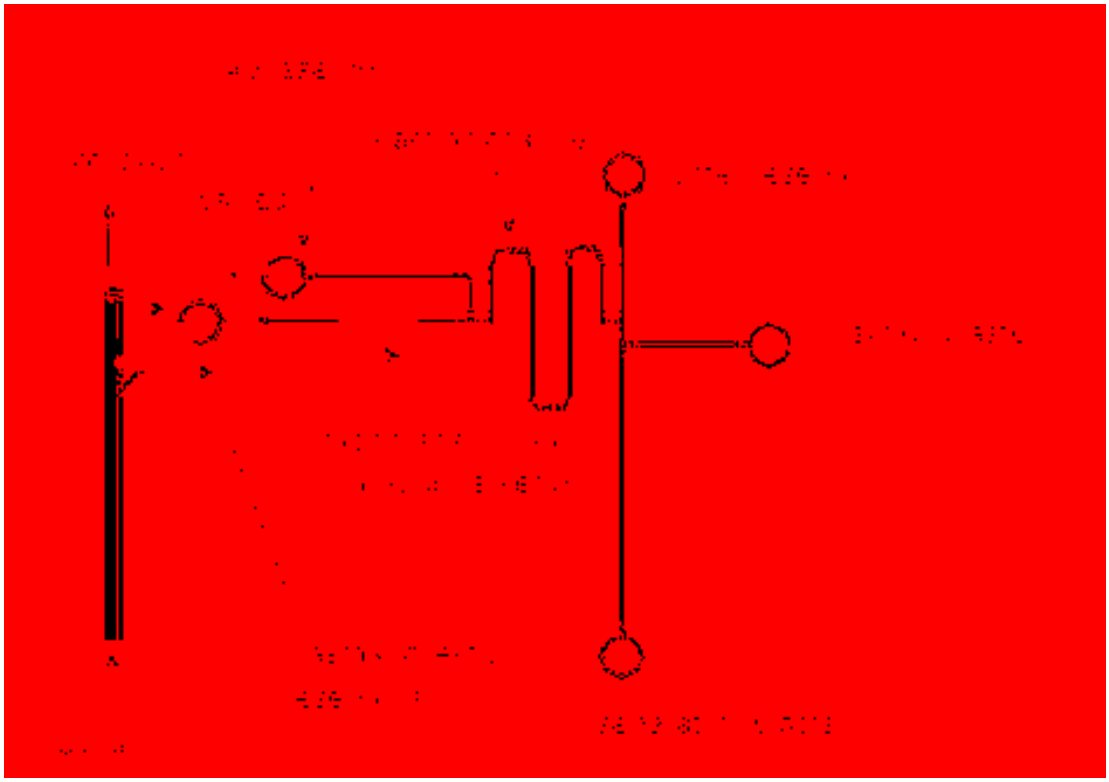

Figure 6.1 Microchip device with integrated plasma extraction module.

6.2.2 Microfluidic neutrophil isolation and procalcitonin detection for sepsis diagnosis

Sepsis is a serious complication caused by bacteria or other microbial organisms and is the leading cause of mortality in critically ill patients.[5] Delay in diagnosis and immediate therapy results in higher mortality.[6] The gold standard for sepsis diagnosis is the broth culture method but this can take as long as 24 hours to arrive at a definitive diagnosis.[5] There is a need to accurately determine in timely and cost-effective manner if the observed inflammatory response is due to bacterial infection. Thus, interest increased in sepsis biomarkers that can provide additional information from already established clinical assessments and investigation.[6] Several biomarkers are routinely measured in hospital laboratories such as C-reactive protein and

cytokines (i.e., interleukins 6 and 8, and tumor necrosis factor). However these markers are also elevated in other chronic inflammatory conditions.[6, 7]

Procalcitonin, a precursor of the hormone calcitonin, was observed to increase from its normal level (<0.1 ng/mL) at 4 hours after the onset of infection, peaking between 8 and 24 hours.[5] Another marker is CD64, a glycoprotein expressed on the neutrophil membrane, which was reported to be upregulated in newborn sepsis.[7,8] Flow cytometry analysis of cell surface markers is a fast and efficient method, but flow cytometry is expensive, bulky and requires special training.

Integrated microfluidic devices that could analyze both CD64 and serum proteins could address the shortcomings of traditional sepsis diagnostics. Figure 6.2 illustrates a modification of Figure 6.1 that would selectively isolate neutrophils from other blood cells to measure CD64 and analyze protein sepsis markers.

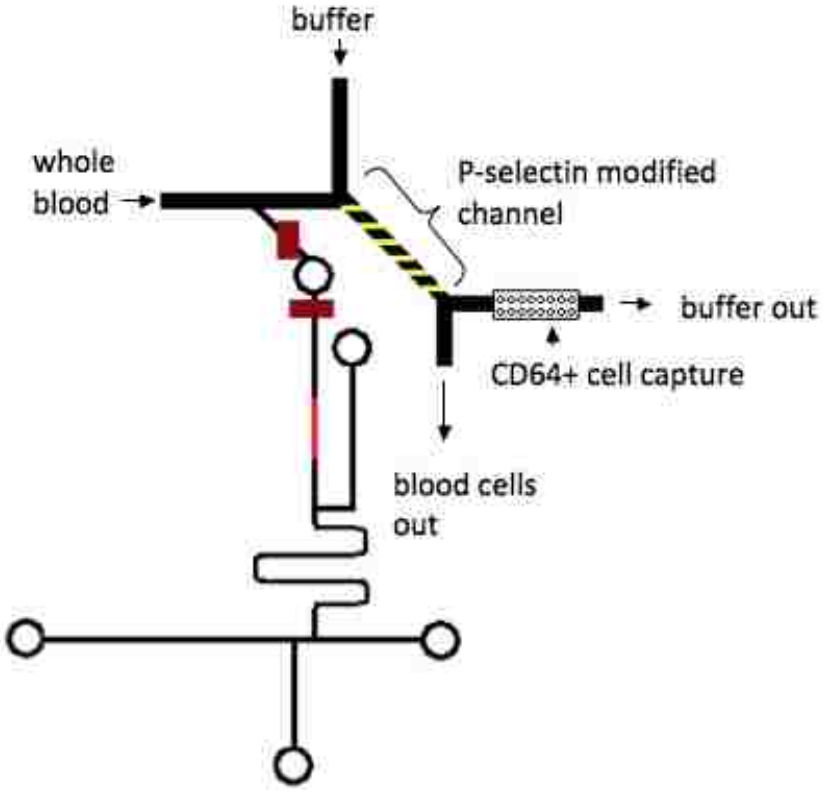

Figure 6.2 CD64+ neutrophil and procalcitonin detection for sepsis diagnosis in microfluidic devices.

Neutrophils can be selectively isolated from other blood cells by using affinity flow fractionation described by Bose et al.[9] They immobilized P-selectin, a protein that specifically interacts with neutrophils, in asymmetric patterns on the surface of a microfluidic channel. When the neutrophil attached to P-selectin, the cell was displaced laterally into the buffer stream and could reattach to the molecular marker. When it reached the non-patterned region it was quickly eluted. Using this technique they were able to obtain intact neutrophils with >92% purity. Isolated neutrophils will be drawn to the channel with immunoaffinity posts that will selectively bind for CD64+ cells. A similar approach to that used for detecting circulating tumor cells in polymeric microfluidic devices will be used in the cell capture module.[10] Adding this cell capture

module will eliminate the need for flow cytometry detection of CD64+ neutrophils. The isolated plasma will be processed and probed for procalcitonin as described in section 6.2.1. The combined cell surface marker and protein biomarker analysis may facilitate faster differential diagnosis of sepsis, so proper therapy can be immediately administered.

Combining cell flow fractionation, target cell capture, protein depletion, and immunoaffinity microchip electrophoresis in microfluidic devices would allow analysis of whole blood without off-chip preparation. The aim is to be able to analyze a ten microliter volume to make this testing compatible with infants and older patients. The ability to analyze small sample volumes may lead to a shorter analysis time that is beneficial for time-sensitive conditions. The ligands used for target marker identification can be changed to fit the needed tests thus making these devices applicable for immunoassays of other disease markers.

6.3 REFERENCES

1. Nakashima, Y.; Hata, S.; Yasuda, T., Blood plasma separation and extraction from a minute amount of blood using dielectrophoretic and capillary forces. *Sensor Actuat B-Chem* **2010,** *145* (1), 561-569.

2. Yang, S.; Undar, A.; Zahn, J. D., A microfluidic device for continuous, real time blood plasma separation. *Lab Chip* **2006,** *6* (7), 871-880.

3. Fekete, Z.; Nagy, P.; Huszka, G.; Tolner, F.; Pongracz, A.; Furjes, P., Performance characterization of micromachined particle separation system based on Zweifach-Fung effect. *Sensor Actuat B-Chem* **2012,** *162* (1), 89-94.

4. Zhang, W. H.; Lin, S. C.; Wang, C. M.; Hu, J.; Li, C.; Zhuang, Z. X.; Zhou, Y. L.; Mathies, R. A.; Yang, C. Y. J., PMMA/PDMS valves and pumps for disposable microfluidics. *Lab Chip* **2009,** *9* (21), 3088-3094.

5. Jin, M.; Khan, A. I., Procalcitonin: Uses in the Clinical Laboratory for the Diagnosis of Sepsis. *Labmedicine* **2010,** *41* (3), 173-177.

6. Kibe, S.; Adams, K.; Barlow, G., Diagnostic and prognostic biomarkers of sepsis in critical care. *J Antimicrob Chemoth* **2011,** *66*, Ii33-Ii40.

7. Bhandari, V.; Wang, C.; Rinder, C.; Rinder, H., Hematologic profile of sepsis in neonates: Neutrophil CD64 as a diagnostic marker. *Pediatrics* **2008,** *121* (1), 129-134.

8. Rudensky, B.; Sirota, G.; Erlichman, M.; Yinnon, A. M.; Schlesinger, Y., Neutrophil CD64 Expression as a Diagnostic Marker of Bacterial Infection in Febrile Children Presenting to a Hospital Emergency Department. *Pediatr Emerg Care* **2008,** *24* (11), 745-748.

9. Bose, S.; Singh, R.; Hanewich-Hollatz, M.; Shen, C.; Lee, C. H.; Dorfman, D. M.; Karp, J. M.; Karnik, R., Affinity flow fractionation of cells via transient interactions with asymmetric molecular patterns. *Sci Rep-Uk* **2013,** *3*, doi:10.1038/srep02329.

10. Ohnaga, T.; Shimada, Y.; Moriyama, M.; Kishi, H.; Obata, T.; Takata, K.; Okumura, T.; Nagata, T.; Muraguchi, A.; Tsukada, K., Polymeric microfluidic devices exhibiting sufficient capture of cancer cell line for isolation of circulating tumor cells. *Biomed Microdevices* **2013,** *15* (4), 611-616.